arXiv:1611.08673v3 [cond-mat.quant-gas] 1 Feb 2017

Multipolar Kondo Effect in $^1S_0$-$^3P_2$ Mixture of ^{173}Yb Atoms

Igor Kuzmenko[1], Tetyana Kuzmenko[1], Yshai Avishai[1,2,4] and Gyu-Boong Jo[3]
[1] *Department of Physics, Ben-Gurion University of the Negev Beer-Sheva, Israel*
[2] *NYU-Shanghai, Pudong, Shanghai, China,*
[3] *Department of Physics, The Hong Kong University of Science and Technology, Clear Water Bay, Kowloon, Hong Kong, China*
[4] *Yukawa Institute for Theoretical Physics, Kyoto University, Kyoto 606-8502, Japan*

Whereas in the familiar Kondo effect the exchange interaction is *dipolar*, it can also be *multipolar*, as has been realized in a recent experiment. Here we study multipolar Kondo effect in a Fermi gas of cold ^{173}Yb atoms. Making use of different AC polarizability of the electronic ground state Yb($^1S_0$) and the long-lived metastable state Yb*($^3P_2$), it is suggested that the latter atoms can be localized and serve as a dilute concentration of magnetic impurities while the former ones remain itinerant. The exchange mechanism between the itinerant Yb and the localized Yb* atoms is analyzed and shown to be antiferromagnetic. The quadruple and octuple interactions act to enhance the Kondo temperature T_K that is found to be experimentally accessible. The bare exchange Hamiltonian needs to be decomposed into dipole (d), quadruple (q) and octuple (o) interactions in order to retain its form under renormalization group (RG) analysis, in which the corresponding exchange constants ($\lambda_{\rm d}$, $\lambda_{\rm q}$ and $\lambda_{\rm o}$) flow independently. Numerical solution of the RG scaling equations reveals a few finite fixed points, indicating an over-screening, which suggests a non-Fermi liquid phase. The impurity contribution to the magnetic susceptibility is calculated in the weak coupling regime ($T \gg T_K$).

PACS numbers: 31.25.-v,32.80.Pj,72.15.Qm

I. INTRODUCTION

Background In its most elementary form, the (single channel) Kondo model describes the physics of a magnetic impurity (of spin operator $\mathbf{S}$), immersed in a host metal with a single continuous band of noninteracting electrons (of spin operator $\mathbf{s}$, with $s=\frac{1}{2}\hbar$)[1–4]. The impurity and the band electrons are coupled via an antiferromagnetic exchange interaction $J\mathbf{s}\cdot\mathbf{S}$ of strength $J>0$. The corresponding Hamiltonian $H_{\rm s-d}$ has an SU(2) symmetry. The Kondo model can naturally be generalized into the Coqblin-Schrieffer model whose Hamiltonian $H_{\rm C-S}$ has an SU(N) symmetry[4–7]. Renormalization group (RG) analysis shows that the respective low energy fixed point in either model is stable and that the corresponding fixed point Hamiltonian describes regular or singular Fermi liquid (FL), in which the impurity is fully or under screened.

A seminal paper by Nozières and Blandin (NB) back in 1980, discusses the fixed points of $H_{\rm s-d}$ under the assumption that a few electron channels participate in the impurity screening[8]. More precisely, suppose that by some mechanism, there are N independent electron channels contributing to screening. Then, under favourable conditions on the corresponding exchange constants, together with the (hereafter referred as NB inequality) $N>2S$, the impurity is *over-screened*. The Hamiltonian of such over-screened Kondo system flows at low temperature to a new fixed point in which it displays a non-Fermi liquid (NFL) behavior. Searching for an experimental manifestation of over-screened Kondo effect in solid state systems was notoriously frustrating, but eventually it was demonstrated in a specifically designed quantum-dot system[9].

Another route to over-screening in the Kondo effect is *single channel over-screening by large spin Fermi-sea*[10]. It is expected to occur when a magnetic impurity is immersed in a host Fermi-sea with a continuous band of noninteracting fermions of spin operator $\mathbf{s}$, with $s>\frac{1}{2}\hbar$. This system is shown to be equivalent to that with $N(s)$ independent electron channels where

$$N(s)=\frac{2}{3}\,s(s+1)(2s+1). \tag{1}$$

Since $N(s)$ is a cubic function of s, (for example $N(\frac{5}{2})=35$), the NB inequality $N>2S$ (that is a necessary but not sufficient condition for over-screening) can easily be satisfied. While it is hard (albeit possible) to perceive its realization in solid state systems, the revelation and the possible control of a gas composed of cold fermionic atoms within a periodic optical lattice potential turned this scenario to be realistic also outside the realm of solid-state systems[11,12]. Indeed, we have recently suggested a general framework for a pertinent experiment to test this scenario of over-screening and analyzed the conditions and parameter range for its realization[13]. It can be performed in a few laboratories that specialize in controlling cold fermionic atoms.

In both cases (multi-channel and/or large spin over screening), the corresponding Hamiltonian has an SU(2) symmetry, and the exchange interaction is *dipolar*. An extension of the SU(2) multi-channel over-screening scenario into over-screened multi-channel SU(N) Kondo

model is discussed in Ref.[14].

In the present work we focus on an experimentally accessible cold atom system and examine the concept of large spin Kondo over-screening beyond SU(2), in the sense that the exchange interaction is *multipolar*. This is motivated by a recent experiment where a multipolar Kondo effect (KE) is realized in solid state system[12]. For the cold atom arena, a concrete experimental candidate system is that of fermionic alkali-earth-like isotopes such as ^{173}Yb atoms[15–18]. The underlying idea is to localize an ^{173}Yb atom in its long lived excited ^{3}P$_2$ state with atomic spin $F = \frac{3}{2}$, in a Fermi sea of non (or weakly)-interacting itinerant ^{173}Yb atoms in their ground state ^{1}S$_0$ with atomic spin $I = \frac{5}{2}$. For that purpose, it should be demonstrated that an antiferromagnetic exchange interaction exists between the impurity Yb*(^{3}P$_2$) and the itinerant Yb(^{1}S$_0$) atoms. Intuitively, in that case we might expect an over-screening by large spin scenario, since the angular momentum of the itinerant atoms is larger than that of the impurity atom ($I = \frac{5}{2} > F = \frac{3}{2}$). However, quantitative analysis turns out to be extremely complicated, due to several factors. First, elucidation and calculation of the exchange interaction is rather involved, and requires sophisticated multiple expansions to handle the pertinent angular momentum algebra. Second, identifying and constructing the explicit form of the exchange term is rather tedious, and, unfortunately, the pertinent Kondo Hamiltonian does not have a definite symmetry. Third, in order to identify the NFL fixed points, perturbative RG calculations within the poor-man scaling procedure must go at least up to third order and the relevant expressions are long and involve multiple summations on angular momentum quantum numbers. Finally, elucidating the NFL physics requires the use of non-perturbative techniques (Bethe ansatz or conformal field theory) which are still not developed for this class of Hamiltonians.

It is worthwhile stressing at this early stage a central point distinguishing multipolar from an SU(2) over-screening resulting from our analysis: If the spin F of the impurity and the spin I of itinerant fermions satisfy the inequalities

$$F \geq 3/2, \quad I \geq 3/2, \quad N(I) > 2S,$$

the NB fixed point $j^* = 1/N(I)$ is unstable, and the stable fixed point is another non Fermi liquid phase. The reason is that in the process of carrying out Schrieffer-Wolf transformations, one usually restricts oneself to second order perturbation theory. However, when quadruple, octuple and higher exchange interactions are present, new interactions are generated within the Schrieffer-Wolf procedure. At high temperature these interactions are weaker than the lowest order (dipole) interaction. But at low temperature, these interactions turn the NB fixed point to be unstable.

Organization: The paper is organized as follows: In section II the question of experimental realization is addressed. Specifically, we substantiate the feasibility of fabricating a system consisting of a Fermi gas of ^{173}Yb atoms in their ground state (electronic configuration ^{1}S$_0$) and a small concentration of ^{173}Yb atoms in their long lived excited state (electronic configuration ^{3}P$_2$) trapped in a suitably designed optical potential. The rest of the paper is devoted to theoretical analysis. Exchange interaction between ^{173}Yb($^1S_0$) and ^{173}Yb*($^3P_2$) atoms is analyzed in section III, while the Kondo Hamiltonian H_K is derived in section IV. The main technical endeavors are related to the decomposition of H_K into 2^n poles components ($n = 1, 2, 3$), and the numerical estimates of the pertinent coupling constants. In section V the perturbative RG calculations pertaining to H_K are detailed up to second order. Although the derivation of these corrections is rather technical, we find it useful to present it within the main text because it starts from the standard diagrams of poor-man's scaling analysis, and the analysis that enables us to overcome the complexities stemming from the relevant spin algebra is quite instructive. At the end of this section we write down and solve the relevant scaling equations (up to second order). The solutions enable us to elucidate the Kondo temperature T_K, as explained in section VI. However, to find stable fixed points that are candidates for NFL behavior, one must expand the perturbative RG calculations up to third order. These calculations are carried out in section VII. Despite its highly technical nature, we include it in the main text, for the same reasons as for section V. The most significant result that emerges is a list of seven possible fixed points. Yet, further analysis is required in order to sort out the stable ones, by linearizing the RG equations and identifying relevant and irrelevant exponents. At the end of this procedure, only three stable points are left. In section X we derive an expression for the first physical observable related to this system, namely, the impurity contribution to the magnetic susceptibility in the weak coupling regime $T > T_K$. A short summary listing our main achievements is presented in section XI. Numerous technical issues are discussed in the Appendix.

II. EXPERIMENTAL FEASIBILITY

Recent development of producing degenerate Bose and Fermi gases of alkaline-earth-like atoms has attracted a great deal of interests in utilizing such atoms for the study of many-body physics (in the context of quantum simulation)[19–21] and the realization of quantum computation[22,23]. The enlarged SU(N) spin symmetry for the fermionic isotopes of alkaline-earth-like atoms expands our capability in exploring large spin physics in low dimensions[19] and a two-orbital Fermi gas with SU(N) interactions[20,21,24] in which the interactions can be tuned by the orbital Feshbach resonance[16]. In addition, a narrow optical transition between the singlet and the triplet state enables to realize a spin-orbit coupled Fermi gas with minimal heating[25–27], and a long-lived triplet state holds the promise in studying the Kondo effect.

It has recently been demonstrated that in such a systems, the Kondo temperature can be increased due to the

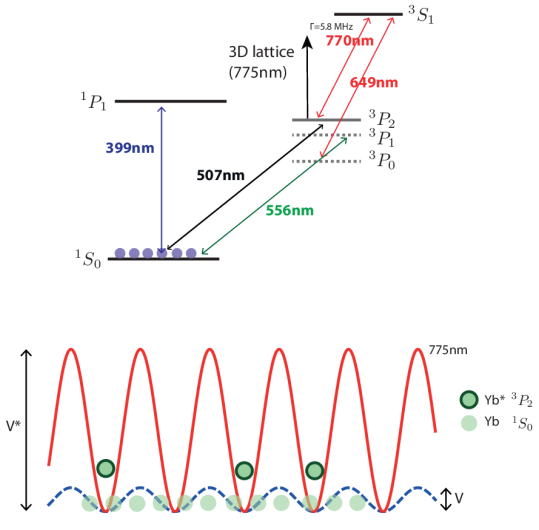


FIG. 1: (color online) Schematic diagram of the experimental system. A small portion of the ytterbium atoms in the ^{1}S$_0$ ground state (labeled by Yb atoms) are optically pumped into the ^{3}P$_2$ excited state via the resonant ^{1}S$_0$-^{3}P$_2$ transition or the intermediate ^{1}S$_0$-^{3}D$_2$ transition. The ytterbium atoms in the metastable state (labeled by Yb* atoms) is tightly confined by a three-dimensional optical lattice generated by the near-resonant 775 nm light. The Yb atoms is, however, itinerant as the effective lattice depth V is $V \ll V^*$.

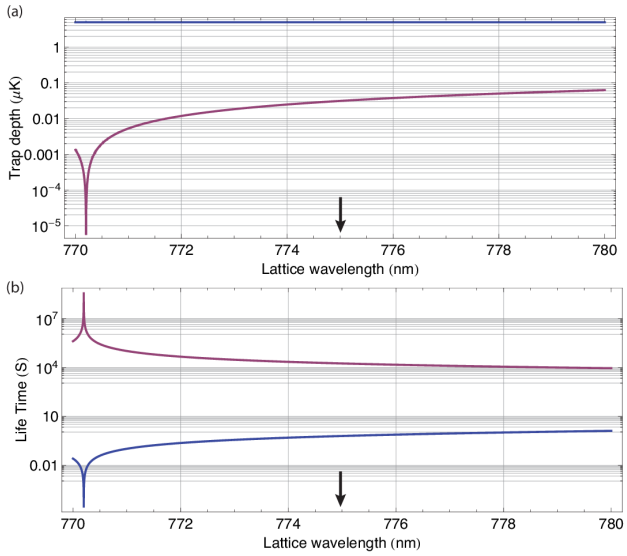


FIG. 2: (color online) (a) The optical lattice depth V of the ^{1}S$_0$ ground-state atoms (purple curve) is calculated for the different values of the lattice light wavelength when the lattice depth of the Yb* atoms (blue curve) is set to $V^* = k_B \times 5\mu$K. Near the wavelength of 775 nm that is far-detuned from the resonant ^{3}P$_2$-^{3}S$_1$ transition of 770.2 nm, the ground-state atoms Yb see the lattice potential depth less than a few $h\times$kHz and thus become itinerant. The spontaneous light scattering for the meta-stable Yb* atoms is suppressed down to $\sim 1s^{-1}$ that should be sufficiently long enough for observing many-body physics in this system. In (b), the life time of Yb (purple curve) and Yb* (blue curve) atoms is shown when the lattice depth is set to the value shown in above Fig 1(a).

spin-exchange interaction and the confinement-induced resonance effect[17].

More concretely, making use of different AC polarizabillities of the ground state and the metastable state, the laters can be localized and serve as local moments. Then, Kondo effect is expected to occur due to an exchange interaction between the atoms in the ground state ^{1}S$_0$ and the atoms in the metastable ^{3}P$_J$ state. Such scenario, pertaining to spin-exchange interactions between ^{1}S$_0$ and ^{3}P$_0$ states has been explored in our previous work where it is shown to realize an SU(6) Coqblin-Schrieffer model[28].

Here, we consider ytterbium atoms in the metastable ^{3}P$_2$ (Yb*) state as magnetic impurities for itinerant ground-state ^{1}S$_0$ (Yb) atoms. To realize the Kondo model proposed in this work, we begin with a Fermi gas of the ground-state ^{173}Yb atoms confined in a shallow harmonic trap. The harmonic potential can be produced by far-detuned lights, for example at the wavelength of 1064 nm, which results a state-independent potential for both Yb and Yb* atoms. Subsequently, a small portion, about 10% of the ground state ^{1}S$_0$ atoms will be directly transferred to ^{3}P$_2$ using a narrow line-width 507 nm optical transition ^{1}S$_0$−^{3}P$_2$[29]. Alternatively, the ground state atoms may be pumped into the state ^{3}D$_2$ with a 404 nm light and then spontaneously decay to the ^{3}P$_2$ state[30]. During the pumping process, a three-dimensional optical lattice potential may be applied to suppress the recoil kick in the Lamb Dicke regime. After the pumping, atoms in the metastable-state ^{3}P$_2$ will be selectively localized by a spin-dependent three-dimensional optical lattice potential generated by the lights near the ^{3}P$_2$-^{3}S$_1$ transition of 770.2 nm. By choosing the wavelength of the 3D lattice suitably, only Yb* atoms will be tightly confined within the lattice while Yb atoms are still itinerant. With the lattice wavelength of 775 nm, for example, the optical lattice depth V^* for Yb* atoms can be $V^* \sim h\times 100$ kHz (or $k_B \times 5\mu$K) that is much larger than the typical Fermi energy of a few kHz in ytterbium atomic system (see Fig. 2), resulting the small Lamb Dicke parameter. Within this optical lattice potential, ^{1}S$_0$ Yb atoms should be still itinerant with the potential depth of $V \sim h\times 0.2$ kHz (or $k_B \times 10n$K). The total spontaneous scattering rate of the ^{3}P$_2$ state is about $\sim 1s^{-1}$ resulting negligible heating of Yb* atoms.

In the proposed experiment, ytterbium atoms in different orbitals, Yb and Yb* atoms, can be selectively detected to extract the thermodynamic quantities that will be discussed later. The Yb atom in the ^{1}S$_0$ state are imaged using the 399 nm ^{1}S$_0$-^{1}P$_1$ transition. To image Yb* atoms, we first blast Yb atoms with 399 nm light followed by optical pumping Yb* atoms into the ^{3}P$_1$ state with 770 nm and 649 nm lights (see Fig. 1). The pumped atoms in the ^{3}P$_1$ state then decay to the ^{1}S$_0$ state that can be imaged by 399 nm light[29].

III. EXCHANGE INTERACTION

This section introduces the main ingredients required for the construction of the Kondo Hamiltonian (that is carried out in the next section). The basic notations and numerous algebraic manipulations pertaining to the geometry of multipolar interactions are specified, and the relevant exchange interactions are derived and analyzed.

A. Notations

In this subsection we introduce the definitions and expressions for the 2^n poles required for the representation of the Kondo Hamiltonian in terms of multiple expansion. These 2^n poles result from the spin content of the underlying atomic system.

We consider exchange interaction of itinerant atoms (which are ^{173}Yb atoms in the ground $^1S_0$ state with atomic spin $I = \frac{5}{2}$), and localized impurities (which are the same ^{173}Yb atoms in the long lived excited $^3P_2$ state with atomic spin $F = \frac{3}{2}$). Note that I is contributed solely from the nuclear spin while F is the sum of electronic and nuclear spins. An atom with total angular momentum $F = \frac{3}{2}$ has nontrivial dipole, quadruple and octuple magnetic momenta. They are denoted here as

$$\hat{F}^{\alpha}, \qquad \hat{F}^{\alpha,\alpha'}, \qquad \hat{F}^{\alpha,\alpha',\alpha''},$$

where α, α' and α'' are Cartesian indices. An atom with total angular momentum $I = \frac{5}{2}$ has nontrivial dipole, quadruple, octuple, 16-pole and 32-pole magnetic momenta, denoted here as

$$\hat{I}^{\alpha_1}, \qquad \hat{I}^{\alpha_1,\alpha_2}, \qquad \hat{I}^{\alpha_1,\alpha_2,\alpha_3},$$
$$\hat{I}^{\alpha_1,\alpha_2,\alpha_3,\alpha_4}, \qquad \hat{I}^{\alpha_1,\alpha_2,\alpha_3,\alpha_4,\alpha_5}.$$

When an expression applies for both itinerant atoms and impurities, we use the notations $\hat{S}^{\alpha}$, $\hat{S}^{\alpha,\alpha''}$, $\hat{S}^{\alpha,\alpha',\alpha''}$ for the dipole, quadruple and octuple momentums. Here $\hat{S}$ denotes the operators $\hat{F}$ or $\hat{I}$.

B. Explicit expressions for 2^n-Pole Momenta

The magnetic dipole operator is collinear with the vector of its spin (more precisely its total angular momentum) operator. When a particle has spin S, the vector $\mathbf{S}$ of the spin matrices (generators of the $2S+1$-dimensional representation of the SU(2) group) are,

$$S^z_{s,s'} = s\ \delta_{s,s'}, \tag{2a}$$
$$S^+_{s,s'} = \mathcal{L}(S,s)\ \delta_{s,s'+1}, \tag{2b}$$
$$S^-_{s,s'} = \mathcal{L}(S,s')\ \delta_{s',s+1}, \tag{2c}$$

where s, s' are magnetic quantum numbers such that $|s| \le S$, and

$$\mathcal{L}(S,s) = \sqrt{(S+s)(S-s+1)}.$$

Next, the quadruple moment operators are represented by symmetric traceless matrices $S^{\alpha,\alpha'}$ ($\alpha, \alpha' = x, y, z$ are Cartesian indices) defined as,

$$\hat{S}^{\alpha,\alpha'} = \left\{\hat{S}^{\alpha},\ \hat{S}^{\alpha'}\right\} - \frac{2}{3}\ \hat{\mathbf{S}}^2\ \delta^{\alpha,\alpha'}, \tag{3}$$

where

$$\left\{\hat{S}^{\alpha},\ \hat{S}^{\alpha'}\right\} = \hat{S}^{\alpha}\hat{S}^{\alpha'} + \hat{S}^{\alpha'}\hat{S}^{\alpha}.$$

The quadruple operators satisfy the following equalities,

$$\hat{S}^{\alpha,\alpha'} = \hat{S}^{\alpha',\alpha}, \qquad \sum_{\alpha}\hat{S}^{\alpha,\alpha} = 0. \tag{4}$$

Continuing this analysis, the octuple moment operators are represented by matrices,

$$\hat{S}^{\alpha,\alpha',\alpha''} = \left\{\hat{S}^{\alpha},\ \hat{S}^{\alpha'},\ \hat{S}^{\alpha''}\right\} - \frac{1}{5}\left(3\ \hat{\mathbf{S}}^2 - 1\right)\times$$
$$\times \sum_{\alpha_1,\alpha_1',\alpha_1''} P^{\alpha,\alpha',\alpha''}_{\alpha_1,\alpha_1',\alpha_1''}\delta^{\alpha_1,\alpha_1'}\ \hat{S}^{\alpha_1''}. \tag{5}$$

Here the symbol $P^{\alpha,\alpha',\alpha''}_{\alpha_1,\alpha_1',\alpha_1''}$ denotes permutation of the indices α, α', α'',

$$P^{\alpha,\alpha',\alpha''}_{\alpha_1,\alpha_1',\alpha_1''} = \delta_{\alpha,\alpha_1}\ P^{\alpha',\alpha''}_{\alpha_1',\alpha_1''} + \delta_{\alpha,\alpha_1'}\ P^{\alpha',\alpha''}_{\alpha_1'',\alpha_1} +$$
$$+\delta_{\alpha,\alpha_1''}\ P^{\alpha',\alpha''}_{\alpha_1,\alpha_1'}, \tag{6}$$

the symbol $P^{\alpha,\alpha'}_{\alpha_1,\alpha_1'}$ denotes permutation of the indices α, α',

$$P^{\alpha,\alpha'}_{\alpha_1,\alpha_1'} = \delta_{\alpha,\alpha_1}\delta_{\alpha',\alpha_1'} + \delta_{\alpha,\alpha_1'}\delta_{\alpha',\alpha_1}. \tag{7}$$

The symbol $\{\hat{S}^{\alpha}, \hat{S}^{\alpha'}, \hat{S}^{\alpha''}\}$ is fully symmetric product of $\hat{S}^{\alpha}$, $\hat{S}^{\alpha'}$ and $\hat{S}^{\alpha''}$,

$$\left\{\hat{S}^{\alpha_1},\ \hat{S}^{\alpha_2},\ \hat{S}^{\alpha_3}\right\} = \sum_{\{\alpha'\}_3} P^{\alpha_1,\alpha_2,\alpha_3}_{\alpha_1',\alpha_2',\alpha_3'}\ \hat{S}^{\alpha_1'}\hat{S}^{\alpha_2'}\hat{S}^{\alpha_3'},$$

where $\{\alpha'\}_3 = \{\alpha_1', \alpha_2', \alpha_3'\}$. The octuple operators are symmetric with all the indices,

$$\hat{S}^{\alpha,\alpha',\alpha''} = \hat{S}^{\alpha',\alpha,\alpha''} = \hat{S}^{\alpha,\alpha'',\alpha'}.$$

Moreover, they are constructed in such a way that the trace over any two indices vanishes that is,

$$\sum_{\alpha'}\hat{S}^{\alpha,\alpha',\alpha'} = 0.$$

For the itinerant atoms with spin $I = \frac{5}{2}$, we also need to consider the 16-pole and 32-pole momentum operators. The 16-pole matrices are defined as,

$$I^{\alpha_1,\alpha_2,\alpha_3,\alpha_4} = \left\{\hat{I}^{\alpha_1},\ \hat{I}^{\alpha_2},\ \hat{I}^{\alpha_3},\ \hat{I}^{\alpha_4}\right\} -$$
$$- \frac{95}{28}\sum_{\{\alpha'\}_4} P^{\alpha_1,\alpha_2,\alpha_3,\alpha_4}_{\alpha_1',\alpha_2',\alpha_3',\alpha_4'}\ \delta_{\alpha_1',\alpha_2'}\ \hat{I}^{\alpha_3',\alpha_4'} +$$
$$+ \frac{707}{48}\sum_{\{\alpha'\}_4} P^{\alpha_1,\alpha_2,\alpha_3,\alpha_4}_{\alpha_1',\alpha_2',\alpha_3',\alpha_4'}\ \delta_{\alpha_1',\alpha_2'}\ \delta_{\alpha_3',\alpha_4'}, \tag{8}$$

where $\{\alpha'\}_4 = \{\alpha'_1, \alpha'_2, \alpha'_3, \alpha'_4\}$,

$$\left\{\hat{I}^{\alpha_1},\ \hat{I}^{\alpha_2},\ \hat{I}^{\alpha_3},\ \hat{I}^{\alpha_4}\right\} = \sum_{\{\alpha'\}_4} P^{\alpha_1,\alpha_2,\alpha_3,\alpha_4}_{\alpha'_1,\alpha'_2,\alpha'_3,\alpha'_4} \times \\ \times \hat{I}^{\alpha'_1}\hat{I}^{\alpha'_2}\hat{I}^{\alpha'_3}\hat{I}^{\alpha'_4}.$$

The symbol $P^{\alpha_1,\alpha_2,\alpha_3,\alpha_4}_{\alpha'_1,\alpha'_2,\alpha'_3,\alpha'_4}$ denotes permutation of the indices α_1, α_2, α_3, α_4,

$$P^{\alpha_1,\alpha_2,\alpha_3,\alpha_4}_{\alpha'_1,\alpha'_2,\alpha'_3,\alpha'_4} = \delta_{\alpha_1,\alpha'_1}\ P^{\alpha_2,\alpha_3,\alpha_4}_{\alpha'_2,\alpha'_3,\alpha'_4} + \delta_{\alpha_1,\alpha'_2}\ P^{\alpha_2,\alpha_3,\alpha_4}_{\alpha'_3,\alpha'_4,\alpha'_1} + \\ + \delta_{\alpha_1,\alpha'_3}\ P^{\alpha_1,\alpha_2,\alpha_4}_{\alpha'_4,\alpha'_1,\alpha'_2} + \delta_{\alpha_1,\alpha'_4}\ P^{\alpha_2,\alpha_3,\alpha_4}_{\alpha'_1,\alpha'_2,\alpha'_3}. \quad (9)$$

The 16-pole matrices are symmetric with respect all their indices. They constructed in such a way that the trace over any two indices vanishes namely,

$$\sum_{\alpha} I^{\alpha_1,\alpha_2,\alpha,\alpha'} = 0.$$

Finally, the 32-pole operators are represented by matrices,

$$I^{\alpha_1,\alpha_2,\alpha_3,\alpha_4,\alpha_5} = \left\{\hat{I}^{\alpha_1},\ \hat{I}^{\alpha_2},\ \hat{I}^{\alpha_3},\ \hat{I}^{\alpha_4},\ \hat{I}^{\alpha_5}\right\} - \\ - \frac{145}{108}\sum_{\{\alpha'\}_5} P^{\alpha_1,\alpha_2,\alpha_3,\alpha_4,\alpha_5}_{\alpha'_1,\alpha'_2,\alpha'_3,\alpha'_4,\alpha'_5}\ \delta_{\alpha'_1,\alpha'_2}\ \hat{I}^{\alpha'_3,\alpha'_4,\alpha'_5} - \\ - \frac{3271}{112}\sum_{\{\alpha'\}_5} P^{\alpha_1,\alpha_2,\alpha_3,\alpha_4,\alpha_5}_{\alpha'_1,\alpha'_2,\alpha'_3,\alpha'_4,\alpha'_5}\ \delta_{\alpha'_1,\alpha'_2}\ \delta_{\alpha'_3,\alpha'_4}\ \hat{I}^{\alpha'_5}. \quad (10)$$

Here $\{\alpha'\}_5 = \{\alpha'_1, \alpha'_2, \alpha'_3, \alpha'_4, \alpha'_5\}$, the symbol $P^{\{\alpha\}_5}_{\{\alpha'\}_5}$ denotes permutation of the indices α_1, α_2, α_3, α_4, α_5, whereas $\hat{I}^{\alpha}$ and $\hat{I}^{\alpha,\alpha',\alpha''}$ are dipole and octuple matrices already defined previously.

C. Casimir Operators

For each set of 2^n-pole operators there corresponds a Casimir operator. We will need these operators and write their expressions below for $n = 1, 2, 3$, and for both impurity atoms ($F = \frac{3}{2}$) and itinerant atoms ($I = \frac{5}{2}$). The general definitions of dipole, quadruple and octuple Casimir operators are,

$$\mathcal{S}_{\rm d} = \sum_{\alpha}\left(\hat{S}^{\alpha}\right)^2,$$
$$\mathcal{S}_{\rm q} = \sum_{\alpha,\alpha'}\left(\hat{S}^{\alpha,\alpha'}\right)^2,$$
$$\mathcal{S}_{\rm o} = \sum_{\alpha,\alpha',\alpha''}\left(\hat{S}^{\alpha,\alpha',\alpha''}\right)^2.$$

Explicit expressions for Casimir operators $\mathcal{S}_{\rm d,q,o} \equiv \mathcal{F}_{\rm d,q,o}$ and $\mathcal{S}_{\rm d,q,o} \equiv \mathcal{I}_{\rm d,q,o}$ for atoms with spin $F = \frac{3}{2}$ and $I = \frac{5}{2}$ respectively read,

$$\mathcal{F}_{\rm d} = \frac{15}{4}\ \hat{1}_4, \qquad \mathcal{F}_{\rm q} = 30\ \hat{1}_4, \qquad \mathcal{F}_{\rm o} = \frac{567}{2}\ \hat{1}_4, \quad (11)$$

where $\hat{1}_4$ is the 4×4 identity matrix.

$$\mathcal{I}_{\rm d} = \frac{35}{4}\ \hat{1}_6, \qquad \mathcal{I}_{\rm q} = \frac{560}{3}\ \hat{1}_6, \qquad \mathcal{I}_{\rm o} = 6804\ \hat{1}_6, \quad (12)$$

where $\hat{1}_6$ is the 6×6 identity matrix.

D. Exchange Interaction

When the distance between itinerant Yb(^{1}S$_0$) and impurity Yb*(^{3}P$_2$) atoms is of the same order as the atomic size R_0, there is an *indirect exchange interaction* between them[28]. Heuristically it is described in two steps [see Fig. 3 for illustration]: 1) A $6p$ electron tunnels from the excited Yb(^{3}P$_2$) atom to the ground state Yb(^{1}S$_0$) atom. As a result, we have two ions with parallel electronic orbital angular momenta. 2) Then, one electron from the $6s$ orbital tunnels from the negatively charged ion to the $6s$ orbital of the positively charged ion. The net outcome is that the atoms "exchange their identity" specified by their electronic quantum states: one atom transforms from the ground state to the excited state, whereas the other atom transforms from the excited state to the ground state. The detailed calculations of the pertinent exchange interaction is relegated to the Appendix I (see also Ref.[28]). They employ two-particle wave functions

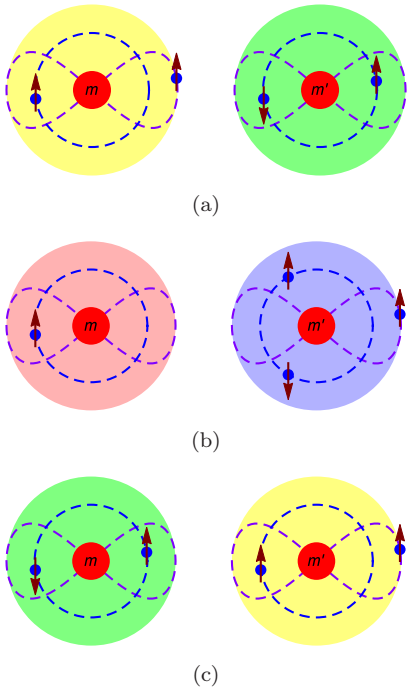


FIG. 3: (color line) Illustration of exchange interaction between ytterbium atoms. Panel (a): Initial quantum state - the first atom is in the meta-stable state (light yellow disk) and the second one is in the ground state (light green disk); panel (b): virtual state - the first atom is positively ionized (light red disk), and the second one is negatively charged (light blue disk); panel (c): final state - the first atom is in the ground state and the other one is in the meta-stable state. For all the panels, arrows denote the electronic spin, m or m' is nuclear spin of the first or second atom.

describing the motion of two atoms in the optical potential, taking into account the atom-atom interaction. For short distance between the atoms, (where the exchange interaction is essential), the two-atom wave function is determined mainly by the inter-atomic van der Waals potential[28]. The exchange interaction strength is given by,

$$\lambda_0 \;=\; \frac{\sqrt{2M\epsilon_F}}{\pi\hbar}\,\Gamma^2\!\left(\frac{3}{2}\right)\int\limits_{r_0}^{\infty} g(R)R^2dR. \qquad (13)$$

Here $r_0 = 3.6673$ Å is found from the condition $W(r_0) = 0$, where $W(R)$ is the van der Waals potential (F2) between an itinerant atom and the impurity. $a_{\rm g}$ is given by eq. (E8) in Appendix E. $g(R)$ is derived in Appendix I,

$$g(R) \;=\; \frac{t_{\rm s}(R)\;t_{\rm p}(R)}{3\;\Delta\epsilon}\;\mathfrak{R}(R). \qquad (14)$$

Here $t_{\rm s}$ and $t_{\rm p} = \frac{1}{3}(t_0 + 2t_1)$ are tunneling rates for the $6s$ and $6p$ electrons, see eqs. (H4) and (H7) in Appendix H. $\Delta\epsilon = \varepsilon_{\rm ion} + \varepsilon_{\rm ea} - \epsilon_{\rm x} = 4.1104$ eV is the energy which should be paid to get positively and negatively charged ions from two neutral atoms, where $\varepsilon_{\rm ion} = 6.2542$ eV is the ionization energy[34], $\varepsilon_{\rm ea} = 0.3$ eV is the electron affinity[35] and $\epsilon_{\rm x} = 2.4438$ eV is the excitation energy of the $^3{\rm P}_2$ state[34]. The function $\mathfrak{R}(R)$ [eq. (G4) in Appendix G] encodes the deformation of the wave function of the itinerant fermions at short distance from the impurity where the van der Waals interaction is significant[28],

$$\mathfrak{R}(R) \;=\; \frac{8c}{R^2K(R)}\left\{1+\left(\frac{a_w-\bar{a}}{\bar{a}}\right)^2\right\}.$$

Here $K(R) = \frac{1}{\hbar}\sqrt{-MW(R)}$, $a_w = 20.9973$ Å and $\bar{a} = 42.9984$ Å [see Appendices F and G for details].

Section III main points: In subsections III A, III B and III C we introduced multiple operators: A 2^n pole operator is an expression involving n spin operators, with appropriate coefficients. These operators, explicitly calculated in this section, are the building blocks of the exchange interaction of the multipolar Kondo Hamiltonian to be introduced in the next section. Finally, in subsection III D the basic mechanism for exchange interaction between two atoms ^{173}Yt(^{3}P$_2$)-^{173}Yt(^{1}S$_0$) is explained. It is similar but not identical with the exchange interaction between two atoms ^{173}Yt(^{3}P$_0$)-^{173}Yt(^{1}S$_0$) discussed in Ref.[28] because here, the total electronic spin of one of the atoms is not zero.

IV. THE KONDO HAMILTONIAN

We are now in a position to write down the Hamiltonian describing the scattering of itinerant ^{173}Yb(^{1}S$_0$) and localized ^{173}Yb(^{3}P$_2$) atoms. Recall that the itinerant atom is in the ground state with total atomic spin $I = \frac{5}{2}$ (which is the nuclear spin), and the trapped atom is in the long lived excited state with its total atomic spin being $F = \frac{3}{2}$. The latter serves as a localized impurity described by the Hubbard operators $X^{f=F_z,f'=F'_z}$,

$$X^{f,f'} \;=\; \big|F,f\big\rangle\big\langle F,f'\big|,$$

where $|F,f\rangle$ is the wave function of the localized impurity with total spin F and magnetic quantum number f. The itinerant atoms form Fermi gas. They are described by the annihilation and creation operators $c_{\mathbf{k},i}$ and $c^\dagger_{\mathbf{k},i}$, where i is the (nuclear) magnetic quantum number and $\mathbf{k}$ is the wave vector of itinerant atom. The interaction between the atoms, consisting of potential scattering and exchange terms, reads,

$$H_K \;=\; \frac{\lambda_0}{a_{\rm g}^2}\sum_j\sum_{f,f'}\sum_{i,i'}\sum_{\mathbf{k},\mathbf{k}'} C^{F,f}_{J,j;I,i}C^{F,f'}_{J,j;I,i'}\times \\ \times X^{f,f'}\;c^\dagger_{\mathbf{k}',i'}c_{\mathbf{k},i}, \qquad (15)$$

were $C^{F,f}_{J,j;I,i}$ are the Clebsch-Gordan coefficients, $a_{\rm g}$ is given by eq. (E8). The integer j is an electronic magnetic quantum number of the Yb atom in the ^{3}P$_2$ state, $|j| \le J$, where $J = 2$ is the total electronic angular momentum. The coupling λ_0 is given by eq. (13).

The Hamiltonian (15) conserves the z component of the total angular momentum that is,

$$i + f' \;=\; i' + f.$$

The selection rules for the Hamiltonian (15) are,

$$\Delta f \;=\; f - f' = 0,\;\; \pm 1,\;\; \pm 2,\;\; \pm 3. \qquad (16)$$

We shall now rewrite this *same Hamiltonian* as a sum of terms representing potential, dipole, quadruple and octuple interactions,

$$H_K \;=\; H_{\rm p} + H_{\rm d} + H_{\rm q} + H_{\rm o}. \qquad (17)$$

The precise expressions for these multipolar components are given in the next subsection. As will be evident from the discussion below, this form of the Hamiltonian is more complicated than its initial form (15). The reason for using the equivalent form (17) is that the form (15) of the Hamiltonian *changes under poor-man's scaling procedure*, and that violates the spirit of the RG formalism. We need to express the Hamiltonian in such a way that its structure is unchanged under the poor-man's scaling procedure, albeit the coupling constants renormalize. As we shall show below, this is indeed the case once we use the form (17).

A. Bare exchange coefficients and structure of multiple terms

The four terms in the decomposition (17) involve four exchange coefficients $\lambda_{p,d,q,o}$, each one being proportional

to λ_0. The proportionality constants are just simple geometric factors to be written down below. Before that, let us specify the structure of the four parts of H_K.

The first term on the right hand side of eq. (17), $H_{\rm p}$, is potential scattering,

$$H_{\rm p} = \frac{\lambda_{\rm p}}{a_{\rm g}^2} \sum_f \sum_i \sum_{\mathbf{k},\mathbf{k}'} X^{f,f}\ c^\dagger_{\mathbf{k}',i} c_{\mathbf{k},i}. \tag{18}$$

The second term on the right hand side of eq. (17), $H_{\rm d}$, is dipole interaction,

$$H_{\rm d} = \frac{\lambda_{\rm d}}{a_{\rm g}^2} \sum_\alpha \sum_{f,f'} \sum_{i,i'} \sum_{\mathbf{k},\mathbf{k}'} F^\alpha_{f,f'} I^\alpha_{i',i}\ X^{f,f'}\ c^\dagger_{\mathbf{k}',i'} c_{\mathbf{k},i}, \tag{19}$$

where $\hat{\mathbf{F}} = (\hat{F}^x, \hat{F}^y, \hat{F}^z)$ and $\hat{\mathbf{I}} = (\hat{I}^x, \hat{I}^y, \hat{I}^z)$ are vectors of the spin-F and spin-I matrices and $\lambda_{\rm d}$ is a coupling constant of the dipole interaction. The third term on the right hand side of eq. (17), $H_{\rm q}$, is quadruple interaction,

$$\begin{aligned} H_{\rm q} \ &= \ \frac{\lambda_{\rm q}}{a_{\rm g}^2} \sum_{\alpha,\alpha'} \sum_{f,f'} \sum_{i,i'} \sum_{\mathbf{k},\mathbf{k}'} F^{\alpha,\alpha'}_{f,f'} I^{\alpha',\alpha}_{i',i} \times \\ &\times X^{f,f'}\ c^\dagger_{\mathbf{k}',i'} c_{\mathbf{k},i}, \end{aligned} \tag{20}$$

where $\hat{F}^{\alpha,\alpha'}$ or $\hat{I}^{\alpha,\alpha'}$ are the quadruple matrices of the particle with spin F or I, $\lambda_{\rm q}$ is a coupling of the quadruple interaction. Finally, the fourth term on the right hand side of eq. (17), $H_{\rm o}$, is octuple interaction,

$$\begin{aligned} H_{\rm o} \ &= \ \frac{\lambda_{\rm o}}{a_{\rm g}^2} \sum_{\alpha,\alpha',\alpha''} \sum_{f,f'} \sum_{i,i'} \sum_{\mathbf{k},\mathbf{k}'} F^{\alpha,\alpha',\alpha''}_{f,f'} I^{\alpha'',\alpha',\alpha}_{i',i} \times \\ &\times X^{f,f'}\ c^\dagger_{\mathbf{k}',i'} c_{\mathbf{k},i}, \end{aligned} \tag{21}$$

where $\hat{F}^{\alpha,\alpha',\alpha''}$ or $\hat{I}^{\alpha,\alpha',\alpha''}$ are the matrices of the octuple momentum of the particle with spin F or I, $\lambda_{\rm o}$ is a coupling of the octuple interaction.

On the bare level (before starting the poor-man's scaling procedure), there is a single coupling constant λ_0. Therefore, all the four coefficients $\lambda_{\rm p}$, $\lambda_{\rm d}$, $\lambda_{\rm q}$ and $\lambda_{\rm o}$ are simply related to λ_0. Straightforward analysis shows that the Hamiltonians (15) and (17) are identical provided,

$$\begin{aligned} \lambda_{\rm p} &= \frac{\lambda_0}{6}, \qquad & \lambda_{\rm d} &= \frac{26\lambda_0}{525}, \\ \lambda_{\rm q} &= -\frac{\lambda_0}{840}, \qquad & \lambda_{\rm o} &= -\frac{\lambda_0}{1890}. \end{aligned} \tag{22}$$

Note that on deriving the exchange Hamiltonian (15), we neglect the spin-orbit and hyperfine interactions. It can be shown that taking into account the spin-orbit and hyperfine interactions modify the Hamiltonian (15), but leave the Hamiltonian (17), [as well as the dipole, quadruple and octuple interactions (19), (20) and (21)] unchanged, except for slight modifications of the couplings $\lambda_{\rm d}$, $\lambda_{\rm q}$ and $\lambda_{\rm o}$. Indeed, as it is shown in Appendix M, the Hamiltonian (17) obeys spin-rotation SU(2) symmetry. The spin-orbit and hyperfine interactions satisfy the same SU(2) symmetry[39]. As a result, the spin-orbit and hyperfine interactions cannot change the Hamiltonian (17).

B. The total Hamiltonian

Having established the explicit expression for the Kondo Hamiltonian, we can now write down the total Hamiltonian of the system by adding the kinetic energy of the itinerant atoms and the atomic energy of the impurity atom. Thus,

$$H \ = \ H_0 + H_K, \qquad H_0 \ = \ H_{\rm c} + H_{\rm imp}, \tag{23}$$

where $H_{\rm c}$ is the Hamiltonian of the itinerant atoms without impurity and $H_{\rm i}$ is the Hamiltonian of the isolated impurity,

$$H_{\rm c} \ = \ \sum_{i,\mathbf{k}} \epsilon_{\mathbf{k}} c^\dagger_{\mathbf{k},i} c_{\mathbf{k},i}, \tag{24}$$

$$H_{\rm imp} \ = \ \varepsilon_{\rm imp} \sum_f X^{f,f}. \tag{25}$$

The Kondo Hamiltonian H_K is given by eq. (17).

Section IV main points: The simple form (15) of the exchange Hamiltonian involves a single bare coupling constant λ_0, but in this form, it does not keep its structure under the RG transformation (introduced in the next section). It is then necessary to decompose the bare Hamiltonian (15) into a sum of terms with *different multi-polarities*, $H_{\rm d}$, $H_{\rm q}$, $H_{\rm o}$ as was carried out above. The prefactors relating the bare coefficients $\lambda_{\rm d}$, $\lambda_{\rm q}$, $\lambda_{\rm o}$ to λ_0 are explicitly calculated above. However, as will be shown in the next section, $\lambda_{\rm d}$, $\lambda_{\rm q}$, $\lambda_{\rm o}$ are renormalized *differently*.

V. SECOND ORDER POOR MAN'S SCALING

We now apply the poor man's scaling RG procedure in term of which we first determine the Kondo temperature and (later on) derive scaling equations for the exchange coefficients and identify the fixed points. As far as dipolar interaction is concerned, this procedure is quite standard, but some technical modifications are required for treating multipolar exchange interactions. We start, as usual, by dividing the "conduction" band of (neutral) itinerant atoms defined by $\{\epsilon\}$, such that $|\epsilon - \epsilon_F| < D$ (where ϵ_F is the Fermi energy) into three parts. The first part contains energies of particle and hole states within a reduced conduction band $|\epsilon - \epsilon_F| < D'$ ($D' = D - \delta D$) which are retained and the second and third parts contains energies of particle and hole states within narrow intervals $D' < |\epsilon - \epsilon_F| < D$ which, within the RG procedure are to be integrated out[4].

Second order corrections to the Kondo Hamiltonian are schematically illustrated in Fig. 4. Here the solid blue line describes the quantum state of the localized impurity. The dashed purple curve restricted from one side by the red dot describes itinerant atom (before or after scattering) whose energy is close to the Fermi energy. The dashed green curves restricted by red dots from both

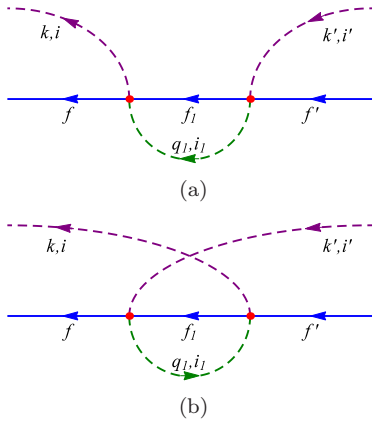


FIG. 4: (color online) "Particle" [panel (a)] and "hole" [panel (b)] second order diagrams for the Kondo Hamiltonian (15). The solid lines correspond to the localized impurity atom, the purple dashed curves describes itinerant atoms before or after the scattering, and the green dashed curves describe itinerant atom in the virtual state near the top edge [panel (a)] or bottom edge [panel (b)] of the conduction band.

sides describe itinerant atom in the virtual state with the energy within the interval $D' < \epsilon - \epsilon_F < D$ (as in Fig. 4(a)) or $-D < \epsilon - \epsilon_F < -D'$ (as in Fig. 4(b)). The red dots denote the Kondo Hamiltonian (17). Since H_K has three terms, the second order corrections to H_K can be written as,

$$\delta H_2 \;=\; \sum_{\beta,\beta'} \delta H^{(2)}_{\beta,\beta'}. \tag{26}$$

Here $\beta, \beta' = \mathrm{d}, \mathrm{q}, \mathrm{o}$ for dipole, quadruple and octuple interaction,

$$\delta H^{(2)}_{\beta,\beta'} \;=\; \frac{1}{2}\sum_{\mathrm{e},\mathrm{e}'} H_\beta \Big|\mathrm{e}\Big\rangle \Big\langle \mathrm{e}\Big|\frac{1}{\epsilon_0 - H_0}\Big|\mathrm{e}'\Big\rangle \Big\langle \mathrm{e}'\Big| H_{\beta'} + \\ + \;\frac{1}{2}\sum_{\mathrm{e},\mathrm{e}'} H_{\beta'} \Big|\mathrm{e}\Big\rangle \Big\langle \mathrm{e}\Big|\frac{1}{\epsilon_0 - H_0}\Big|\mathrm{e}'\Big\rangle \Big\langle \mathrm{e}'\Big| H_{\beta}, \tag{27}$$

where $|\mathrm{e}\rangle$ and $|\mathrm{e}'\rangle$ are quantum states with a hole near the Fermi energy and an atom with energy in the interval $D' < \epsilon < D$, or a hole on an energy level in the interval $-D < \epsilon < -D'$ and an additional atom near the Fermi level. H_0 is the Hamiltonian of itinerant atoms without impurity. For $\delta D \ll D$, we can use the approximation,

$$\Big\langle \mathrm{e}\Big|\frac{1}{\epsilon_0 - H_0}\Big|\mathrm{e}'\Big\rangle \;\approx\; -\frac{1}{D}\,\delta_{\mathrm{e},\mathrm{e}'}.$$

Explicit expressions for the operators $\delta H^{(2)}_{\beta,\beta'}$ are derived in Appendix J. Combining all the differentials $\delta H^{(2)}_{\beta,\beta'}$, we see that integrating out the virtual states near the band edges to lowest order results in a new Hamiltonian of the *same form* as eq. (17) but with renormalized coupling constants $\lambda_\beta(D) \to \lambda_\beta(D') = \lambda_\beta(D) + \delta\lambda_\beta$, where $\beta = \mathrm{d}, \mathrm{q}, \mathrm{o}$. Consequently, we arrive at the following second order poor man's scaling equations for the dimensionless couplings $\Lambda_\beta = \lambda_\beta \rho_0$,

$$\frac{\partial \Lambda_\mathrm{d}}{\partial \ln D} \;=\; -\Lambda_\mathrm{d}^2 - \frac{9216}{25}\,\Lambda_\mathrm{q}^2 - \frac{1469664}{25}\,\Lambda_\mathrm{o}^2, \tag{28a}$$

$$\frac{\partial \Lambda_\mathrm{q}}{\partial \ln D} \;=\; -12\Lambda_\mathrm{d}\Lambda_\mathrm{q} - \frac{1458}{5}\,\Lambda_\mathrm{q}\Lambda_\mathrm{o}, \tag{28b}$$

$$\frac{\partial \Lambda_\mathrm{o}}{\partial \ln D} \;=\; -18\Lambda_\mathrm{d}\Lambda_\mathrm{o} - \frac{64}{9}\,\Lambda_\mathrm{q}^2 + \frac{306}{5}\,\Lambda_\mathrm{o}^2. \tag{28c}$$

Here ρ_0 is the density of states of itinerant atoms at the Fermi energy ϵ_F,

$$\rho_0 \;=\; \frac{1}{2\hbar\omega_\mathrm{g} a_\mathrm{g}^2}, \tag{29}$$

where a_g and ω_g are given by eq. (E8). Note that in the "continuous" limit $\omega_\mathrm{g} \to 0$ and $a_\mathrm{g} \to \infty$, the DOS (29) reduces to

$$\rho_0 \;=\; \frac{M}{4\hbar^2}.$$

The initial values $\Lambda^{(0)}_\beta = \Lambda_\beta(D_0)$ of the couplings Λ_β (where $\beta = \mathrm{d}, \mathrm{q}, \mathrm{o}$) are,

$$\Lambda^{(0)}_\mathrm{d} \;=\; \frac{26}{525}\,\lambda_0\rho_0, \tag{30a}$$

$$\Lambda^{(0)}_\mathrm{q} \;=\; -\frac{\lambda_0\rho_0}{840}, \tag{30b}$$

$$\Lambda^{(0)}_\mathrm{o} \;=\; -\frac{\lambda_0\rho_0}{1890}. \tag{30c}$$

Note that when the initial values of Λ_q and Λ_o are zero, the right hand sides of eqs. (28b) and (28c) vanish and the set of equations (28) reduces to the standard scaling equation for the s-d Kondo model[4],

$$\frac{\partial \Lambda_\mathrm{d}}{\partial \ln D} \;=\; -\Lambda_\mathrm{d}^2. \tag{31}$$

In the next section we elucidate the effect of the quadruple and octuple interactions on the scaling invariant of the RG equations, that is, the Kondo temperature[4] and show that it is rather significant.

It should be noted that the scaling procedure is carried out until the effective bandwidth D essentially exceeds $\hbar\omega_\mathrm{g}$ and T_K [where T_K is the Kondo temperature defined below]. In what follows, we assume that $\hbar\omega_\mathrm{g} < T_K$, and therefore the Kondo temperature is the infrared cutoff parameter of our theory.

Section V main points: In this section we derived the poor-man scaling equations to second-order in the exchange constant. This procedure is quite standard, and yet, there are important differences between the procedure applied here and that employed in the standard Kondo effect. First, as we see from Eqs. (28), there are three coupling constants that satisfy a set of three coupled non-linear scaling equations, and second, within the underlying representation of $SU(2)$ the number of spin projections $2s + 1 > 2$.

VI. KONDO TEMPERATURE

The Kondo temperature is defined as the value of D for which the running coupling constants $\Lambda_\beta(D)$ diverge ($\beta = \mathrm{d}, \mathrm{q}, \mathrm{o}$). We solve the set of equations (28) numerically for different initial values $\Lambda_\beta^{(0)}$. Using eq. (30), we can express $\Lambda_\mathrm{q}^{(0)}$ and $\Lambda_\mathrm{o}^{(0)}$ in terms of $\Lambda_\mathrm{d}^{(0)}$. Then the Kondo temperature is a function of a single parameter, $\Lambda_\mathrm{d}^{(0)}$. The results of these numerical calculations for the Kondo temperature are displayed in Fig. 5, (solid curve). T_K can be approximated by the following expression,

$$T_K \;=\; D_0 \,\exp\left(-\frac{1}{A\Lambda_\mathrm{d}^{(0)}}\right), \quad A \;=\; 13.9561. \qquad (32)$$

The approximation (32) for T_K is displayed in Fig. 5, (dashed curve). It is clearly seen that the dashed and solid curves are close to each other, so that the approximation (32) is satisfactory.

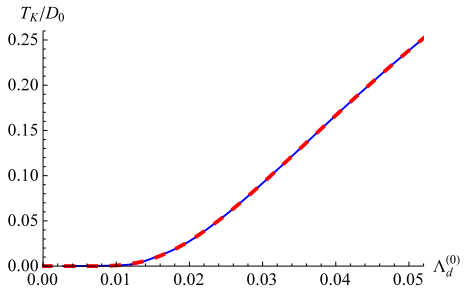


FIG. 5: (color online) Kondo temperature calculated numerically from the set of equations (28) [solid blue curve] and the approximation (32) [dashed red curve].

Note that the scaling equation (31) yields the following expressions for the Kondo temperature,

$$T_K^{(\mathrm{d})} \;=\; D_0 \exp\left(-\frac{1}{\Lambda_\mathrm{d}^{(0)}}\right). \qquad (33)$$

The factor $A \gg 1$ in eq. (32) indicates that the quadruple and octuple interactions are important and act to enhance T_K.

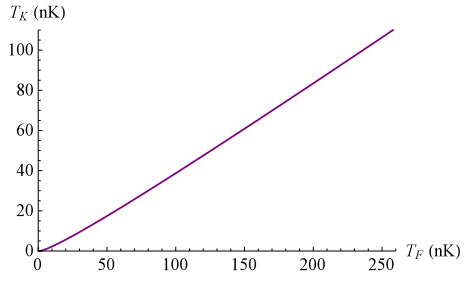


FIG. 6: (color online) Kondo temperature as a function of T_F for $D_0 = 0.5T_F$.

Taking into account eq. (13), we can express the Kondo temperature (32) as a function of the Fermi temperature T_F. The result is shown in Fig. 6. It is seen that T_K varies within the interval 40 nK$< T_K <$ 100 nK for 100 nK$< T_F <$ 250 nK.

VII. THIRD ORDER POOR MAN'S SCALING

Identification of NFL fixed points requires the solution of the poor-man's scaling equation at least up to third order. This task is carried out in the present section. In order to derive the third order correction to the poor-man's scaling equations (28), we need to consider the second order correction to the energy of the system, as encoded in the self energy diagrams shown in Fig. 7, as well as the third order vertex diagrams shown in Fig. 8 (see Ref.[4]). These diagrams are considered below each one in its turn.

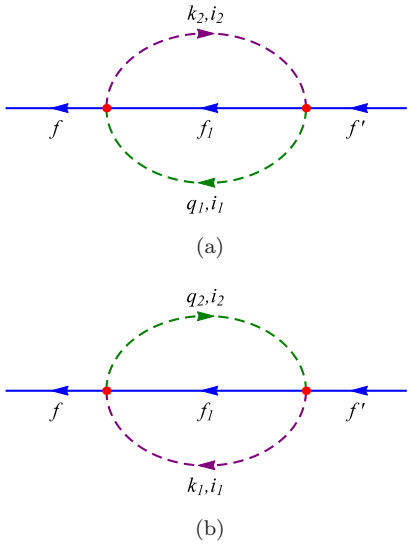


FIG. 7: (color online) "Particle" [panel (a)] and "hole" [panel (b)] second order self energy diagrams. The solid lines correspond to the localized impurity atom, the purple dashed curves restricted by the vertex from one side describe itinerant atoms before or after the scattering, the purple dashed curves restricted by vertex from both sides describe itinerant atoms in the virtual state in the reduced energy band and the green dashed curves describe itinerant atom in the virtual state near the top edge [panel (a)] or bottom edge [panel (b)] of the conduction band.

A. Second Order Self Energy Diagrams

Second order correction to the energy is illustrated by diagrams in Fig. 7.

The second order corrections to the self energy are calculated in Appendix K. Taking into account eqs. (K5), (K8) and (K10), we get

$$\delta E \;=\; -\frac{\delta D}{D}\, E \left\{ \frac{525}{4}\, \lambda_\mathrm{d}^2\rho_0^2 + 13440\, \lambda_\mathrm{q}^2\rho_0^2 + \right.$$
$$\left. + \,3306744\, \lambda_\mathrm{o}^2\rho_0^2 \right\}. \qquad (34)$$

B. Third Order Vertex Diagrams

Now we consider in details the third order contributions to the scaling equations given by diagrams in Fig. 8. The corresponding correction to the Kondo Hamiltonian is decomposed as,

$$\delta H_3 \;=\; \sum_{\beta,\beta'} \delta H^{(3)}_{\beta',\beta,\beta'}, \tag{35}$$

where $\beta, \beta' = \mathrm{d}, \mathrm{q}, \mathrm{o}$ for the dipole, quadruple and octuple interactions,

$$\begin{aligned}\delta H^{(3)}_{\beta',\beta,\beta'} \;=\; & \frac{\lambda_\beta \lambda^2_{\beta'}}{D^2} \sum_{\vec\alpha_\beta,\vec\alpha_{\beta'},\vec\alpha'_{\beta'}} \sum_{f,f'} \left(\hat F^{\vec\alpha_{\beta'}} \hat F^{\vec\alpha_\beta} \hat F^{\vec\alpha'_{\beta'}}\right)_{f,f'} \times \\ & \times X^{f,f'} \sum_{i,i'} \sum_{\mathbf{k},\mathbf{k}'} I^{\vec\alpha_\beta}_{i,i'}\; c^\dagger_{\mathbf{k},i} c_{\mathbf{k}',i'} \times \\ & \times \mathrm{Tr}\left(\hat I^{\vec\alpha_{\beta'}} \hat I^{\vec\alpha'_{\beta'}}\right)\, \mathfrak{G}. \end{aligned} \tag{36}$$

Here $\hat F^{\vec\alpha_\beta}$ or $\hat I^{\vec\alpha_\beta}$ are dipole ($\beta = \mathrm{d}$), quadruple ($\beta = \mathrm{q}$) and octuple ($\beta = \mathrm{o}$) matrices for a localized impurity or itinerant atoms, $\vec\alpha_\mathrm{d} \equiv \alpha$, $\vec\alpha_\mathrm{q} \equiv (\alpha, \alpha')$ and $\vec\alpha_\mathrm{o} \equiv (\alpha, \alpha', \alpha'')$, where α's are Cartesian indices [see eqs. (2), (3) and (5)]. The quantity $\mathfrak{G}$ is

$$\mathfrak{G} \;=\; 2\rho_0^2\; D\; \delta D. \tag{37}$$

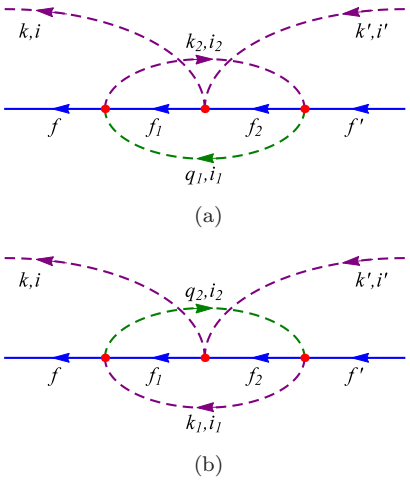


FIG. 8: (color online) "Particle" [panel (a)] and "hole" [panel (b)] third order diagrams for the Kondo Hamiltonian (15). The solid lines correspond to the localized impurity atom, the purple dashed curves restricted by the vertex from one side describe itinerant atoms before or after the scattering, the purple dashed curves restricted by vertex from both sides describe itinerant atoms in the virtual state in the reduced energy band and the green dashed curves describe itinerant atom in the virtual state near the top edge [panel (a)] or bottom edge [panel (b)] of the conduction band.

Explicit expressions for the operators $\delta H^{(3)}_{\beta',\beta,\beta'}$ are derived in Appendix L. It is shown there that $H_K + \delta H_2 + \delta H_3$ has the *same form* as H_K, albeit with proper corrections to the coupling constants $\lambda_\beta + \delta\lambda_\beta$. Therefore we conclude that inclusion of δH_3 does not change the structure of the initial Kondo Hamiltonian, but it gives rise to an additional renormalization of the couplings λ_β.

C. Third Order Poor Man's Scaling Equations

The effective Hamiltonian (which includes energy and vertex renormalization) depends on the energy E[4] which is determined through the Schrödinger equation

$$H\Psi \;=\; E\Psi,$$

and this dependence is given by[4]

$$\tilde H_\mathrm{eff}(E) \;=\; \tilde H_\mathrm{eff}(0) - ES,$$

where the parameter $S = \delta E/E$ does not depend on E, see eq. (34), and

$$\tilde H_\mathrm{eff}(0) \;=\; H_K + \delta H_2 + \delta H_3, \tag{38}$$

δH_2 and δH_3 are given by eqs. (26) and (35). In order to get an effective Hamiltonian, we solve the (implicit) secular equation,

$$\left|\tilde H_\mathrm{eff}(E) - E\right| \;=\; 0,$$

(where $|A|$ denotes the determinant of the square matrix A) which leads to

$$\left|\tilde H_\mathrm{eff}(0) - (1+S)E\right| \;=\; 0.$$

This equation gives an E-independent Hamiltonian,

$$H_\mathrm{eff} \;=\; \left(1+S\right)^{-1/2} \tilde H_\mathrm{eff}(0)\, \left(1+S\right)^{-1/2}.$$

Taking into account that $S \sim \lambda^2$ [see eq. (34)] and keeping the terms up to λ^3, we can write H_eff as,

$$H_\mathrm{eff} \;=\; H_K + \delta H_2 + \delta\tilde H_3, \tag{39}$$

where

$$\delta\tilde H_3 \;=\; \delta H_3 + S H_K. \tag{40}$$

Taking into account the results of subsections VII A and VII B, we can see that the operator $\delta\tilde H_3$ has the same form as the Hamiltonian H_K, (see eq. (17) and the equations below it). Therefore, it gives rise to renormalization of the couplings constants λ_β. The third order poor-man scaling equations for the dimensionless couplings $\Lambda_\beta = \lambda_\beta \rho_0$ are,

$$\frac{\partial \Lambda_\beta}{\partial \ln D} \;=\; \mathfrak{F}_\beta\left(\Lambda_\mathrm{d},\; \Lambda_\mathrm{q},\; \Lambda_\mathrm{o}\right), \tag{41}$$

where $\beta = \mathrm{d}, \mathrm{q}, \mathrm{o}$, the functions $\mathfrak{F}_{\mathrm{d,q,o}}$ are,

$$\begin{aligned}
\mathfrak{F}_{\mathrm{d}} &= -\Lambda_{\mathrm{d}}^2 - \frac{9216}{25}\,\Lambda_{\mathrm{q}}^2 - \frac{1469664}{25}\,\Lambda_{\mathrm{o}}^2 + 35\,\Lambda_{\mathrm{d}}^3 + \\
&\quad +12096\,\Lambda_{\mathrm{d}}\Lambda_{\mathrm{q}}^2 + \frac{21493836}{5}\,\Lambda_{\mathrm{d}}\Lambda_{\mathrm{o}}^2, \qquad (42a)\\
\mathfrak{F}_{\mathrm{q}} &= -12\Lambda_{\mathrm{d}}\Lambda_{\mathrm{q}} - \frac{1458}{5}\,\Lambda_{\mathrm{q}}\Lambda_{\mathrm{o}} + \frac{945}{8}\,\Lambda_{\mathrm{q}}\Lambda_{\mathrm{d}}^2 + \\
&\quad +17472\,\Lambda_{\mathrm{q}}^3 + \frac{15380348}{5}\,\Lambda_{\mathrm{q}}\Lambda_{\mathrm{o}}^2, \qquad (42b)\\
\mathfrak{F}_{\mathrm{o}} &= -18\Lambda_{\mathrm{d}}\Lambda_{\mathrm{o}} - \frac{64}{9}\,\Lambda_{\mathrm{q}}^2 + \frac{306}{5}\,\Lambda_{\mathrm{o}}^2 + \frac{1365}{8}\,\Lambda_{\mathrm{o}}\Lambda_{\mathrm{d}}^2 + \\
&\quad +12096\,\Lambda_{\mathrm{o}}\Lambda_{\mathrm{q}}^2 + \frac{16769916}{5}\,\Lambda_{\mathrm{o}}^3. \qquad (42c)
\end{aligned}$$

The symmetry of the scaling equations (41) should be noted: $\mathfrak{F}_{\mathrm{d}}$ and $\mathfrak{F}_{\mathrm{o}}$ are even with respect to the inversion transformation $\Lambda_{\mathrm{q}} \to -\Lambda_{\mathrm{q}}$, whereas $\mathfrak{F}_{\mathrm{q}}$ is odd. Therefore we can safely conclude that the scaling equations (41) are invariant with respect to the inversion $\Lambda_{\mathrm{q}} \to -\Lambda_{\mathrm{q}}$. The fixed points of the scaling equations (41) are found from the conditions, $\mathfrak{F}_{\mathrm{d,q,o}} = 0$. Numerical solution of the last set of equations yields seven fixed points in 3D parameter space, $P_n = (\Lambda_{\mathrm{d}}^{(n)}, \Lambda_{\mathrm{q}}^{(n)}, \Lambda_{\mathrm{o}}^{(n)})$, $n = 1, 2, \ldots 7$:

$$\begin{aligned}
P_1&=\big(0.0285714, 0, 0\big), \qquad (43a)\\
P_2&=\big(0.0193713, \text{-}0.00192056, \text{-}0.000158648\big), \qquad (43b)\\
P_3&=\big(0.0193713, 0.00192056, \text{-}0.000158648\big), \qquad (43c)\\
P_4&=\big(0.0147126, \text{-}0.00101842, 0.00026056\big), \qquad (43d)\\
P_5&=\big(0.0140075, 0, \text{-}0.000264616\big), \qquad (43e)\\
P_6&=\big(0.0140587, 0, 0.000246764\big), \qquad (43f)\\
P_7&=\big(0.0147126, 0.00101842, 0.00026056\big). \qquad (43g)
\end{aligned}$$

There is one more fixed point, $P_0 = (0, 0, 0)$, but it is unstable, see scaling equations (28).

The scaling pattern of the parameters Λ_β ($\beta = \mathrm{d}, \mathrm{q}, \mathrm{o}$) depends on the initial values of the parameters. The initial values of Λ_β are given by eq. (30) [see also eq. (22)]. They consist of the dimensionless parameter $\lambda_0\rho_0$ which is calculated from a microscopic model of interaction of a Yb atom in the $^1\mathrm{S}_0$ state with an Yb atom in the $^3\mathrm{P}_2$ state, see eq. (13). It is seen that Λ_{d} is positive, whereas Λ_{q} and Λ_{o} are negative.

To proceed further, it is necessary to study the scaling of Λ_{d}, Λ_{q} and Λ_{o} near the fixed points $P_n = (\Lambda_{\mathrm{d}}^{(n)}, \Lambda_{\mathrm{q}}^{(n)}, \Lambda_{\mathrm{o}}^{(n)})$. For this purpose we introduce the variables x_{d}, x_{q} and x_{o},

$$\begin{aligned}
\Lambda_{\mathrm{d}} &= \Lambda_{\mathrm{d}}^{(n)} + x_{\mathrm{d}},\\
\Lambda_{\mathrm{q}} &= \Lambda_{\mathrm{q}}^{(n)} + x_{\mathrm{q}},\\
\Lambda_{\mathrm{o}} &= \Lambda_{\mathrm{o}}^{(n)} + x_{\mathrm{o}},
\end{aligned}$$

and assume that x_β [$\beta = \mathrm{d}, \mathrm{q}, \mathrm{o}$] are small. Expanding the functions $\mathfrak{F}_\beta$, eq. (42), in x_β to first (linear) order we get,

$$\mathfrak{F}_\beta\big(\Lambda_{\mathrm{d}},\ \Lambda_{\mathrm{q}},\ \Lambda_{\mathrm{o}}\big) = \sum_{\beta'=\mathrm{d,q,o}} A_{\beta,\beta'}\ x_{\beta'} + O\big(x^2\big),$$

where

$$A_{\beta,\beta'} = \left(\frac{\partial \mathfrak{F}_\beta}{\partial \Lambda_{\beta'}}\right)_{P_n},$$

the derivative is taken at the fixed point P_n. Thereby we get a set of linear differential equations for x_β,

$$\begin{aligned}
\frac{\partial x_{\mathrm{d}}}{\partial \ln D} &= A_{\mathrm{d,d}}\ x_{\mathrm{d}} + A_{\mathrm{d,q}}\ x_{\mathrm{q}} + A_{\mathrm{d,o}}\ x_{\mathrm{o}}, \qquad (44a)\\
\frac{\partial x_{\mathrm{q}}}{\partial \ln D} &= A_{\mathrm{q,d}}\ x_{\mathrm{d}} + A_{\mathrm{q,q}}\ x_{\mathrm{q}} + A_{\mathrm{q,o}}\ x_{\mathrm{o}}, \qquad (44b)\\
\frac{\partial x_{\mathrm{o}}}{\partial \ln D} &= A_{\mathrm{o,d}}\ x_{\mathrm{d}} + A_{\mathrm{o,q}}\ x_{\mathrm{q}} + A_{\mathrm{o,o}}\ x_{\mathrm{o}}. \qquad (44c)
\end{aligned}$$

The solution of the set of equations (44) is of the form,

$$x_\beta \ \propto\ D^\gamma,$$

where the Lyapunov exponent γ is an eigenvalue of the set of equations (44). The set of three linear equations has, as a rule, three eigenvalues. A fixed point P_n is stable when all x_β tend to zero as D tends to zero. This occurs when all γ's are positive. Accordingly, we now write down the numerical values of the triples $(\gamma_1, \gamma_2, \gamma_3)$ for each one of the fixed points P_1 – P_7 in its turn and determine its stability (s=stable, u=unstable).

$$\begin{aligned}
&P_1 : (\gamma_1, \gamma_2, \gamma_3)=(0.0285714, \text{-}0.246429, \text{-}0.375) \ \Rightarrow\ \text{u.}\\
&P_2 : (\gamma_1, \gamma_2, \gamma_3)=(0.341287, \text{-}0.228946, 0.163813) \ \Rightarrow\ \text{u.}\\
&P_3 : (\gamma_1, \gamma_2, \gamma_3)=(0.341287, \text{-}0.228946, 0.163813) \ \Rightarrow\ \text{u.}\\
&P_4 : (\gamma_1, \gamma_2, \gamma_3)=(0.44974, 0.320668, 0.0632014) \ \Rightarrow\ \text{s.}\\
&P_5 : (\gamma_1, \gamma_2, \gamma_3)=(0.434777, 0.14764, 0.14764) \ \Rightarrow\ \text{s.}\\
&P_6 : (\gamma_1, \gamma_2, \gamma_3)=(0.40609, 0.271873, \text{-}0.0300051) \ \Rightarrow\ \text{u.}\\
&P_7 : (\gamma_1, \gamma_2, \gamma_3)=(0.44974, 0.320668, 0.0632014) \ \Rightarrow\ \text{s.}
\end{aligned}$$

Note that P_1 is the NB fixed point, that in this case is unstable. Accordingly, only P_4, P_5 and P_7 are stable. Elucidation of these three stable fixed points such that the corresponding fixed point Hamiltonians display non-Fermi liquid behavior (see section IX) is one of the central results of the present work.

Section VII main points: A necessary condition for arriving at a novel fixed point is to check that such point is a *finite solution of third order scaling equations*. Derivation and solutions of these equations is carried out in this section. As expected, the calculations are rather involved due to the occurrence of higher multiples, third order diagrams and spin $s > \frac{1}{2}$. Nevertheless, these cumbersome calculations should not mask the important physical consequence that there are three candidates for stable finite fixed points P_4, P_5 and P_7, that correspond to non-Fermi liquid ground-states.

VIII. ANALYSIS OF THE SCALING EQUATIONS

Let us consider the scaling equations (41) in some details. Note that when $\Lambda_{\mathrm{q}} = \Lambda_{\mathrm{o}} = 0$, then we recover the

s-d model as a special case. In this case, scaling of $\Lambda_{\rm d}$ depends on the sign of $\Lambda_{\rm d}^{(0)}$. For $\Lambda_{\rm d}^{(0)} > 0$ $\Lambda_{\rm d}(D)$ flows towards the Nosièr-Blandin fixed point P_1, eq. (43a) indicating an over-screened KE. When $\Lambda_{\rm d}^{(0)} < 0$, $\Lambda_{\rm d}(D)$ flows towards zero which means that there is no KE. When $\Lambda_{\rm q}^{(0)}$ and/or $\Lambda_{\rm o}^{(0)}$ are nontrivial, the scenario is more complicated. In order to analyze scaling, we consider the following equations,

$$\frac{\partial \Lambda_{\rm q}}{\partial \Lambda_{\rm d}} = \frac{\mathfrak{F}_{\rm q}(\Lambda_{\rm d},\Lambda_{\rm q},\Lambda_{\rm o})}{\mathfrak{F}_{\rm d}(\Lambda_{\rm d},\Lambda_{\rm q},\Lambda_{\rm o})}, \tag{45a}$$

$$\frac{\partial \Lambda_{\rm o}}{\partial \Lambda_{\rm d}} = \frac{\mathfrak{F}_{\rm o}(\Lambda_{\rm d},\Lambda_{\rm q},\Lambda_{\rm o})}{\mathfrak{F}_{\rm d}(\Lambda_{\rm d},\Lambda_{\rm q},\Lambda_{\rm o})}, \tag{45b}$$

where $\mathfrak{F}_{\rm d,q,o}$ are given by eq. (42). Solving the set of equations (45), we get $\Lambda_{\rm q}$ and $\Lambda_{\rm o}$ as functions of $\Lambda_{\rm d}$. Numerical solution of the set of equations is illustrated in Figs. 9 and 10. It is seen that there are the following scaling regimes:

- All the couplings Λ_β flow to zero when D vanishes. In this case there is no KE.
- The couplings Λ_β flow to one of the stable fixed points. In this case, there is KE.

First, we should determine for which values of the couplings $\Lambda_\beta^{(0)}$ there is KE, and for which ones there is no KE. Our numerical analysis shows that when $\Lambda_{\rm d} > 0$, there is *always* KE (see Fig. 10). Therefore we investigate the case $\Lambda_{\rm d}^{(0)} < 0$. The result of our numerical calculations for this case is shown in Fig. 9. Let us analyze the different scaling regimes displayed in this figure.

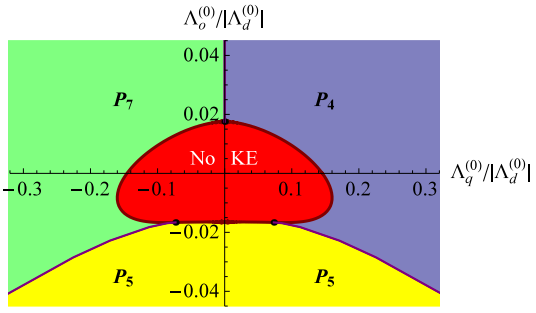


FIG. 9: (color online) Scaling of $\Lambda_{\rm d}$, $\Lambda_{\rm q}$ and $\Lambda_{\rm o}$ for $\Lambda_{\rm d}^{(0)} = -0.00105$ and different values of $\Lambda_{\rm q}^{(0)}$ and $\Lambda_{\rm o}^{(0)}$. The red area: all Λ's frow to zero and there is no KE. Yellow area: Λ's flow to the fixed point P_5. Blue area: Λ's flow to the fixed point P_4. Green area: Λ's flow to the fixed point P_7.

When the effective bandwidth decreases, the coupling $\Lambda_{\rm d}$ increases from its negative initial value and tends to 0. At this stage, it is important to determine whether $|\Lambda_{\rm q}(D)|$ and $|\Lambda_{\rm o}(D)|$ decrease faster or slower than $|\Lambda_{\rm d}(D)|$. In other words, we should consider the dimensionless parameters $\mathcal{K}_\beta$ (β =d,q,o), defined as,

$$\mathcal{K}_\beta = \frac{\partial \ln|\Lambda_\beta(D_0)|}{\partial \ln D_0}.$$

(For $\Lambda_{\rm d} < 0$, all $\mathcal{K}_\beta$ are positive). When $\mathcal{K}_{\rm d} < \mathcal{K}_{\rm q,o}$, the couplings $\Lambda_{\rm q,o}$ vanish faster than $\Lambda_{\rm d}$. As a result, the Kondo Hamiltonian renormalizes towards the s-d model Hamiltonian with ferromagnetic coupling $\Lambda_{\rm d}(D)$. This coupling flows towards zero when D vanishes. This is the case when Λ_β are in the red area in Fig. 9 (see also dark red arrowed curves in Fig. 10).

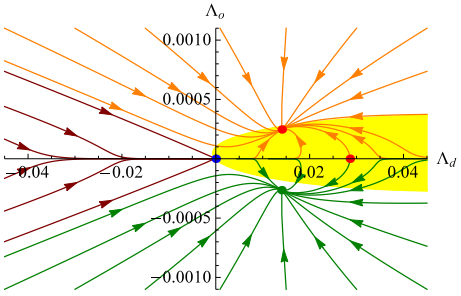


FIG. 10: (color online) Scaling of $\Lambda_{\rm d}$ and $\Lambda_{\rm o}$ for $\Lambda_{\rm q} = 0$. Dark red arrowed lines: the couplings rescale to zero. Green lines: the couplings renormalize towards the stable fixed point P_5, eq. (43e). Orange lines: the couplings renormalize towards the saddle fixed point P_6, eq. (43f). When $\Lambda_{\rm q}$ is very small but not zero, the couplings renormalize towards the fixed points P_4 or P_7, eqs. (43d) or (43g) depending either the initial value of $\Lambda_{\rm q}$ is negative or positive.

When $\mathcal{K}_{\rm q} < \mathcal{K}_{\rm d}$ and/or $\mathcal{K}_{\rm o} < \mathcal{K}_{\rm d}$, then $\Lambda_{\rm d}$ vanishes when $\Lambda_{\rm q}$ an/or $\Lambda_{\rm o}$ assume finite values. At this point, Λ_β continues to flow [see eqs. (41) and (42)]. $\Lambda_{\rm d}$, for example, changes its sign and the couplings Λ_β flow towards one of the fixed points, P_4, P_5 or P_7 (blue, yellow and green areas in Fig. 9). Note that quadruple and octuple interaction give rise to exotic property of the KE: The effective dipole coupling $\Lambda_{\rm d}(T)$ as a function of temperature turns from ferromagnetic at high temperature to antiferromagnetic at low temperature. This property is shown in Fig. 10, see orange and green arrowed curves.

It should be noted that when $\Lambda_{\rm q} = 0$, the function $\mathfrak{F}_{\rm q} = 0$ [see eq. (42b)]. Therefore, when $\Lambda_{\rm q}^{(0)} = 0$, then $\Lambda_{\rm q}(D) = 0$ for any $D < D_0$. Consider renormalization of $\Lambda_{\rm d}$ and $\Lambda_{\rm o}$ in the plane $\Lambda_{\rm q} = 0$. Numerical solution of eq. (45b) for $\Lambda_{\rm q}(0) = 0$ is displayed in Fig. 10. It is seen that the couplings flow to one of the fixed points, P_0, P_5 or P_6, eq. (43). In order to check stability of the solution, we apply the Lyapunov method for stability. For this purpose, we consider the scaling equation for $\Lambda_{\rm q}(D)$,

$$\frac{\partial \Lambda_{\rm q}}{\partial \ln D} = \mathfrak{F}_{\rm q}(\Lambda_{\rm d},\Lambda_{\rm q},\Lambda_{\rm o}),$$

with infinitesimal initial condition $\Lambda_{\rm q}^{(0)}$. Keeping just the linear power of $\Lambda_{\rm q}$ on the right hand side of the last equation we may write,

$$\frac{\partial \Lambda_{\rm q}}{\partial \ln D} = \Lambda_{\rm q}\, \mathcal{A}_{\rm q}(\Lambda_{\rm d},\Lambda_{\rm o}), \tag{46}$$

where

$$\mathcal{A}_{\rm q}(\Lambda_{\rm d},\Lambda_{\rm o}) = \lim_{\Lambda_{\rm q}\to 0}\left(\frac{\partial \mathfrak{F}_{\rm q}(\Lambda_{\rm d},\Lambda_{\rm q},\Lambda_{\rm o})}{\partial \Lambda_{\rm q}}\right).$$

The solution of eq. (46) is,

$$\frac{\Lambda_{\rm q}(D)}{\Lambda_{\rm q}^{(0)}} = \exp\left\{ -\int_{D}^{D_0} \mathcal{A}_{\rm q}\Big(\Lambda_{\rm d}(D'),\Lambda_{\rm o}(D')\Big)\ \frac{dD'}{D'}\right\}. \quad (47)$$

Note that when D vanishes, $\Lambda_{\rm d}$ and $\Lambda_{\rm o}$ flow to one of the fixed points (43), where $\mathcal{A}_{\rm q}$ takes a finite value. In this case the integral on the right hand side of eq. (47) diverges. Thus, we conclude that when $\mathcal{A}_{\rm q}$ is positive along all the scaling trajectories of $\Lambda_{\rm d}(D)$ and $\Lambda_{\rm o}(D)$, then $\Lambda_{\rm q}(D)$ flows to zero, and the solution displayed in Fig. 10 is stable. When $\mathcal{A}_{\rm q}$ is negative, then $\Lambda_{\rm q}(D)$ flows away from zero, and the solution displayed in Fig. 10 is unstable. The interval of $\Lambda_{\rm d}$ and $\Lambda_{\rm o}$ where the solution displayed in Fig. 10 is unstable is marked by yellow.

Finally, we just state our result pertaining to scaling of the couplings satisfying the initial conditions (30). Numerical analysis shows that for any positive λ_0, the couplings flow towards the fixed point P_5.

Section VIII main points: Analysis of the flow pattern for a system of three coupled non-linear scaling equations is rather rich and complicated. To some extent, in Figs. 9 and 10, we worked out the analogue of the celebrated Anderson-Yuval equations (derived for the anisotropic Kondo effect), as adapted for the present model. Unlike the former case, however, where the fixed points are at infinity, the present analysis leads to the occurrence of finite fixed points.

IX. GROUND STATE OF THE SYSTEM

Before studying experimental issues it is useful to elucidate the nature of the ground state. This will determine whether the pertinent Kondo physics at the stable points is that of over-screening or under screening. The variational method is an appropriate tool for that purpose, which is not based on perturbation theory. It can be shown that the minimal energy can be reached when the number of atoms over the fully occupied Fermi sphere is $\mathcal{N} = I + \frac{1}{2}$. For $I = \frac{5}{2}$, $\mathcal{N} = 3$. Such a three particle wave function is described by the three atomic spin S. The maximal value of the spin is $S = \frac{9}{2}$. This value can be get as following: according to the Pauli principle, the magnetic quantum numbers satisfy the inequalities $i_1 \neq i_2$, $i_2 \neq i_3$ and $i_3 \neq i_1$. Therefore the maximal magnetic quantum number of the three atoms is $S = \frac{9}{2}$.

A simple form of variational wave function is,

$$\big|L,m\big\rangle \ = \ \sum_{f,\{i\}_3,\{\mathbf{k}\}_3} C^{L,m}_{S,s;F,f}\ \psi_L(\mathbf{k}_1)\ \psi_L(\mathbf{k}_2)\psi_L(\mathbf{k}_3)\times \\ \times C^{S,s}_{I,i_1;I,i_2;I,i_3}\ c^\dagger_{\mathbf{k}_1,i_1}\ c^\dagger_{\mathbf{k}_2,i_2}\ c^\dagger_{\mathbf{k}_3,i_3}\ \big|f;\Omega\big\rangle, \quad (48)$$

where $|f;\Omega\rangle$ describes the impurity with magnetic quantum number f and a Fermi sea with all the levels below the Fermi energy occupied and all the levels above the Fermi energy free. $C^{L,m}_{S,s;F,f}$ are the appropriate Clebsch-Gordan coefficients, and $L = S+F, S+F-1, S+F-2, \ldots, S-F$ is the total angular momentum of the four atomic system. $C^{S,s}_{I,i_1;I,i_2;I,i_3}$ are so called three particle Clebsch-Gordan coefficients. Here we use the fact that $H_{\rm d}$, $H_{\rm q}$ and $H_{\rm o}$ commute with each other (see Appendix M for details), and therefore the four-atomic orbital angular momentum L is a good quantum number.

In order to find $\psi_L(\mathbf{k})$, we apply the Schrödinger equation

$$H\big|L,m\big\rangle \ = \ \varepsilon\big|L,m\big\rangle.$$

Then we get

$$\big(\epsilon_{\mathbf{k}} - \varepsilon\big)\psi_L(\mathbf{k}) + g_L \sum_{\mathbf{k}'} \Theta(\epsilon_{\mathbf{k}'} - \epsilon_F)\psi_L(\mathbf{k}') = 0. \quad (49)$$

Here

$$g_L \ = \ \lambda_{\rm d}\ \mathcal{D}_L + \lambda_{\rm q}\ \mathcal{Q}_L + \lambda_{\rm o}\ \mathcal{O}_L, \quad (50)$$

where

$$\begin{aligned}
\mathcal{D}_L \ &= \ \frac{1}{2}\ \Big\{L(L+1) - F(F+1) - I(I+1)\Big\},\\
\mathcal{Q}_L \ &= \ 4\ \mathcal{D}_L^2 + 2\ \mathcal{D}_L - \frac{4}{3}\ F(F+1)\ S(S+1),\\
\mathcal{O}_L \ &= \ 36\mathcal{D}_L^3 + 72\mathcal{D}_L^2 + 12\mathcal{D}_L - \\
&\quad -\frac{12}{5}\ \big(3S(S+1)-1\big)\ \big(2F(F+1)-1\big)\ \mathcal{D}_L - \\
&\quad -18\ S(S+1)\ F(F+1).
\end{aligned}$$

The solution of eq. (49) is,

$$\psi_L(\mathbf{k}) \ = \ \frac{A_L}{\varepsilon_L - \epsilon_{\mathbf{k}}},$$

where A_L is a normalization constant. The energy ε_L can be found from the equation,

$$g_L \sum_{\mathbf{k}} \frac{\Theta(\epsilon_{\mathbf{k}} - \epsilon_F)}{\varepsilon_L - \epsilon_{\mathbf{k}}} + 1 \ = \ 0. \quad (51)$$

We are interested in the energies ε_L which are below the Fermi energy ϵ_F. This is the case when $g_L < 0$. Introducing the density of states [see eq. (G3) below], we can write,

$$\varepsilon_L - \epsilon_F \ = \ D_0 \exp\left(-\frac{1}{|g_L|\ \rho_0}\right).$$

The energy of the ground state is found as

$$\varepsilon_{\rm gs} \ = \ \min_L \varepsilon_L.$$

Thus, the problem of finding the ground state reduces to that of finding a minimum of g_L. In order to check whether the magnetic impurity is over-screened or under-screened, we consider the operator

$$\big(\mathbf{L}\cdot\mathbf{F}\big) = \frac{1}{2}\ \big\{L(L+1) + F(F+1) - S(S+1)\big\}. \quad (52)$$

When $(\mathbf{L}\cdot\mathbf{F})<0$, there is over-screened KE. Using eq. (52), we get the condition of over-screened KE,

$$L(L+1)+F(F+1)-S(S+1)\ <\ 0. \tag{53}$$

When $S=\frac{9}{2}$ and $F=\frac{3}{2}$, the condition (53) is fulfilled when $L=3$ or 4. Note that the condition (53) is sufficient but not necessary for overscreened KE: When the condition (53) is fulfilled, there is overscreened KE with non Fermi liquid ground state. When the condition (53) is not fulfilled, we cannot say about the nature of the ground state.

We now apply our analysis for elucidating the nature of the stable fixed points P_4, P_5 and P_7. For the fixed point P_4, the ground state corresponds to the energy level with $L=3$, and therefore there is an overscreened KE. Similarly, for the fixed point P_5, the ground state corresponds to the energy level with $L=4$, and therefore there is overscreened KE. Finally, for the fixed point P_7, the ground state corresponds to the energy level with $L=5$, and therefore we cannot conclude whether the impurity is overscreened or underscreened. As an example, when the initial values of the couplings $\lambda_{\rm d}$, $\lambda_{\rm q}$ and $\lambda_{\rm o}$ are given by eq. (30), the Kondo Hamiltonian flows toward the fixed point P_5, and therefore we can conclude that there is an overscreened KE. It is important to stress that the exchange interaction between the overscrened spin of the impurity and the rest of the Fermi gas is *antiferromagnetic* and therefore, the Fermi liquid fixed point $\Lambda_\beta\to\infty$ is unstable[8] ($\beta={\rm d,q,o}$). Since the two fixed points, $\Lambda_\beta=0$ and $\Lambda_\beta\to\infty$, are unstable, there is at least one *stable and finite fixed point* Λ_β in between[8].

Section IX main points: After the candidates for stable fixed points are identified, it is necessary to elucidate the ground-state wave functions at these points. This is required in order to evaluate physical observables and to determine whether over-screening does occur. This task is carried out above, and, as we find, the nature of the system (whether there is or there is no over-screening) depends on the initial value of the bare constants $\lambda_{\rm d}$, $\lambda_{\rm q}$ and $\lambda_{\rm o}$.

X. MAGNETIC SUSCEPTIBILITY

The formalism developed so far enables us to calculate a few thermodynamic quantities. Here we will be content by focusing on an important experimental observable that is relevant for the pertinent system, namely, the impurity contribution to the magnetic susceptibility. We will calculate it here in the weak coupling regime, wherein it is expected that the general form of the susceptibility is dominated by logarithmic functions of $\frac{D}{T}$. Whereas for dipolar exchange interaction (governed by the $s-d$ Hamiltonian), the derivation is quite standard, the derivation and handling of the spin algebra in the present case of multipolar exchange interactions is much more involved.

In order to derive an expression for the magnetic susceptibility of the atomic gas with the Kondo impurity, we note that the itinerant atoms are in the electronic spin-singlet state, whereas the impurity is in the electronic spin-triplet state. Therefore interaction of itinerant atoms with the magnetic field is proportional to the nuclear magneton $\mu_{\rm n}$, whereas the interaction of the impurity with the magnetic field is proportional to the Bohr magneton μ_B. The interaction of the itinerant atoms and the impurity with the magnetic field $\mathbf{B}=B\mathbf{e}_z$ is described by the Hamiltonian,

$$\begin{aligned} H_B\ &=\ -g_{\rm Yb}\mu_{\rm n}\sum_{i,i',\mathbf{k}}\left(\mathbf{B}\cdot\mathbf{I}_{i,i'}\right)\,c^\dagger_{\mathbf{k},i}c_{\mathbf{k},i'}\,- \\ &\quad -g\mu_B\sum_f\left(\mathbf{B}\cdot\mathbf{F}_{f,f'}\right)\,X^{f,f'}, \end{aligned} \tag{54}$$

where $g_{\rm Yb}=-0.2592$ is the nuclear g-factor of $^{173}{\rm Yb}$[32], g is electronic g-factor of Yb atom in the $^3{\rm P}_2$ state,

$$g\ =\ \frac{3J(J+1)+S(S+1)-L(L+1)}{2J(J+1)}\ =\ \frac{3}{2}, \tag{55}$$

where for the $^3{\rm P}_2$ configuration, $J=2$ and $L=S=1$. Then the impurity magnetization $\mathbf{M}_{\rm imp}=M_{\rm imp}\mathbf{e}_z$ can be written as[4],

$$M_{\rm imp}=g\mu_B\,\left\langle\hat{F}^z\right\rangle+g_{\rm Yb}\mu_{\rm n}\,\Big\{\left\langle\hat{I}^z\right\rangle-\left\langle\hat{I}^z\right\rangle_0\Big\}, \tag{56}$$

where $\langle\cdots\rangle$ indicates a thermal average with respect to the total Hamiltonian $H+H_B$, and $\langle\cdots\rangle_0$ with respect to H_0+H_B,

$$\begin{aligned} \left\langle\mathcal{O}\right\rangle\ &=\ \frac{{\rm tr}\big(e^{-\beta(H+H_B)}\,\mathcal{O}\big)}{{\rm tr}\ e^{-\beta(H+H_B)}}, \\ \left\langle\mathcal{O}\right\rangle_0\ &=\ \frac{{\rm tr}\big(e^{-\beta(H_0+H_B)}\,\mathcal{O}\big)}{{\rm tr}\ e^{-\beta(H_0+H_B)}}. \end{aligned}$$

Here H and H_0 are given by eq. (23).

The magnetic interaction described by the Hamiltonian (54) has a standard form of a scalar product of the external magnetic field and the magnetic dipole momentum operators of the impurity and itinerant atoms. It reflects the fact that (usually), only the dipole moment contributes to the linear magnetization of atoms. However, somewhat unexpectedly, the Kondo Hamiltonian (17) gives rise to nontrivial contributions of the quadruple and octuple magnetic moments to the linear magnetization of the system. This requires an analysis that is distinct from the one the standard treatment of magnetic susceptibility as applied to the $s-d$ Hamiltonian. In this section we derive the magnetic susceptibility as a function of temperature in the weak coupling regime, $T\gg T_K$.

A. Contributions to $M_{\rm imp}$ due to H_K

First, let us recall the expression for the magnetization of an isolated atom. To linear order in the magnetic field

B, the magnetization of a single ^{173}Yb atom in the $^3P_2$ state with $F=\frac{3}{2}$ is,

$$M^{(0)}_{\rm imp} \;=\; \frac{F(F+1)}{3T}\,\big(g\mu_B\big)^2 B. \tag{57}$$

Next, consider the contributions to $M_{\rm imp}$ due to H_K,

$$\delta M_{\rm imp} \;=\; M_{\rm imp} - M^{(0)}_{\rm imp}.$$

By definition, this contribution is given by,

$$\begin{aligned}\delta M_{\rm imp} \;&=\; g\mu_B\,\Big\{\big\langle \hat{F}^z\big\rangle - \big\langle \hat{F}^z\big\rangle_0\Big\} + \\ &+\; g_{\rm Yb}\mu_{\rm n}\,\Big\{\big\langle \hat{I}^z\big\rangle - \big\langle \hat{I}^z\big\rangle_0\Big\}.\end{aligned} \tag{58}$$

Assume that the couplings λ's are small and expand $\delta M_{\rm imp}$ with powers of H_K,

$$\delta M_{\rm imp} \;=\; \sum_{n=1}^{\infty}\delta M^{(n)}_{\rm imp}, \tag{59}$$

where $\delta M^{(n)}_{\rm imp}$ is proportional to λ^n_β. Below we will calculate $\delta M^{(1)}_{\rm imp}$ and $\delta M^{(2)}_{\rm imp}$.

1. Corrections linear with λ's

The correction $\delta M^{(1)}_{\rm imp}$ can be written as,

$$\delta M^{(1)}_{\rm imp} \;=\; \sum_\beta \Big\{\delta M_{{\rm f};\beta} + \delta M_{{\rm i};\beta}\Big\}. \tag{60}$$

Here

$$\delta M_{{\rm f};\beta} \;=\; -g\mu_B\int_0^\beta \Big\langle \hat{F}^z H_\beta(\tau)\Big\rangle_0\, d\tau, \tag{61}$$

$$\delta M_{{\rm i};\beta} \;=\; -g_{\rm Yb}\mu_{\rm n}\int_0^\beta \Big\langle \hat{I}^z H_\beta(\tau)\Big\rangle_0\, d\tau, \tag{62}$$

where $\beta = {\rm d},{\rm q},{\rm o}$ for dipole, quadruple and octuple interactions, $H_{\rm d,q,o}$ are given by eqs. (19), (20) and (21). The expectation values $\langle F^{\vec{\alpha}_\beta}\rangle$, $\langle I^{\vec{\alpha}_\beta}\rangle$, $\langle F^z F^{\vec{\alpha}_\beta}\rangle$ and $\langle I^z I^{\vec{\alpha}_\beta}\rangle$ [where $\hat{F}^{\vec{\alpha}_\beta}$ or $\hat{I}^{\vec{\alpha}_\beta}$ are dipole ($\beta={\rm d}$), quadruple ($\beta={\rm q}$) and octuple ($\beta={\rm o}$) matrices for a localized impurity or itinerant atoms, α's are the Cartesian indices] are calculated in Appendix O. Then $\delta M^{(1)}_{\rm imp}$ is,

$$\delta M^{(1)}_{\rm imp} \;=\; -\frac{175B}{4T}\;g\mu_B\;g_{\rm Yb}\mu_{\rm n}\;\Lambda_{\rm d}. \tag{63}$$

Note that the factor $\frac{175}{4}$ comes from,

$$\frac{2}{9}\;F(F+1)\;I(I+1)(2I+1) \;=\; \frac{175}{4}.$$

If instead of itinerant atoms with spin $I=\frac{5}{2}$, we use atoms with spin $s=\frac{1}{2}$, the last expression turns to

$$\frac{2}{9}\;F(F+1)\;s(s+1)(2s+1) \;=\; \frac{F(F+1)}{3},$$

which agrees with eq. (3.2) from Ref.[4].

2. Corrections quadratic with λ's

Calculating the second order correction, $\delta M^{(2)}_{\rm imp}$, we get $\delta M_{\rm imp}$ up to λ^2,

$$\begin{aligned}\delta M_{\rm imp} \;&=\; -M^{(0)}_{\rm imp}\,\mathcal{N}_I\;\frac{g\mu_B}{g_{\rm Yb}\mu_{\rm n}}\;\times \\ &\times\;\left\{\Lambda_{\rm d} - \mathfrak{F}^{(2)}_{\rm d}\;\ln\left(\frac{D}{T}\right)\right\},\end{aligned} \tag{64}$$

where $M^{(0)}_{\rm imp}$ is given by eq. (57),

$$\mathcal{N}_I \;=\; \frac{2}{3}\;I\big(I+1\big)\big(2I+1\big), \tag{65}$$

$$\mathfrak{F}^{(2)}_{\rm d} = -\Lambda^2_{\rm d} - \frac{9216}{25}\;\Lambda^2_{\rm q} - \frac{1469664}{25}\;\Lambda^2_{\rm o}. \tag{66}$$

$\mathfrak{F}^{(2)}_{\rm d}$ can be get from eq. (42a) neglecting the terms of order λ^3.

The condition imposing the invariance of the magnetization under the poor mans scaling transformation is

$$\frac{\partial}{\partial \ln D}\left\{\Lambda_{\rm d} - \mathfrak{F}^{(2)}_{\rm d}\ln\left(\frac{D}{T}\right)\right\} \;=\; 0. \tag{67}$$

Within the accuracy of this equation, when differentiating the second term, we should neglect any implicit dependence on D through the couplings Λ_β ($\beta={\rm d},{\rm q},{\rm o}$). The renormalization procedure should proceed until the bandwidth D is reduced to the temperature T. At this point, the second order of the perturbation theory vanishes and the magnetization takes the form,

$$M_{\rm imp} \;=\; M^{(0)}_{\rm imp}\left\{1 - \frac{g_{\rm Yb}\mu_{\rm n}}{g\mu_B}\;\mathcal{N}_I\;\Lambda_{\rm d}(T)\right\}, \tag{68}$$

where $\mathcal{N}_I$ is given by eq. (65), $\Lambda_{\rm d}(T)$ is the solution of the second order scaling equation (28).

It is useful to write the magnetic susceptibility $\chi_{\rm imp} = \partial M_{\rm imp}/\partial B$ as,

$$\chi_{\rm imp}(T) \;=\; \chi^{(0)}_{\rm imp} + \delta\chi_{\rm imp}(T), \tag{69}$$

where $\chi^{(0)}_{\rm imp}$ is the susceptibility of the isolated impurity atom, and $\delta\chi_{\rm imp}(T)$ is correction to the susceptibility due to the Kondo interaction. Explicitly,

$$\chi^{(0)}_{\rm imp} \;=\; \frac{\chi_0}{3}\;\frac{T_K}{T}\;F(F+1), \tag{70}$$

$$\delta\chi_{\rm imp} = -\frac{g_{\rm Yb}\mu_{\rm n}}{g\mu_B}\;\chi^{(0)}_{\rm imp}\;\mathcal{N}_I\;\Lambda_{\rm d}, \tag{71}$$

where

$$\chi_0 \;=\; \frac{\big(g\mu_B\big)^2}{T_K}.$$

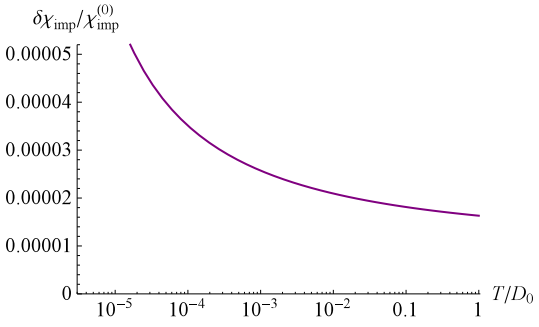


FIG. 11: (color online) The ratio $\delta\chi_{\rm imp}/\chi^{(0)}_{\rm imp}$ as a function of T for $\lambda_0\rho_0 = 0.7$ and so that $\Lambda^{(0)}_{\rm d} = 0.03467$, $\Lambda^{(0)}_{\rm q} = -0.00083$, $\Lambda^{(0)}_{\rm o} = -0.00037$.

The ratio $\delta\chi_{\rm imp}/\chi^{(0)}_{\rm imp}$ as a function of temperature is shown in Fig. 11. It is seen that $\delta\chi_{\rm imp}/\chi^{(0)}_{\rm imp} \ll 1$ since the ratio,

$$\frac{g_{\rm Yb}\ \mu_{\rm n}}{g\ \mu_B} \ = \ -9.411\cdot 10^{-5},$$

is small. When T approaches the Kondo temperature, $\delta\chi_{\rm imp}$ diverges as $1/\ln(T/T_K)$ which indicates breaking down of the underlying perturbation theory.

Section X main points: An appropriate candidate (smoking gun) for an experimental test of the Kondo effect in the pertinent system is the growth of the magnetic susceptibility with decreasing temperature. The magnetic susceptibility can be readily extracted from the relative atom number fluctuation[40] or from the thermodynamic potential obtained by the density profile for one-component Bose gases[41], two-component Fermi gases[42], and very recently SU(N) fermions trapped in optical lattices[43]. We believe that similar measurements are feasible in a system composed of ^{1}S$_0$-^{3}P$_2$ ytterbium mixture. The rate of growth is indeed small in the weak coupling regime, $T \gg T_K$, and it dominates the temperature behaviour of the susceptibility in the strong coupling regime, $T < T_K$. In the present work t we confined ourselves to the weak coupling regime because as far as we know, there is yet no solid theory of the multipolar Kondo effect in the strong coupling regime. Certainly, working out this problem is an urgent task but it goes beyond the scope of the present study.

XI. CONCLUSION

Let us then briefly summarize our results. Our main arena concerns the Kondo physics in an ultracold Fermi gas of ^{173}Yb (^{1}S$_0$) atoms (in their electronic ground-state) in which a few ^{173}Yb (^{3}P$_2$) atoms (in a long lived excited state) are trapped in a specially designed optical potential. The main objectives are: 1) To explore the feasibility of experimental realization; 2) To calculate the exchange interaction between the itinerant ^{173}Yb(^{1}S$_0$) and ^{173}Yb(^{3}P$_2$) atoms and to verify that it is an antiferromagnetic exchange; 3) To construct the Kondo Hamiltonian and to identify its underlying symmetry; 4) To carry out the corresponding poor-man scaling, to identify the stable fixed points and to determine whether some of them display non-Fermi liquid behavior; 5) To calculate some experimentally accessible observable in such a system.

As far as objective 1) is concerned, we have considered a mixture of ^{1}S$_0$ and ^{3}P$_2$ ytterbium fermions that can be readily prepared in a current experiment, in which a state-dependent optical potential using a strong ^{3}P$_2$-^{3}S$_1$ transition tightly confines ^{3}P$_2$ atoms while makes ground-state ^{1}S$_0$ atoms itinerant. By properly choosing the wavelength of the optical potential, we have shown that the spontaneous light scattering can be sufficiently reduced to observe a many-body effect. The localized and itinerant atoms can be then independently detected with the combination of optical pumping and blast. Finally a ^{1}S$_0$-^{3}P$_2$ mixture of ytterbium atoms has a magnetic Feshbach resonance by which the interaction strength between localized and itinerant atoms can be further controlled[38]. Such novel features may open a new route to investigate the Kondo effect with tunable atom-atom interactions in this system. Calculating the exchange interaction proceeds along similar lines as in our previous paper[28].

The main difficulty is encountered in achieving goals (3) and (4). It is required to write down the Kondo Hamiltonian in terms of multiple expansion, since otherwise, the RG procedure is inapplicable. This requires a technically tedious procedure related to the pertinent spin algebra. Moreover, identifying the corresponding fixed points requires calculations of RG diagrams to third order in the exchange constant, which turn out to be rather involved. Details of the calculations are explained in the Appendices.

Having overcame these technical difficulties, we have found seven fixed points for $\lambda_{\rm d}$ and $\lambda_{\rm q}$ and $\lambda_{\rm o}$. Three of them, P_4, P_5 and P_7 [eqs. (43d), (43e) and (43g)] are stable, and the other fixed points are unstable. The fixed points found here are distinct from the NB non Fermi liquid fixed point described in our previous paper[28], in which we studied the Kondo physics in a ^{1}S$_0$-^{3}P$_0$ mixture of ^{173}Yb atoms. In the present work, the NB non Fermi liquid fixed point corresponds to P_1 in the list (43d), and is *unstable*.

The remaining task, that is, elucidating the Kondo physics *in the strong coupling regime* for the new stable fixed points P_4, P_5 and P_7 (identified here) is beyond the scope of our present study. It is perceived that the standard techniques that are applied to the dipolar Kondo effect such as Bethe Ansatz and conformal field theory might work also in this case albeit with non-trivial modifications.

Acknowledgement

Y.A, I.K and T.K acknowledge many years of collaboration and discussions pertaining to the Kondo Physics with their colleague and their close friend

Konstantin Abramovich Kikoin

His sudden death left us shocked and wordless.

The authors thank S. Zhang for useful discussion. G.B.J acknowledges financial support from the Hong Kong Research Grants Council (Project No. 26300014/16300215/16311516) and from the Croucher Foundation. The research of Y.A is partially supported by grant 400/12 of the Israeli Science Foundation.

Appendix A: Commutation Relations for Angular Momentum Operators

The spin matrices satisfy the following commutation relations,

$$\left[\hat{S}^{\alpha},\ \hat{S}^{\alpha'}\right] \ = \ i\sum_{\alpha''}\epsilon^{\alpha,\alpha',\alpha''}\ \hat{S}^{\alpha''}, \tag{A1}$$

where $\alpha, \alpha', \alpha''$ are Cartesian indices, $\epsilon^{\alpha,\alpha',\alpha''}$ are the Levi-Civita symbols. Eq. (A1) shows that the matrices S^{α} are generators of the $(2S+1)$-dimensional irreducible representation of the SU(2) group. The commutator of the spin matrices with the matrices representing the quadruple moment are,

$$\left[\hat{S}^{\alpha_1}, \hat{S}^{\alpha_2,\alpha_2'}\right] \ = \ i\sum_{\alpha_3,\alpha_3'}\sum_{\alpha_4} P^{\alpha_2,\alpha_2'}_{\alpha_3,\alpha_3'} \times \\ \times\epsilon^{\alpha_1,\alpha_3,\alpha_4}\ \hat{S}^{\alpha_3',\alpha_4}, \tag{A2}$$

where $P^{\alpha_2,\alpha_2'}_{\alpha_3,\alpha_3'}$ is given by eq. (7). Similarly, the commutator of the spin matrices with the matrices representing the octuple moment are,

$$\left[\hat{S}^{\alpha_1},\ \hat{S}^{\alpha_2,\alpha_2',\alpha_2''}\right] \ = \ i\sum_{\alpha_3,\alpha_3',\alpha_3''}\sum_{\alpha_4} P^{\alpha_2,\alpha_2',\alpha_2''}_{\alpha_3,\alpha_3',\alpha_3''} \times \\ \times\epsilon^{\alpha_1,\alpha_3,\alpha_4}\ \hat{S}^{\alpha_3',\alpha_3'',\alpha_4}, \tag{A3}$$

where $P^{\alpha_2,\alpha_2',\alpha_2''}_{\alpha_3,\alpha_3',\alpha_3''}$ is given by eq. (6).

Now consider commutation relations for matrices representing quadruple moment operators. For atoms with spin $F=\frac{3}{2}$, the commutators are,

$$\left[\hat{F}^{\alpha_1,\alpha_1'},\ \hat{F}^{\alpha_2,\alpha_2'}\right] \ = \ i\sum_{\alpha_3,\alpha_3'}\sum_{\alpha_4,\alpha_4'}\sum_{\alpha_5} P^{\alpha_1,\alpha_1'}_{\alpha_3,\alpha_3'}\ P^{\alpha_2,\alpha_2'}_{\alpha_4,\alpha_4'} \times \\ \times\epsilon^{\alpha_3,\alpha_4,\alpha_5}\left(\frac{2}{3}\ \hat{F}^{\alpha_3',\alpha_4',\alpha_5} + \right. \\ \left. + \frac{12}{5}\ \delta_{\alpha_3',\alpha_4'}\ \hat{F}^{\alpha_5}\right), \tag{A4}$$

where $\hat{F}^{\alpha}$ and $\hat{F}^{\alpha,\alpha',\alpha''}$ are the spin and octuple momentum matrices for atoms with spin $F=\frac{3}{2}$.

For atoms with spin $I=\frac{5}{2}$, the commutators are,

$$\left[\hat{I}^{\alpha_1,\alpha_1'},\ \hat{I}^{\alpha_2,\alpha_2'}\right] \ = \ i\sum_{\alpha_3,\alpha_3'}\sum_{\alpha_4,\alpha_4'}\sum_{\alpha_5} P^{\alpha_1,\alpha_1'}_{\alpha_3,\alpha_3'}\ P^{\alpha_2,\alpha_2'}_{\alpha_4,\alpha_4'} \times \\ \times\epsilon^{\alpha_3,\alpha_4,\alpha_5}\left(\frac{2}{3}\ \hat{I}^{\alpha_3',\alpha_4',\alpha_5} + \right. \\ \left. + \frac{32}{5}\ \delta_{\alpha_3',\alpha_4'}\ \hat{I}^{\alpha_5}\right), \tag{A5}$$

where $\hat{I}^{\alpha}$ and $\hat{I}^{\alpha,\alpha',\alpha''}$ are the spin and octuple momentum matrices for atoms with spin $I=\frac{5}{2}$.

In the next level of complexity we consider commutators of the matrices representing quadruple and octuple operators. For atoms with spin $F=\frac{3}{2}$, the commutators are,

$$\left[\hat{F}^{\alpha_1,\alpha_1'},\ \hat{F}^{\alpha_2,\alpha_2',\alpha_2''}\right] \ = \ \frac{3i}{10}\sum_{\alpha_3,\alpha_3'}\sum_{\alpha_4,\alpha_4',\alpha_4''}\sum_{\alpha_5} P^{\alpha_1,\alpha_1'}_{\alpha_3,\alpha_3'}\ P^{\alpha_2,\alpha_2',\alpha_2''}_{\alpha_4,\alpha_4',\alpha_4''}\ \epsilon^{\alpha_3,\alpha_4,\alpha_5} \times \\ \times\left\{5\ \delta_{\alpha_3',\alpha_4'}\ \hat{F}^{\alpha_4'',\alpha_5} - \delta_{\alpha_4',\alpha_4''}\ \hat{F}^{\alpha_3',\alpha_5}\right\}, \tag{A6}$$

while for atoms with spin $I=\frac{5}{2}$, the commutators are,

$$\left[\hat{I}^{\alpha_1,\alpha_1'},\ \hat{I}^{\alpha_2,\alpha_2',\alpha_2''}\right] \ = \ \frac{i}{4}\sum_{\alpha_3,\alpha_3'}\sum_{\alpha_4,\alpha_4',\alpha_4''}\sum_{\alpha_5} P^{\alpha_1,\alpha_1'}_{\alpha_3,\alpha_3'}\ P^{\alpha_2,\alpha_2',\alpha_2''}_{\alpha_4,\alpha_4',\alpha_4''}\ \epsilon^{\alpha_3,\alpha_4,\alpha_5} \times \\ \times\left\{\hat{I}^{\alpha_3',\alpha_4',\alpha_4'',\alpha_5} + \frac{162}{7}\ \delta_{\alpha_3',\alpha_4'}\ \hat{I}^{\alpha_4'',\alpha_5} - \frac{162}{35}\ \delta_{\alpha_4',\alpha_4''}\ \hat{I}^{\alpha_3',\alpha_5}\right\}, \tag{A7}$$

where $\hat{I}^{\alpha_1,\alpha_2,\alpha_3,\alpha_4}$ is a tensor of the 16-pole momentum.

Now we arrive at the calculations of commutators of the matrices representing octuple operators. For atoms with

spin $F=\frac{3}{2}$, the commutators are,

$$\begin{aligned}\left[\hat{F}^{\alpha_1,\alpha_1',\alpha_1''},\ \hat{F}^{\alpha_2,\alpha_2',\alpha_2''}\right] &= \frac{i}{10}\sum_{\alpha_3,\alpha_3',\alpha_3''}\sum_{\alpha_4,\alpha_4',\alpha_4''}\sum_{\alpha_5} P^{\alpha_1,\alpha_1',\alpha_1''}_{\alpha_3,\alpha_3',\alpha_3''}\ P^{\alpha_2,\alpha_2',\alpha_2''}_{\alpha_4,\alpha_4',\alpha_4''}\ \epsilon^{\alpha_3,\alpha_4,\alpha_5}\times\\ &\times\left[\delta_{\alpha_3',\alpha_3''}\ \hat{F}^{\alpha_4,\alpha_4',\alpha_5}+\delta_{\alpha_4',\alpha_4''}\ \hat{F}^{\alpha_3,\alpha_3',\alpha_5}\right]-\\ &-\frac{i}{2}\sum_{\alpha_3,\alpha_3',\alpha_3''}\sum_{\alpha_4,\alpha_4',\alpha_4''}\sum_{\alpha_5} P^{\alpha_1,\alpha_1',\alpha_1''}_{\alpha_3,\alpha_3',\alpha_3''}\ P^{\alpha_2,\alpha_2',\alpha_2''}_{\alpha_4,\alpha_4',\alpha_4''}\ \epsilon^{\alpha_3,\alpha_4,\alpha_5}\ \delta_{\alpha_3',\alpha_4'}\ \hat{F}^{\alpha_3'',\alpha_4'',\alpha_5}-\\ &-\frac{27i}{50}\sum_{\alpha_3,\alpha_3',\alpha_3''}\sum_{\alpha_4,\alpha_4',\alpha_4''}\sum_{\alpha_5} P^{\alpha_1,\alpha_1',\alpha_1''}_{\alpha_3,\alpha_3',\alpha_3''}\ P^{\alpha_2,\alpha_2',\alpha_2''}_{\alpha_4,\alpha_4',\alpha_4''}\ \epsilon^{\alpha_3,\alpha_4,\alpha_5}\ \delta_{\alpha_3',\alpha_3''}\ \delta_{\alpha_4',\alpha_4''}\ \hat{F}^{\alpha_5}+\\ &+\frac{27i}{10}\sum_{\alpha_3,\alpha_3',\alpha_3''}\sum_{\alpha_4,\alpha_4',\alpha_4''}\sum_{\alpha_5} P^{\alpha_1,\alpha_1',\alpha_1''}_{\alpha_3,\alpha_3',\alpha_3''}\ P^{\alpha_2,\alpha_2',\alpha_2''}_{\alpha_4,\alpha_4',\alpha_4''}\ \epsilon^{\alpha_3,\alpha_4,\alpha_5}\ \delta_{\alpha_3',\alpha_4'}\ \delta_{\alpha_3'',\alpha_4''}\ \hat{F}^{\alpha_5}. \end{aligned}\tag{A8}$$

For atoms with spin $I=\frac{5}{2}$, the commutators are,

$$\begin{aligned}\left[\hat{I}^{\alpha_1,\alpha_1',\alpha_1''},\ \hat{I}^{\alpha_2,\alpha_2',\alpha_2''}\right] &= \frac{3i}{40}\sum_{\alpha_3,\alpha_3',\alpha_3''}\sum_{\alpha_4,\alpha_4',\alpha_4''}\sum_{\alpha_5} P^{\alpha_1,\alpha_1',\alpha_1''}_{\alpha_3,\alpha_3',\alpha_3''}\ P^{\alpha_2,\alpha_2',\alpha_2''}_{\alpha_4,\alpha_4',\alpha_4''}\ \epsilon^{\alpha_3,\alpha_4,\alpha_5}\hat{I}^{\alpha_3',\alpha_3'',\alpha_4',\alpha_4'',\alpha_5}-\\ &-\frac{17i}{30}\sum_{\alpha_3,\alpha_3',\alpha_3''}\sum_{\alpha_4,\alpha_4',\alpha_4''}\sum_{\alpha_5} P^{\alpha_1,\alpha_1',\alpha_1''}_{\alpha_3,\alpha_3',\alpha_3''}\ P^{\alpha_2,\alpha_2',\alpha_2''}_{\alpha_4,\alpha_4',\alpha_4''}\ \epsilon^{\alpha_3,\alpha_4,\alpha_5}\times\\ &\times\left[\delta_{\alpha_3',\alpha_3''}\ \hat{I}^{\alpha_4,\alpha_4',\alpha_5}+\delta_{\alpha_4',\alpha_4''}\ \hat{I}^{\alpha_3,\alpha_3',\alpha_5}\right]+\\ &+\frac{17i}{6}\sum_{\alpha_3,\alpha_3',\alpha_3''}\sum_{\alpha_4,\alpha_4',\alpha_4''}\sum_{\alpha_5} P^{\alpha_1,\alpha_1',\alpha_1''}_{\alpha_3,\alpha_3',\alpha_3''}\ P^{\alpha_2,\alpha_2',\alpha_2''}_{\alpha_4,\alpha_4',\alpha_4''}\ \epsilon^{\alpha_3,\alpha_4,\alpha_5}\ \delta_{\alpha_3',\alpha_4'}\ \hat{I}^{\alpha_3'',\alpha_4'',\alpha_5}-\\ &-\frac{972i}{175}\sum_{\alpha_3,\alpha_3',\alpha_3''}\sum_{\alpha_4,\alpha_4',\alpha_4''}\sum_{\alpha_5} P^{\alpha_1,\alpha_1',\alpha_1''}_{\alpha_3,\alpha_3',\alpha_3''}\ P^{\alpha_2,\alpha_2',\alpha_2''}_{\alpha_4,\alpha_4',\alpha_4''}\ \epsilon^{\alpha_3,\alpha_4,\alpha_5}\ \delta_{\alpha_3',\alpha_3''}\ \delta_{\alpha_4',\alpha_4''}\ \hat{I}^{\alpha_5}+\\ &+\frac{972i}{35}\sum_{\alpha_3,\alpha_3',\alpha_3''}\sum_{\alpha_4,\alpha_4',\alpha_4''}\sum_{\alpha_5} P^{\alpha_1,\alpha_1',\alpha_1''}_{\alpha_3,\alpha_3',\alpha_3''}\ P^{\alpha_2,\alpha_2',\alpha_2''}_{\alpha_4,\alpha_4',\alpha_4''}\ \epsilon^{\alpha_3,\alpha_4,\alpha_5}\ \delta_{\alpha_3',\alpha_4'}\ \delta_{\alpha_3'',\alpha_4''}\ \hat{I}^{\alpha_5}, \end{aligned}\tag{A9}$$

where $\hat{I}^{\alpha_1,\alpha_2,\alpha_3,\alpha_4,\alpha_5}$ are matrices of the 32-pole momentum.

Appendix A main points: In the main text we have underline the important role of the 2^n pole operators as building blocks of the exchange terms appearing in the Kondo Hamiltonian. In this appendix we elaborated upon some technical points related to the geometric structure of these operators.

Appendix B: Single Electronic Wave Functions

The electronic wave functions in atomic Yb play the key role in calculating the exchange interaction. In this section we introduce the corresponding wave functions that are used for these calculations. Recall that an Yb atom has two valence electrons outside a closed shell. The ground state of Yb is $^1\mathrm{S}_0$, whose electronic configuration is $6s^2$. The low lying excited states are $^3\mathrm{P}_J$ (angular momentum $J=0,1,2$), with electronic configuration $6s6p$. The single electron wave functions of the $6s$ and $6p$ electronic orbitals are denoted as $\psi_{\mathrm{s}}(r)$ and $\psi_{L_z}(\mathbf{r})$, where $L_z=0,\pm1$ is a magnetic quantum number. The latter can be written as,

$$\psi_{L_z}(\mathbf{r}) \ = \ \sqrt{4\pi}\ \psi_{\mathrm{p}}(r)Y_{1L_z}(\theta,\phi),\tag{B1}$$

where $\mathbf{r}=(r,\theta,\phi)$ are spherical coordinates, $\psi_{\mathrm{p}}(r)$ is a radial wave function of the $6p$ orbital and $Y_{1L_z}(\theta,\phi)$ is a spherical harmonic. The wave functions $\psi_{\mathrm{s}}(r)$ and $\psi_{\mathrm{p}}(r)$ are normalized by the conditions,

$$4\pi\int_0^\infty \left|\psi_\nu(r)\right|^2 r^2dr \ = \ 1, \qquad \nu \ = \ \mathrm{s},\mathrm{p}.$$

Asymptotic expression for the single electron spatial wave functions: When the distance r between nucleus and the valence electron exceeds the radius of the inner (closed shell) orbitals (which is smaller than the atomic radius), the single electron wave function $\psi_{\mathrm{s}}(r)$ and the radial wave function $\psi_{\mathrm{p}}(r)$ can be approximated by the following expressions,

$$\psi_\nu(r) \ = \ \sqrt{\frac{2\mathcal{A}_\nu\ \kappa_\nu^3}{\pi\Gamma\left(\frac{2+\beta_\nu}{\beta_\nu}\right)}}\ \left(2\kappa_\nu r\right)^{\frac{1-\beta_\nu}{\beta_\nu}}\ e^{-\kappa_\nu r}.\tag{B2}$$

Here the parameters κ_ν and β_ν are determined by the ionization energy ε_ν of the atom in the ground [$\nu = \mathrm{s}$] or excited [$\nu = \mathrm{p}$] state,

$$\kappa_\nu \;=\; \frac{\sqrt{2m_e\varepsilon_\nu}}{\hbar}, \qquad \beta_\nu \;=\; \kappa_\nu a_B,$$

where m_e is the electron mass and a_B is the Bohr's radius. Taking the values

$$\varepsilon_\mathrm{s} \;=\; 6.2542 \text{ eV}, \qquad \varepsilon_\mathrm{p} \;=\; 3.8104 \text{ eV},$$

we get

$$\kappa_\mathrm{s} \;=\; 1.2812 \text{ Å}^{-1}, \qquad \beta_\mathrm{s} \;=\; 0.67680, \quad \text{(B3a)}$$
$$\kappa_\mathrm{p} \;=\; 1.0004 \text{ Å}^{-1}, \qquad \beta_\mathrm{p} \;=\; 0.52936. \quad \text{(B3b)}$$

The dimensionless parameter $\mathcal{A}_\mathrm{s}$ or $\mathcal{A}_\mathrm{p}$ encodes the behavior of the function $\psi_\mathrm{s}(r)$ or $\psi_\mathrm{p}(r)$ inside the atom. In the following, we will consider $\mathcal{A}_\mathrm{s}$ and $\mathcal{A}_\mathrm{p}$ as fitting parameters.

Appendix B main points: In this section the electronic wave functions of the Yb atoms are calculated. The most important interaction that determines these wave functions is the Coulomb interaction with the atomic nucleus. A few words about the role of spin-orbit and hyperfine interactions are in order. Spin orbit interaction results in splitting of the $6s6p$ electronic configuration into the $^3\mathrm{P}_0$, $^3\mathrm{P}_1$, $^3\mathrm{P}_2$ and $^1\mathrm{P}_1$ quantum states. We consider here the $^3\mathrm{P}_2$ state. Hyperfine interaction splits the $^3\mathrm{P}_2$ state into the states with total atomic orbital momentum $F = \frac{1}{2}, \frac{3}{2}, \frac{5}{2}, \ldots, \frac{9}{2}$. The Hamiltonian (H1) consists of only the Coulomb interaction since it yields the main contribution to the tunnelling rates. Taking into account also spin-orbit and hyperfine interactions modifies the expressions for the tunnelling rates and, as a result, modifies the Hamiltonian (15). However, both the spin-orbit and the hyperfine interactions satisfy SU(2) spin-rotational symmetry, and therefore the Hamiltonian (17) [which is also SU(2) invariant] is unchanged. The sole effect of the spin-orbit and hyperfine interactions on the Kondo Hamiltonian (17) comprises a slight modification of the couplings λ_d, λ_q and λ_o.

Appendix C: Wave Functions of Yb Atoms in the $^1\mathbf{S}_0$ and $^3\mathbf{P}_2$ States

In this section we present the wave functions of the ground and meta-stable states of the neutral ytterbium atom, as well as the wave functions of the positively and negatively charged ions in their respective virtual states.

1. Wave Functions of Neutral Atom

Electronic configuration of the ^{173}Yb atom in the ground $^1\mathrm{S}_0$ state is $6s^2$. The nuclear spin is $I = \frac{5}{2}$. The wave function of the ground state is,

$$\begin{aligned}\langle \mathbf{r}_a, \mathbf{r}_b \big| \mathrm{g}, i\rangle &= \Psi_{\mathrm{g},i}(\mathbf{r}_a, \mathbf{r}_b) \\ &= \psi_\mathrm{s}(r_a)\psi_\mathrm{s}(r_b)\chi_\mathrm{S}(a,b)\mathcal{X}_i, \end{aligned} \quad \text{(C1)}$$

where $\mathbf{r}_a$ and $\mathbf{r}_b$ are the positions of electrons, i is a nuclear magnetic quantum number, $i = \pm\frac{1}{2}, \pm\frac{3}{2}, \pm\frac{5}{2}$ and $\mathcal{X}_i$ is the spin wave function of the nucleus with nuclear magnetic quantum number i. The position of the nucleus is chosen as the origin of the frame of coordinates. The spatial wave function is symmetric with respect to the permutation of the electrons. According to the Pauli principle, the Yb atom with the $6s^2$ electronic configuration is in the spin singlet state. The corresponding spin wave function $\chi_\mathrm{S}(a,b)$ is,

$$\chi_\mathrm{S}(a,b) \;=\; \frac{1}{\sqrt{2}}\Big\{\tilde{\chi}_\uparrow(a)\tilde{\chi}_\downarrow(b) - \tilde{\chi}_\downarrow(a)\tilde{\chi}_\uparrow(b)\Big\}, \quad \text{(C2)}$$

where $\tilde{\chi}_\sigma(a)$ or $\tilde{\chi}_\sigma(b)$ is a wave function of a single electron with spin $\sigma = \uparrow, \downarrow$.

Consider now the Yb* atom in the long lived $^3\mathrm{P}_2$ excited state. The corresponding electronic wave functions are,

$$\Psi_{J_z}(\mathbf{r}_a, \mathbf{r}_b) \;=\; \sum_{L_z,S_z} C^{J,J_z}_{L,L_z;S,S_z}\; \tilde{\Psi}_{L_z,S_z}(\mathbf{r}_a, \mathbf{r}_b), \quad \text{(C3)}$$

where $C^{J,J_z}_{L,L_z;S,S_z}$ are the Clebsch-Gordan coefficients, $L = 1$ is the angular momentum of the $6s6p$ electronic configuration, $S = 1$ is the total electronic spin, $J = 2$ is the total electronic angular momentum. $\tilde{\Psi}_{L_z,S_z}(\mathbf{r}_a, \mathbf{r}_b)$ describes valence electrons of Yb atom in the $6s6p$ configuration with the electronic angular magnetic quantum number L_z and the spin magnetic quantum number S_z ($L_z, S_z = 0, \pm 1$),

$$\begin{aligned}\tilde{\Psi}_{L_z,S_z}(\mathbf{r}_a, \mathbf{r}_b) \;=\; \frac{1}{\sqrt{2}}\Big\{&\psi_\mathrm{s}(r_a)\psi_{L_z}(\mathbf{r}_b) - \\ &- \psi_{L_z}(\mathbf{r}_a)\psi_\mathrm{s}(r_b)\Big\}\; \chi_{S_z}(a,b). \end{aligned} \quad \text{(C4)}$$

The spin triplet wave functions $\chi_{S_z}(a,b)$ are,

$$\chi_{S_z}(a,b) \;=\; \sum_{\sigma,\sigma'} C^{1,S_z}_{\frac{1}{2},\sigma;\frac{1}{2},\sigma'}\; \tilde{\chi}_\sigma(a)\tilde{\chi}_{\sigma'}(b), \quad \text{(C5)}$$

where $C^{1,S_z}_{\frac{1}{2},\sigma;\frac{1}{2},\sigma'}$ are the Clebsch-Gordan coefficients, $\tilde{\chi}_\sigma(a)$ and $\tilde{\chi}_\sigma(b)$ are wave function of single electron with spin $\sigma = \uparrow, \downarrow$.

2. Hyperfine Splitting

The hyperfine interaction between the electrons with angular momentum $J = 2$ and the nucleus with spin $I = \frac{5}{2}$ results in the splitting of the $(2J+1)(2I+1)$ fold degenerate level into five energy levels with given total angular momentum F [$F = \frac{1}{2}, \frac{3}{2}, \frac{5}{2}, \frac{7}{2}$ and $\frac{9}{2}$]. Every level is $2F+1$ fold degenerate. We focus here on the

state with $F = \frac{3}{2}$. The corresponding wave functions are,

$$\Psi_{\mathrm{x},f}(\mathbf{r}_a,\mathbf{r}_b) \;=\; \sum_{J_z,i} C^{F,f}_{J,J_z;I,i}\; \Psi_{J_z}(\mathbf{r}_a,\mathbf{r}_b)\; \mathcal{X}_i, \quad \text{(C6)}$$

where $C^{F,f}_{J,J_z;I,i}$ are the Clebsch-Gordan coefficients, $f = \pm\frac{1}{2}, \pm\frac{3}{2}$ is the total atomic magnetic quantum number, and $\Psi_{J_z}(\mathbf{r}_a,\mathbf{r}_b)$ are the electronic wave functions (C3) of the Yb(^{3}P$_2$) quantum states. The wave function $\mathcal{X}_i$ is the spin function of the nucleus of the ^{173}Yb atom with nuclear magnetic quantum number i [$i = \pm\frac{1}{2}, \pm\frac{3}{2}, \pm\frac{5}{2}$]. Finally, using eqs. (C3) and (C5), we can express the wave functions (C6) in terms of the single-electronic wave functions,

$$\begin{aligned}\Psi_{\mathrm{x},f}(\mathbf{r}_a,\mathbf{r}_b) \;=\; & \frac{1}{\sqrt{2}} \sum_{J_z,i} C^{F,f}_{J,J_z;I,i} \times \\ & \times \sum_{L_z,S_z} C^{J,J_z}_{L,L_z;S,S_z} \sum_{\sigma,\sigma'} C^{1,S_z}_{\frac{1}{2},\sigma;\frac{1}{2},\sigma'} \times \\ & \times \Big\{ \psi_{\mathrm{s}}(r_a)\psi_{L_z}(\mathbf{r}_b) - \psi_{L_z}(\mathbf{r}_a)\psi_{\mathrm{s}}(r_b) \Big\} \times \\ & \times \tilde{\chi}_{\sigma}(a)\; \tilde{\chi}_{\sigma'}(b)\; \mathcal{X}_i. \end{aligned} \quad \text{(C7)}$$

In what follows, we use also a bracket notation of the wave functions (C7) of the excited ^{3}P$_2$ state with $F = \frac{3}{2}$,

$$\big\langle \mathbf{r}_a,\mathbf{r}_b \big| \mathrm{x},f \big\rangle \;=\; \Psi_{\mathrm{x},f}(\mathbf{r}_a,\mathbf{r}_b), \quad \text{(C8)}$$

where $f = \pm\frac{1}{2}, \pm\frac{3}{2}$ is a total atomic magnetic quantum number.

3. Electronic Wave Function of Two Neutral Atoms

Electronic wave functions of two ^{173}Yb atoms, one in the ground state, and the other one in the excited state,

$$\begin{aligned}\big\langle \mathbf{r}_{1a},\mathbf{r}_{1b};\mathbf{r}_{2c},\mathbf{r}_{2d} \big| \mathrm{g},i;\; \mathrm{x},f \big\rangle = \frac{1}{4!} \sum_{P_{a,b,c,d}} P_{a,b,c,d} \times \\ \times\; \Psi_{\mathrm{g},i}(\mathbf{r}_{1a},\mathbf{r}_{1b}) \Phi_{\mathrm{x},f}(\mathbf{r}_{2c},\mathbf{r}_{2d}), \end{aligned} \quad \text{(C9)}$$

where $\Psi_{\mathrm{g},i}(\mathbf{r}_a,\mathbf{r}_b)$ is the wave function (C1) of the ^{173}Yb atom in the ground ^{1}S$_0$ state with nuclear spin $I = \frac{5}{2}$ and $i = \pm\frac{1}{2}, \pm\frac{3}{2}, \pm\frac{5}{2}$, $\Psi_{\mathrm{x},f}(\mathbf{r}_c,\mathbf{r}_d)$ are the wave functions (C7) of the Yb atom in the excited ^{3}P$_2$ state with $F = \frac{3}{2}$ and $f = \pm\frac{1}{2}, \pm\frac{3}{2}$. $\mathbf{r}_{j\nu} = \mathbf{r}_\nu - \mathbf{R}_j$ ($j = 1,2$ and $\nu = a,b,c,d$), $\mathbf{r}_\nu$ and $\mathbf{R}_j$ are the position vectors of the electrons and the nuclei. $P_{a,b,c,d}$ denotes permutation of the electrons, it equals 1 or -1 for even or odd number of permutations.

Appendix D: Wave Functions of Positively and Negatively Charged Ions

The wave function of a positively charged Yb atom with $6s$ electronic configuration reads,

$$\Psi_{\mathrm{h},\sigma,i}(\mathbf{r}_a) \;=\; \psi_{\mathrm{s}}(r_a)\tilde{\chi}_\sigma(a)\mathcal{X}_i, \quad \text{(D1)}$$

where the index h ("hole") indicates positive charging of the atom. The wave function of negatively charged Yb atom with $6s^2 6p$ electronic configuration is,

$$\begin{aligned}\Psi_{\mathrm{e},L_z,\sigma,i}(\mathbf{r}_a,\mathbf{r}_b,\mathbf{r}_c) \;=\; & \\ =\; \frac{\mathcal{X}_i}{\sqrt{3}} \Big\{ & \psi^{\mathrm{e}}_{L_z}(\mathbf{r}_a)\psi^{\mathrm{e}}_{\mathrm{s}}(r_b)\psi^{\mathrm{e}}_{\mathrm{s}}(r_c)\tilde{\chi}_\sigma(a)\chi_{\mathrm{S}}(b,c) + \\ & + \psi^{\mathrm{e}}_{L_z}(\mathbf{r}_b)\psi^{\mathrm{e}}_{\mathrm{s}}(r_c)\psi^{\mathrm{e}}_{\mathrm{s}}(r_a)\tilde{\chi}_\sigma(b)\chi_{\mathrm{S}}(c,a) + \\ & + \psi^{\mathrm{e}}_{L_z}(\mathbf{r}_c)\psi^{\mathrm{e}}_{\mathrm{s}}(r_a)\psi^{\mathrm{e}}_{\mathrm{s}}(r_b)\tilde{\chi}_\sigma(c)\chi_{\mathrm{S}}(a,b) \Big\}. \end{aligned} \quad \text{(D2)}$$

This wave function is antisymmetric with respect to permutation of any pair of electrons. Electronic wave functions of two ^{173}Yb ions, one positively charged and the second one negatively charged, are,

$$\begin{aligned}\big\langle \mathbf{r}_{1a},\mathbf{r}_{2b},\mathbf{r}_{2c},\mathbf{r}_{2d} \big| \mathrm{h},\sigma,i;\; \mathrm{e},L_z,\sigma',i' \big\rangle = \\ = \frac{1}{4!} \sum_{a',b',c',d'} P^{a',b',c',d'}_{a,b,c,d}\; \big(-1\big)^P\; \Psi_{\mathrm{h},\sigma,i}(\mathbf{r}_{1a'}) \times \\ \times\; \Psi_{\mathrm{e},L_z,\sigma',i'}(\mathbf{r}_{2b'},\mathbf{r}_{2c'},\mathbf{r}_{2d'}), \end{aligned} \quad \text{(D3)}$$

where $\Psi_{\mathrm{h},\sigma,i}(\mathbf{r}_a)$ and $\Psi_{\mathrm{e},L_z,\sigma',i'}(\mathbf{r}_b,\mathbf{r}_c,\mathbf{r}_d)$ are the wave functions (D1) and (D2) of the positively and negatively charged ions. $P^{a',b',c',d'}_{a,b,c,d}$ is a permutation operator, see eq. (9). The factor $(-1)^P$ indicates the Pauli principle, it equals 1 for even permutations of electrons and -1 for odd permutations. $\mathbf{r}_{j\nu} = \mathbf{r}_\nu - \mathbf{R}_j$ ($j = 1,2$ and $\nu = a,b,c,d$), $\mathbf{r}_\nu$ and $\mathbf{R}_j$ are the position vectors of the electrons and the nuclei.

Appendices C and D main points: To calculate the exchange interaction we are guided by the analysis in subsection III D and especially Fig. 3. That is, we need to know not only the electronic wave functions of a single atom but also the wave functions of two neutral atoms as well as the wave functions of positively and negatively charged ions This later task is carried out in these three sections.

Appendix E: Trapping of Yb and Yb* Atoms by Optical Potential

The Yb(^{1}S$_0$) and Yb*(^{3}P$_2$) atoms are trapped by a state-dependent trapping potentials $V_{\mathrm{g,x}}(\mathbf{R})$,

$$V_{\mathrm{g}} \;=\; V^{(0)}_{\mathrm{g}}\; k^2_{\mathrm{g}} R^2, \qquad R \;=\; \big|\mathbf{R}\big|, \quad \text{(E1)}$$

$$V_{\mathrm{x}} \;=\; V^{(0)}_{\mathrm{x}} \sum_\alpha \sin^2\big(k_{\mathrm{x}} X_\alpha\big), \quad \text{(E2)}$$

where α is a Cartesian index. The potential parameters are tuned such that

$$V^{(0)}_{\mathrm{g}} k^2_{\mathrm{g}} \;\ll\; V^{(0)}_{\mathrm{x}} k^2_{\mathrm{x}}, \quad \text{(E3)}$$

and therefore the atoms in the ground state are considered as itinerant atoms, and the atom in the excited state plays a role of the impurity.

In the adiabatic (Born-Oppenheimer) approximation (which is well substantiated in atomic physics), the wave function of a single ytterbium atom is expressed as a product of the wave functions $\Psi(\mathbf{R})$ (for the rigid ion core) and $\psi(\mathbf{r}_a, \mathbf{r}_b)$ (for the valence electrons). The former is considered as a point particle of mass M whose position vector in Cartesian coordinates is $\mathbf{R} = (X, Y, Z)$. Strictly speaking, we should describe the system by many-particle wave function $\Psi(\mathbf{R}_0; \{\mathbf{R}\}_{\mathcal{N}})$, where $\mathcal{N}$ is the number of itinerant atoms, $\{\mathbf{R}\}_{\mathcal{N}} = \{\mathbf{R}_1, \mathbf{R}_2, ..., \mathbf{R}_{\mathcal{N}}\}$, $\mathbf{R}_j$ is the position of an itinerant atom ($j = 1, 2, \ldots, \mathcal{N}$) and $\mathbf{R}_0$ is the position of the impurity atom. When the distances between all the atoms exceed the range of the van der Waals interaction, the many-particle wave function splits into a sum of products of single-particle wave functions. When an itinerant atom is placed close to the impurity and all other atoms are far away, the many particle wave function is a product of a two-particle wave function describing interacting pair of atoms, and single particle wave functions describing motion of the other itinerant atoms. Usually, the density of itinerant atoms is low and the probability to find two or more itinerant atoms close to the impurity is negligibly small. Here we derive two atomic wave functions that are appropriate at large distance between the Yb and Yb* atoms, and consequently the interaction between the atoms can safely be neglected. The two atomic wave functions appropriate for short inter atomic distance are derived in Sec. F.

In order to find the wave functions and energies of the itinerant Yb atoms and the impurity atom in the 3D potential well, we need to solve the following Schrödinger equation for $\Psi_\nu(\mathbf{R})$ ($\nu = \mathrm{g}, \mathrm{x}$ for the itinerant atoms or the impurity),

$$\frac{\hbar^2 \mathbf{K}^2}{2M}\, \Psi_\nu(\mathbf{R}) + V_\nu(\mathbf{R})\Psi_\nu(\mathbf{R}) \;=\; \varepsilon\, \Psi_\nu(\mathbf{R}). \quad \text{(E4)}$$

Consider first the impurity atom. When the corresponding energy level $\varepsilon_{\rm imp}$ is deep enough, the wave function of the bound state near the potential minimum at $\mathbf{R} = 0$ can be approximated within the harmonic potential picture as,

$$\Psi_{\rm x}(R) \;=\; \frac{1}{\left(\pi a_{\rm x}^2\right)^{1/4}}\, \exp\left(-\frac{R^2}{2a_{\rm x}^2}\right), \quad \text{(E5)}$$

where

$$k_{\rm x} a_{\rm x} \;=\; \sqrt{\frac{\hbar\omega_{\rm x}}{V_{\rm x}^{(0)}}}, \qquad \omega_{\rm x} \;=\; \sqrt{\frac{2V_{\rm x}^{(0)} k_{\rm x}^2}{M}}. \quad \text{(E6)}$$

The corresponding energy $\varepsilon_{\rm imp}$ is,

$$\varepsilon_{\rm imp} \;=\; \frac{3}{2}\, \hbar\omega_{\rm x}.$$

Second, consider the wave function of the itinerant atoms, for which the shallow potential wells are not deep enough to form bound states. Quantum states of atoms in subject to the isotropic potential (E1) are described by the radial quantum number n [$n = 0, 1, 2, \ldots$], orbital quantum number L [$L = 0, 1, 2, \ldots$] and projection m of the orbital moment on the axis z [$m = L, L+1, \ldots, L$]. Due to the centrifugal barrier, only the atoms with $L = 0$ can approach the impurity and be involved in the exchange interaction with it. The wave functions of the states with $L = 0$ found from the Schrödinger equation (E4) are,

$$\Psi_{\rm g}^n(\mathbf{R}) \;=\; \frac{\mathcal{N}_n}{\sqrt{4\pi}}\, L_n^{(\frac{1}{2})}\left(\frac{R^2}{a_{\rm g}^2}\right)\, \exp\left(-\frac{R^2}{2a_{\rm g}^2}\right), \quad \text{(E7)}$$

where $L_n^{(\frac{1}{2})}(\rho)$ are generalized Laguerre polynomials. The normalization factor is

$$\mathcal{N}_n \;=\; \left(\frac{2}{\pi a_{\rm g}^6}\right)^{1/4} \sqrt{\frac{2^{n+2} n!}{(2n+1)!!}}.$$

The parameters $a_{\rm g}$ and $\omega_{\rm g}$ are defined through,

$$k_{\rm g} a_{\rm g} \;=\; \sqrt{\frac{\hbar\omega_{\rm g}}{V_{\rm g}^{(0)}}}, \qquad \omega_{\rm g} \;=\; \sqrt{\frac{2V_{\rm g}^{(0)} k_{\rm g}^2}{M}}. \quad \text{(E8)}$$

The corresponding energy levels are

$$\varepsilon_n \;=\; \hbar\omega_{\rm g}\left(2n + \frac{3}{2}\right). \quad \text{(E9)}$$

The inequality (E3) imply

$$\omega_{\rm g} \ll \omega_{\rm x}.$$

Within this framework, the spectrum is nearly continuous and the ytterbium atoms in the ground-state form a Fermi gas. The Fermi energy ϵ_F is such that $\epsilon_F \gg \omega_{\rm g}$, hence the Fermi gas is 3D. and the nuclei.

Appendix E main points: The scattering and exchange interaction between the ground and trapped excited Yb atoms occurs inside the trap. Its analysis requires the knowledge of the wave function inside the state dependent traps (trapping potentials V_g for the ground-state and V_x for the excited state). The corresponding wave functions of the atoms (as point particles) inside their respective traps are constructed in this section. Scattering analysis is carried out in the next section.

Appendix F: Scattering of the Itinerant Atoms by Localized Impurities

In order to elucidate the behavior of the two atom wave function within the interval $|\mathbf{R}_1 - \mathbf{R}_0| \le c$ [where $\mathbf{R}_0$ and $\mathbf{R}_1$ are positions of the Yb* and Yb atoms, c is given by eq. (F4) below], we adopt the semiclassical technique developed in Ref.[36]. It is important that the trapping

potentials $V_{\rm x}(\mathbf{R}_0)$ and $V_{\rm g}(\mathbf{R}_1)$ change slowly on the distances of order c. Therefore the wave function $\Psi_{\rm r}(\mathbf{R})$ describing relative motions of the atoms satisfies the following Schrödinger equation[28],

$$\left\{\frac{\hbar^2\mathbf{K}^2}{M}+W(\mathbf{R})-\mathcal{E}_{\rm r}\right\}\Psi_{\rm r}(\mathbf{R}) \;=\; 0, \qquad \text{(F1)}$$

where $\mathbf{R}=\mathbf{R}_1-\mathbf{R}_0$. We describe the van der Waals interaction by the potential[33],

$$W(R) \;=\; -\frac{C_6}{R^6}-\frac{C_8}{R^8}+\frac{C_{12}}{R^{12}}. \qquad \text{(F2)}$$

Here $C_6 = 2.649\cdot 10^3\ E_h a_B^6$, $C_8 = 3.21097\cdot 10^5\ E_h a_B^8$ and $C_{12} = 1.41808\cdot 10^9\ E_h a_B^{12}$, where $E_h = 27.2114$ eV and $a_B = 0.529177$ Å.

Since $W(R)$ depends just on the distance R from the impurity, the orbital angular momentum L and its projection m on the axis z are good quantum numbers. Because of the centrifugal barrier, just atoms with $L=0$ can approach close one to another. Therefore we restrict ourselves by considering just the s-wave (i.e., the wave with $L=0$). Solution of the equation (F1) is evident but rather cumbersome (see Refs.[28,36] for details). The wave function of the s-wave satisfying eq. (F1) is

$$\Psi(\mathbf{R}) \;=\; \frac{\psi(R)}{\sqrt{4\pi}\,R}. \qquad \text{(F3)}$$

In order to find the wave function $\psi(R)$, we note that there are different intervals of R where we employ different approximations to solve eq. (F1):

- For $r_0 < R < c$ we apply the Wentzel-Kramers-Brillouin (WKB) approximation;
- For $b_0 < R < c$, we can approximate $W(R)$ by C^6/R^6.

Here $r_0 = 3.6673$ Å is found from the equation $W(r_0)=0$, b_0 is constrained by the inequalities,

$$\frac{C_6}{b_0^6} \;\gg\; \frac{C_8}{b_0^8}, \qquad \frac{C_6}{b_0^6} \;\gg\; \frac{C_{12}}{b_0^{12}}.$$

We take $b_0 = 8$ Å. The parameter c is

$$c \;=\; \left(\frac{MC_6}{\hbar^2}\right)^{1/4} \;=\; 89.9569\ \text{Å}, \qquad \text{(F4)}$$

The intervals $r_0 < R \ll c$ and $b_0 < R < c$ overlap with each other since there is a wide interval $b_0 < R \ll c$ where both the WKB approximation and the approximation $W(R)\approx C_6/R^6$ are valid. Therefore, within this interval, both approaches should give the same solution. We use this condition as a connection constraint for the solutions within the two overlapping intervals.

1. The interval $r_0 < R \ll c$: The wave function calculated within the WKB approximation with quantum corrections[28,36,37] is,

$$\psi^{(1)}(R) \;=\; \frac{A_1}{\sqrt{K(R)}}\,\sin\left(\Phi_{\rm r}(R)+\frac{\pi}{4}\right). \qquad \text{(F5)}$$

Here

$$K(R) \;=\; \frac{1}{\hbar}\,\sqrt{-MW(R)}, \qquad \text{(F6)}$$

$$\Phi_{\rm r}(R) \;=\; \int_{r_0}^{R} K(R')\,dR'. \qquad \text{(F7)}$$

When the distance between the atoms exceeds c, the interaction between the atoms can be neglected and the two-atomic wave function is a product of the single atomic wave functions describing motion of the atoms in the state dependent trapping potential[28]. The wave function and its derivative are continues at $R=c$. Then we have,

$$A_1 = \frac{2\sqrt{kc}}{\pi a_{\rm g}}\,\Gamma\left(\frac{3}{4}\right)\,\sqrt{1+\left(\frac{a_w-\bar{a}}{\bar{a}}\right)^2}, \qquad \text{(F8)}$$

where

$$k \;=\; \frac{\sqrt{M\mathcal{E}_{\rm r}}}{\hbar}, \qquad \text{(F9)}$$

the parameters $\bar{a}$ and a_w are given by eqs. (F12) and (F11) below.

2. The interval $R > b_0$: Within this interval, we can approximate the potential energy by $W(R)\approx C_6/R^6$. The wave function $\psi^{(2)}(R)$ for this interval is,

$$\psi^{(2)}(R) \;=\; A_2\tilde{\psi}_{2A}(R)+B_2\tilde{\psi}_{2B}(R), \qquad \text{(F10)}$$

where $\tilde{\psi}_{2A}(R)$ and $\tilde{\psi}_{2B}(R)$ are,

$$\tilde{\psi}_{2A}(R) \;=\; \sqrt{\frac{2R}{c}}\,J_{1/4}\left(\frac{c^2}{2R^2}\right),$$

$$\tilde{\psi}_{2B}(R) \;=\; \sqrt{\frac{2R}{c}}\,J_{-1/4}\left(\frac{c^2}{2R^2}\right).$$

There is an interval $b_0 < R \ll c$, where we can approximate $W(R)$ by $-C_6/R^6$ and apply the WKB approximation[36]. Therefore, within this interval the equality $\psi^{(1)}(R) = \psi^{(2)}(R)$ is valid. This equality gives[28],

$$A_2 \;=\; -A_1\,\frac{\sqrt{\pi c}}{2}\,\cos\left(\Phi_w+\frac{\pi}{8}\right),$$

$$B_2 \;=\; A_1\,\frac{\sqrt{\pi c}}{2}\,\sin\left(\Phi_w+\frac{3\pi}{8}\right),$$

where

$$\Phi_w \;=\; \int_{r_0}^{\infty} K(R)\,dR \;=\; 346.440832.$$

For $R > c$, the functions $\tilde{\psi}_{2A}(R)$ and $\tilde{\psi}_{2B}(R)$ are well approximated by expressions that are linear with R[28,36],

that is, $\psi^{(2)}(R) \propto R - a_w$, where the scattering length a_w is,

$$a_w = \bar{a}\left\{1 - \tan\left(\Phi_w - \frac{\pi}{8}\right)\right\} = \\ = 20.9973 \text{ Å}, \quad \text{(F11)}$$

$$\bar{a} = \frac{c}{2^{3/2}}\frac{\Gamma(3/4)}{\Gamma(5/4)} = 42.9984 \text{ Å}. \quad \text{(F12)}$$

Appendix F main points: Accurate analysis of low energy scattering of ground and excited states of Yb atoms is crucial for elucidating the exchange constant. In our previous study of Yb(^{1}S$_0$)-Yb(^{3}P$_0$) scattering have already shown that in this case, the atom-atom (van-der Waals) potential should be treated and inspected and adapted carefully in different region of configuration space[28]. In the present section we applied a similar procedure for Yb(^{1}S$_0$)-Yb(^{3}P$_2$) scattering.

Appendix G: Local Density of State

As it is shown in our previous work[28], the van der Waals interaction between itinerant atoms and a localized impurity results in sufficient decreasing of the local density of states (LDOS) of itinerant atoms at short distances from the impurity. We calculate here the LDOS of itinerant atoms interacting with a localized impurity.

The LDOS at short distances between an itinerant atom from the impurity, [that is, $R < b_0$] is defined as[28],

$$\rho(\epsilon, R) = \frac{4\pi}{R^2}\sum_{n=0}^{\infty}\left|\psi_n^{(1)}(R)\right|^2\delta(\epsilon - \varepsilon_n), \quad \text{(G1)}$$

where $\psi_n^{(1)}(R)$ is given by eq. (F5), ε_n is given by eq. (E9). Employing the fact that the function $\sin^2(\Phi_{\rm r}(R) + \pi/4)$ strongly oscillates, whereas the potential and the exchange interactions change smoothly [see Ref.[28]], we can approximate $\sin^2(\Phi_{\rm r}(R) + \pi/4)$ by its averaged value $1/2$ and write the "smooth" part of the LDOS as,

$$\rho(\epsilon, R) = \Re(R)\ \rho_0(\epsilon), \quad \text{(G2)}$$

where $\rho_0(\epsilon)$ is a bare DOS,

$$\rho_0(\epsilon) = \sqrt{\epsilon}\left(\frac{M}{2\hbar^2}\right)^{3/2}\Theta(\epsilon), \quad \text{(G3)}$$

where M is the atomic mass. The factor $\Re(R)$ describes "deformation" of the DOS due to the van der Waals interaction with a localized impurity,

$$\Re(R) = \frac{8c}{R^2\ K(R)}\left[1 + \left(\frac{a_w - \bar{a}}{\bar{a}}\right)^2\right]. \quad \text{(G4)}$$

Here the function $K(R)$ is given by eq. (F6), and the parameters $\bar{a}$ and a_w are given by eqs. (F11) and (F12).

Appendix G Main points: The local density of states of the itinerant atoms calculated in this appendix multiplies the exchange constants to yield the dimensionless exchange constants. These quantities determine the Kondo temperature and are renormalized according to the scaling equations.

Appendix H: Tunneling Rates

We consider here tunnelling of $6s$ electron from the atom in the ground state to the atom in the excited state and tunneling of $6p$ electron from the atom in the excited state to the atom in the ground state.

In order to derive the tunneling rates, we need to start with the two-atom Hamiltonian. We take into account the fact that fine and hyperfine interactions are much weaker than Coulomb interaction, hence they are neglect in these calculations. Then we can write the Hamiltonian as,

$$\mathcal{H} = \sum_{\nu}\frac{\hbar^2\mathbf{k}_\nu^2}{2m_e} + \sum_j\sum_\nu V_{\rm i}(\mathbf{r}_\nu - \mathbf{R}_j) + \\ + \frac{1}{2}\sum_{\nu\neq\nu'}\frac{e^2}{\left|\mathbf{r}_\nu - \mathbf{r}_{\nu'}\right|} + \frac{4e^2}{\left|\mathbf{R}_1 - \mathbf{R}_2\right|}. \quad \text{(H1)}$$

Here $\mathbf{r}_\nu$ and $\mathbf{k}_\nu = -i\partial_{\mathbf{r}_\nu}$ are the position vector and wave vector of electron $[\nu, \nu' = a, b, c, d]$, $\mathbf{R}_j$ is the position vector of the ions $[j = 1, 2]$. In the following, we chose the center of mass of the two atom system at the origin of the coordinate frame. Moreover, the axis connecting two rigid ions are chosen as a X_3 axis. In this frame, the position vectors are $\mathbf{R}_1 = R\mathbf{e}_3/2$ and $\mathbf{R}_2 = -R\mathbf{e}_3/2$, where R is the distance between the atoms.

1. Tunneling Rate of the $6s$ Electron

Tunneling rate of a $6s$ electron is defined as,

$$V^{(\rm s)}_{\sigma,\sigma',L_z,i';f} = \int d^3\mathbf{r}_a d^3\mathbf{r}_b d^3\mathbf{r}_c d^3\mathbf{r}_d \times \\ \times\ \overline{\Psi}_{{\rm h},\sigma,i}(\mathbf{r}_{1a})\overline{\Psi}_{{\rm e},L_z,\sigma',i'}(\mathbf{r}_{2b}, \mathbf{r}_{2c}, \mathbf{r}_{2d}) \times \\ \times\ \mathcal{H}\ \Psi_{{\rm g},i}(\mathbf{r}_{1a}, \mathbf{r}_{1b})\Psi_{{\rm x},f}(\mathbf{r}_{2c}, \mathbf{r}_{2d}), \quad \text{(H2)}$$

where $\overline{\Psi}$ implies complex conjugation of the spatial wave function and Hermitian conjugation of the electronic and nuclear spin wave functions. $\mathbf{r}_{j\nu} = \mathbf{r}_\nu - \mathbf{R}_j$, where $\mathbf{r}_\nu$ and $\mathbf{R}_j$ are the position vectors of the electrons and the nuclei, $j = 1, 2$ and $\nu = a, b, c, d$.

In the next step, we take into account eqs. (C1), (C7), (D1) and (D2), and that enables us to write $V^{(\rm s)}_{\sigma,\sigma',L_z,i';f}$ as

$$V^{(\rm s)}_{\sigma,\sigma',L_z,i';f} = -\frac{t_{\rm s}}{\sqrt{6}}\ C^{F,L_z+i'+\sigma+\sigma'}_{J,L_z+\sigma+\sigma';I,i'} \\ \times C^{J,L_z+\sigma+\sigma'}_{L,L_z;S,\sigma+\sigma'}\ C^{S,\sigma+\sigma'}_{\frac{1}{2},\sigma;\frac{1}{2},\sigma'} \times \\ \times\delta_{f,L_z+i'+\sigma+\sigma'}, \quad \text{(H3)}$$

where

$$t_{\rm s} \;=\; \frac{1}{2}\int d^3\mathbf{r}\,\Big\{V_{\rm i}\big(|\mathbf{r}-\mathbf{R}_1|\big)+V_{\rm i}\big(|\mathbf{r}-\mathbf{R}_2|\big)\Big\}\times \\ \times\psi^*_{\rm s}\big(|\mathbf{r}-\mathbf{R}_2|\big)\;\psi_{\rm s}\big(|\mathbf{r}-\mathbf{R}_1|\big). \qquad \text{(H4)}$$

2. Tunneling Rate of the $6p$ Electron

Tunneling rate of a $6p$ electron is defined as,

$$V^{(\rm p)}_{\sigma,\sigma',L_z,i';f} \;=\; \int d^3\mathbf{r}_a d^3\mathbf{r}_b d^3\mathbf{r}_c d^3\mathbf{r}_d\times \\ \times\,\overline{\Psi}_{{\rm e},L_z,\sigma,i}(\mathbf{r}_{1a},\mathbf{r}_{1b},\mathbf{r}_{1c})\overline{\Psi}_{{\rm h},\sigma',i'}(\mathbf{r}_{2d})\times \\ \times\,\mathcal{H}\;\Psi_{{\rm g},i}(\mathbf{r}_{1a},\mathbf{r}_{1b})\Psi_{{\rm x},f}(\mathbf{r}_{2c},\mathbf{r}_{2d}). \qquad \text{(H5)}$$

Taking into account eqs. (C1), (C7), (D1) and (D2), we can write $V^{(\rm s)}_{\sigma,\sigma',L_z,i';f}$ as

$$V^{(\rm p)}_{\sigma,\sigma',L_z,i';f} \;=\; -\frac{t_{L_z}}{\sqrt{6}}\;C^{F,L_z+i'+\sigma+\sigma'}_{J,L_z+\sigma+\sigma';I,i'} \\ \times C^{J,L_z+\sigma+\sigma'}_{L,L_z;S,\sigma+\sigma'}\;C^{S,\sigma+\sigma'}_{\frac{1}{2},\sigma;\frac{1}{2},\sigma'}\times \\ \times\delta_{f,L_z+i'+\sigma+\sigma'}. \qquad \text{(H6)}$$

where

$$t_{L_z} \;=\; \frac{1}{2}\int d^3\mathbf{r}\,\Big\{V_{\rm i}\big(|\mathbf{r}-\mathbf{R}_1|\big)+V_{\rm i}\big(|\mathbf{r}-\mathbf{R}_2|\big)\Big\}\times \\ \times\psi^*_{L_z}\big(\mathbf{r}-\mathbf{R}_1\big)\;\psi_{L_z}\big(\mathbf{r}-\mathbf{R}_2\big). \qquad \text{(H7)}$$

Here we chose the direction of $\mathbf{R}=\mathbf{R}_1-\mathbf{R}_2$ as an axis of quantization for the angular momentum, and therefore L_z is a good quantum number during the tunneling. We can introduce a matrix $\hat{t}_{\rm p}$ as following,

$$\hat{t}_{\rm p}(\mathbf{e}_z) \;=\; {\rm diag}\big(t_1,t_0,t_1\big),$$

where we take into account the time reversal symmetry $t_1=t_{\bar{1}}$.

When the vector $\mathbf{R}$ is not collinear to the axis z, L_z is not a good quantum number during the tunneling. In this case, $\hat{t}_{\rm p}$ is not a diagonal matrix. Writing $\mathbf{R}$ in the spherical coordinates as,

$$\mathbf{R} \;=\; R\,\mathbf{e}_z, \qquad \mathbf{e}_R \;=\; \big(\sin\theta\cos\phi,\;\sin\theta\sin\phi,\;\cos\theta\big),$$

we can write the matrix $\hat{t}_{\rm p}$ as,

$$\hat{t}_{\rm p}(\mathbf{e}_R)=\frac{t_0+2t_1}{3}\;\hat{E}_3+\frac{t_1-t_0}{3}\;\begin{pmatrix} \frac{1}{4}\left[3\cos(2\theta)+1\right] & -\frac{3}{\sqrt{2}}\;\cos(\theta)\sin(\theta)\;e^{i\phi} & \frac{3}{2}\;\sin^2(\theta)\;e^{2i\phi} \\ -\frac{3}{\sqrt{2}}\;\cos(\theta)\sin(\theta)\;e^{-i\phi} & -\frac{1}{2}\left[3\cos(2\theta)+1\right] & \frac{3}{\sqrt{2}}\;\cos(\theta)\sin(\theta)\;e^{i\phi} \\ \frac{3}{2}\;\sin^2(\theta)\;e^{-i\phi} & \frac{3}{\sqrt{2}}\;\cos(\theta)\sin(\theta)\;e^{-2i\phi} & \frac{1}{4}\left[3\cos(2\theta)+1\right] \end{pmatrix}, \qquad \text{(H8)}$$

where $\hat{E}_3$ is the 3×3 identity matrix.

It is important to stress that due to the centrifugal barrier, only s-wave electrons can approach the impurity and be involved in the exchange interaction. Therefore, we should average $\hat{t}_{\rm p}$ over all the directions of $\mathbf{e}_R$. Integrating $\hat{t}_{\rm p}$ over the angles θ and ϕ gives the identity matrix,

$$\frac{1}{4\pi}\int\limits_0^{2\pi}d\phi\;\int\limits_0^{\pi}\sin\theta d\theta\;\hat{t}_{\rm p} \;=\; \frac{t_0+2t_1}{3}\;\hat{E}_3.$$

The coupling strength appearing in the Kondo Hamiltonian is proportional to the integral of $t_{\rm s}\hat{t}_{\rm p}(\mathbf{R})$ over the angles θ and ϕ. Taking into account the last equality, we conclude that the Kondo Hamiltonian is isotropic.

In what follows, we take $V^{(p)}_{\sigma,\sigma',L_z,i;f'}$ in the form,

$$V^{(\rm p)}_{\sigma,\sigma',L_z,i';f} \;=\; -\frac{t_{\rm p}}{\sqrt{6}}\;C^{F,L_z+i'+\sigma+\sigma'}_{J,L_z+\sigma+\sigma';I,i'} \\ \times C^{J,L_z+\sigma+\sigma'}_{L,L_z;S,\sigma+\sigma'}\;C^{S,\sigma+\sigma'}_{\frac{1}{2},\sigma;\frac{1}{2},\sigma'}\times \\ \times\delta_{f,L_z+i'+\sigma+\sigma'}, \qquad \text{(H9)}$$

where

$$t_{\rm p} \;=\; \frac{t_0+2t_1}{3}.$$

Appendix H main points: Guided by the analysis of the exchange interaction in subsection III D and especially Fig. 3, it is evident that the physics of electron tunneling between Yb atoms plays a crucial role. In the above section, tunneling rates are calculated ab-initio using atomic wave-functions computed in previous appendices.

Appendix I: Exchange Interaction

When an impurity atom is localized at the origin of coordinates and an itinerant atom is placed at position $\mathbf{R}$ so that they are separated by $R=|\mathbf{R}|$, there is an exchange interaction between them. The interaction Hamiltonian

is,

$$\mathcal{H}_{\rm exch}(R) \;=\; \sum_{f,f'}\sum_{i,i'} V_{f,f';i,i'}(R)\times \\ \times X^{f,f'}\;\hat{\psi}^{\dagger}_{i'}(\mathbf{R})\hat{\psi}_{i}(\mathbf{R}), \qquad \text{(I1)}$$

where $X^{f,f'} = |f\rangle\langle f'|$ are Hubbard operators of the localized impurity, $\hat{\psi}_i(\mathbf{R})$ and $\hat{\psi}^{\dagger}_i(\mathbf{R})$ are annihilation and creation operators of itinerant atoms at position $\mathbf{R}$ with the nuclear magnetic quantum number i. The rate $V_{f,f';i,i'}(R)$ is,

$$V_{f,f';i,i'}(R) \;=\; \frac{1}{\Delta\epsilon}\sum_{L_z,\sigma,\sigma'}\Big\{V^{(s)}_{\sigma,\sigma',L_z,i';f}V^{(p)}_{\sigma,\sigma',L_z,i;f'} + \\ +V^{(p)}_{\sigma,\sigma',L_z,i';f}V^{(s)}_{\sigma,\sigma',L_z,i;f'}\Big\} \;= \\ =\; \frac{t_{\rm s}(R)\;t_{\rm p}(R)}{3\;\Delta\epsilon}\sum_{j} C^{F,f}_{J,j;I,i}C^{F,f'}_{J,j;I,i'}. \qquad \text{(I2)}$$

Here $t_{\rm s}$ and $t_{\rm p}$ are given by eqs. (H3) and (H9),

$$\Delta\epsilon = \varepsilon_{\rm ion}+\varepsilon_{\rm ea}+\epsilon_{\rm g}-\epsilon_{\rm x} \;=\; 4.1104 \text{ eV},$$

where $\varepsilon_{\rm ion} = 6.2542$ eV is the ionization energy[34], $\varepsilon_{\rm ea} = 0.3$ eV is the electron affinity[35] and $\epsilon_{\rm x}-\epsilon_{\rm g} = 2.4438$ eV is the excitation energy of the $^3{\rm P}_2$ state[34].

Substituting eq. (I2) into eq. (I1), we get

$$\mathcal{H}_{\rm exch}(R) \;=\; g(R)\sum_{j}\sum_{f,f'}\sum_{i,i'} C^{F,f}_{J,j;I,i}C^{F,f'}_{J,j;I,i'}\times \\ \times X^{f,f'}\;\hat{\psi}^{\dagger}_{i'}(\mathbf{R})\hat{\psi}_{i}(\mathbf{R}), \qquad \text{(I3)}$$

where

$$g(R) \;=\; \frac{t_{\rm s}(R)\;t_{\rm p}(R)}{3\;\Delta\epsilon}. \qquad \text{(I4)}$$

Appendix J: Derivation of $\delta H^{(2)}_{\beta,\beta'}$, Eq. (27)

Here we consider in turn the various multiple contributions to $\delta H^{(2)}_{\beta,\beta'}$ with $\beta,\beta' = {\rm d},{\rm q},{\rm o}$.

1. **Dipole-dipole contribution**: The correction $\delta H^{(2)}_{\rm d,d}$ [eq. (27)] is,

$$\delta H^{(2)}_{\rm d,d} \;=\; -\frac{\lambda_{\rm d}^2}{D}\sum_{\alpha,\alpha'}\sum_{f,f',f''}\sum_{i,i',i''}\sum_{\mathbf{k},\mathbf{k}',\mathbf{q}} F^{\alpha}_{f,f''}F^{\alpha'}_{f'',f'}\times \\ \times X^{f,f'}\,c^{\dagger}_{\mathbf{k},i}c_{\mathbf{k}',i'}\Big(I^{\alpha}_{i,i''}I^{\alpha'}_{i'',i'}\big\langle c_{\mathbf{q},i''}c^{\dagger}_{\mathbf{q},i''}\big\rangle - \\ -I^{\alpha'}_{i,i''}I^{\alpha}_{i'',i'}\big\langle c^{\dagger}_{\mathbf{q},i''}c_{\mathbf{q},i''}\big\rangle\Big). \qquad \text{(J1)}$$

Here the energy of atoms with wave vectors $\mathbf{k},\mathbf{k}'$ belongs to the reduced energy band, whereas the energy of atoms with the wave vector $\mathbf{q}$ is located near the edge of the energy band such that

$$\big|\epsilon_{\mathbf{k}}\big|,\;\big|\epsilon_{\mathbf{k}'}\big| \;<\; D', \qquad D' \;<\; \big|\epsilon_{\mathbf{q}}\big| \;<\; D,$$

where $D > D' = D-\delta D$. When $D' \gg T$ (T is the temperature of the gas), we can write

$$\big\langle c_{\mathbf{q},i''}c^{\dagger}_{\mathbf{q},i''}\big\rangle \;=\; \Theta(\epsilon_{\mathbf{q}}-D)\Theta(-D'-\epsilon_{\mathbf{q}}),$$
$$\big\langle c^{\dagger}_{\mathbf{q},i''}c_{\mathbf{q},i''}\big\rangle \;=\; \Theta(\epsilon_{\mathbf{q}}-D')\Theta(D-\epsilon_{\mathbf{q}}),$$

where $\Theta(\epsilon)$ is the Heaviside theta function equal to 1 for $\epsilon>0$, 0 for $\epsilon<0$ and $\frac{1}{2}$ for $\epsilon=0$. Thus, the correction $H^{(2)}_{\rm d,d}$ can be written as,

$$\delta H^{(2)}_{\rm d,d} \;=\; -\frac{\lambda_{\rm d}^2\rho_0\delta D}{2D}\sum_{\alpha,\alpha'}\sum_{f,f'}\sum_{i,i'}\sum_{\mathbf{k},\mathbf{k}'}\Big[\hat{F}^{\alpha},\hat{F}^{\alpha'}\Big]_{f,f'}\times \\ \times\Big[\hat{I}^{\alpha},\;\hat{I}^{\alpha'}\Big]_{i,i'}X^{f,f'}\;c^{\dagger}_{\mathbf{k},i}c_{\mathbf{k}',i'}, \qquad \text{(J2)}$$

where

$$\big[\hat{A},\hat{B}\big] \;=\; \hat{A}\hat{B}-\hat{B}\hat{A},$$

denotes the commutator of the matrices $\hat{A}$ and $\hat{B}$. ρ_0 is the density of states of itinerant atoms. The commutator of the spin operators $\hat{F}^{\alpha}$ and $\hat{I}^{\alpha}$ are given by eq. (A1). Taking into account the property of the Levi-Civita symbols,

$$\sum_{\alpha,\alpha'}\epsilon^{\alpha,\alpha',\alpha_1}\epsilon^{\alpha,\alpha',\alpha'_1} \;=\; 2\;\delta^{\alpha_1,\alpha'_1}, \qquad \text{(J3)}$$

we get,

$$\delta H^{(2)}_{\rm d,d} \;=\; \frac{\lambda_{\rm d}^2\rho_0\delta D}{D}\sum_{\alpha}\sum_{f,f'}\sum_{i,i'}\sum_{\mathbf{k},\mathbf{k}'}F^{\alpha}_{f,f'}\;I^{\alpha}_{i,i'}\times \\ \times X^{f,f'}\;c^{\dagger}_{\mathbf{k},i}c_{\mathbf{k}',i'}. \qquad \text{(J4)}$$

2. **Dipole-quadruple contribution**: The correction $\delta H^{(2)}_{\rm d,q}$ [eq. (27)] is,

$$\delta H^{(2)}_{\rm d,q} \;=\; -\frac{\lambda_{\rm d}\lambda_{\rm q}\rho_0\delta D}{2D}\sum_{\alpha_1,\alpha_2,\alpha'_2}\sum_{f,f'}\sum_{i,i'}\sum_{\mathbf{k},\mathbf{k}'}\times \\ \times\Big[\hat{F}^{\alpha_1},\hat{F}^{\alpha_2,\alpha'_2}\Big]_{f,f'}\Big[\hat{I}^{\alpha_1},\;\hat{I}^{\alpha_2,\alpha'_2}\Big]_{i,i'}\times \\ \times X^{f,f'}\;c^{\dagger}_{\mathbf{k},i}c_{\mathbf{k}',i'}, \qquad \text{(J5)}$$

where ρ_0 is the density of states (29) of itinerant atoms. The commutators of the spin operators $\hat{F}^{\alpha_1}$ or $\hat{I}^{\alpha_1}$ with the quadruple momentum operators $\hat{F}^{\alpha_2,\alpha'_2}$ or $\hat{I}^{\alpha_2,\alpha'_2}$ are given by eq. (A2) below. Taking into account the property (J3) of the Levi-Civita symbols, we get

$$\delta H^{(2)}_{\rm d,q} \;=\; \frac{6\lambda_{\rm d}\lambda_{\rm q}\rho_0\delta D}{D}\sum_{\alpha,\alpha'}\sum_{f,f'}\sum_{i,i'}\sum_{\mathbf{k},\mathbf{k}'}F^{\alpha,\alpha'}_{f,f'}\;I^{\alpha,\alpha'}_{i,i'}\times \\ \times X^{f,f'}\;c^{\dagger}_{\mathbf{k},i}c_{\mathbf{k}',i'}. \qquad \text{(J6)}$$

3. **Dipole-octuple contribution**: The correction

$\delta H^{(2)}_{\rm d,o}$ [eq. (27)] is,

$$\delta H^{(2)}_{\rm d,o} = -\frac{\lambda_{\rm d}\lambda_{\rm o}\rho_0\delta D}{2D}\sum_{\alpha_1}\sum_{\alpha_2,\alpha_2',\alpha_2''}\sum_{f,f'}\sum_{i,i'}\sum_{\mathbf{k},\mathbf{k}'}\times \times\left[\hat{F}^{\alpha_1},\hat{F}^{\alpha_2,\alpha_2',\alpha_2''}\right]_{f,f'}\left[\hat{I}^{\alpha_1},\ \hat{I}^{\alpha_2,\alpha_2',\alpha_2''}\right]_{i,i'}\times \times X^{f,f'}\ c^\dagger_{\mathbf{k},i}c_{\mathbf{k}',i'}, \quad \text{(J7)}$$

where ρ_0 is the density of states (29) of itinerant atoms. The commutators of spin operators $\hat{F}^{\alpha_1}$ or $\hat{I}^{\alpha_1}$ with octuple momentum operators $\hat{F}^{\alpha_2,\alpha_2',\alpha_2''}$ or $\hat{I}^{\alpha_2,\alpha_2',\alpha_2''}$ are given by eq. (A3) below. Taking into account the property (J3) of the Levi-Civita symbols, we get

$$\delta H^{(2)}_{\rm d,o} = \frac{9\lambda_{\rm d}\lambda_{\rm o}\rho_0\delta D}{D}\sum_{\alpha,\alpha',\alpha''}\sum_{f,f'}\sum_{i,i'}\sum_{\mathbf{k},\mathbf{k}'}\times \times F^{\alpha,\alpha',\alpha''}_{f,f'}\ I^{\alpha,\alpha',\alpha''}_{i,i'}X^{f,f'}\ c^\dagger_{\mathbf{k},i}c_{\mathbf{k}',i'}. \quad \text{(J8)}$$

4. **Quadruple-quadruple contribution**: The correction $\delta H^{(2)}_{\rm q,q}$ [eq. (27)] is,

$$\delta H^{(2)}_{\rm q,q} = -\frac{\lambda^2_{\rm q}\rho_0\delta D}{2D}\sum_{\alpha_1,\alpha_1'}\sum_{\alpha_2,\alpha_2'}\sum_{f,f'}\sum_{i,i'}\sum_{\mathbf{k},\mathbf{k}'} \times\left[\hat{F}^{\alpha_1,\alpha_1'},\hat{F}^{\alpha_2,\alpha_2'}\right]_{f,f'}\left[\hat{I}^{\alpha_1,\alpha_1'},\ \hat{I}^{\alpha_2,\alpha_2'}\right]_{i,i'}\times \times X^{f,f'}c^\dagger_{\mathbf{k},i}c_{\mathbf{k}',i'}, \quad \text{(J9)}$$

where ρ_0 is the density of states (29) of itinerant atoms. The commutators of the quadruple momentum operators $\hat{F}^{\alpha,\alpha'}$ are given by eq. (A4) below, whereas the commutators of the quadruple momentum operators $\hat{I}^{\alpha_2,\alpha_2'}$ are given by eq. (A5) below. Taking into account the property (J3) of the Levi-Civita symbols, we get

$$\delta H^{(2)}_{\rm q,q} = \frac{64\lambda^2_{\rm q}\rho_0\delta D}{9D}\sum_{\alpha,\alpha',\alpha''}\sum_{f,f'}\sum_{i,i'}\sum_{\mathbf{k},\mathbf{k}'}\times \times F^{\alpha,\alpha',\alpha''}_{f,f'}\ I^{\alpha,\alpha',\alpha''}_{i,i'}\ X^{f,f'}\ c^\dagger_{\mathbf{k},i}c_{\mathbf{k}',i'} + + \frac{9216\lambda^2_{\rm q}\rho_0\delta D}{25D}\sum_{\alpha}\sum_{f,f'}\sum_{i,i'}\sum_{\mathbf{k},\mathbf{k}'}\times \times F^{\alpha}_{f,f'}\ I^{\alpha}_{i,i'}\ X^{f,f'}\ c^\dagger_{\mathbf{k},i}c_{\mathbf{k}',i'}. \quad \text{(J10)}$$

5. **Quadruple-octuple contribution**: The correction $\delta H^{(2)}_{\rm q,o}$ [eq. (27)] is,

$$\delta H^{(2)}_{\rm q,o} = -\frac{\lambda_{\rm q}\lambda_{\rm o}\rho_0\delta D}{2D}\sum_{\alpha_1,\alpha_1'}\sum_{\alpha_2,\alpha_2',\alpha_2''}\sum_{f,f'}\sum_{i,i'}\sum_{\mathbf{k},\mathbf{k}'} \times\left[\hat{F}^{\alpha_1,\alpha_1'},\hat{F}^{\alpha_2,\alpha_2',\alpha_2''}\right]_{f,f'}\times \times\left[\hat{I}^{\alpha_1,\alpha_1'},\ \hat{I}^{\alpha_2,\alpha_2',\alpha_2''}\right]_{i,i'}\times \times X^{f,f'}c^\dagger_{\mathbf{k},i}c_{\mathbf{k}',i'}, \quad \text{(J11)}$$

where ρ_0 is the density of states (29) of itinerant atoms.

The commutators of the quadruple momentum operators $\hat{F}^{\alpha_1,\alpha_1'}$ with the octuple operators $\hat{F}^{\alpha_2,\alpha_2',\alpha_2''}$ are given by eq. (A6), whereas the commutators of the quadruple momentum operators $\hat{I}^{\alpha_1,\alpha_1'}$ with the octuple operators $\hat{I}^{\alpha_2,\alpha_2',\alpha_2''}$ are given by eq. (A7). Then eq. (J11) takes the form,

$$\delta H^{(2)}_{\rm q,o} = \frac{1458\lambda_{\rm q}\lambda_{\rm o}}{D_0}\sum_{\alpha,\alpha'}\sum_{f,f'}\sum_{i,i'}\sum_{\mathbf{k},\mathbf{k}'}F^{\alpha,\alpha'}_{f,f'}I^{\alpha',\alpha}_{i',i}\times \times X^{f,f'}\ c^\dagger_{\mathbf{k}',i'}c_{\mathbf{k},i}. \quad \text{(J12)}$$

6. **Octuple-octuple contribution**: The correction $\delta H^{(2)}_{\rm o,o}$ [eq. (27)] is,

$$\delta H^{(2)}_{\rm o,o} = -\frac{\lambda_{\rm q}\lambda_{\rm o}\rho_0\delta D}{2D}\sum_{\alpha_1,\alpha_1',\alpha_1''}\sum_{\alpha_2,\alpha_2',\alpha_2''}\sum_{f,f'}\sum_{i,i'}\sum_{\mathbf{k},\mathbf{k}'} \times\left[\hat{F}^{\alpha_1,\alpha_1',\alpha_1''},\hat{F}^{\alpha_2,\alpha_2',\alpha_2''}\right]_{f,f'}\times \times\left[\hat{I}^{\alpha_1,\alpha_1',\alpha_1''},\ \hat{I}^{\alpha_2,\alpha_2',\alpha_2''}\right]_{i,i'}\times \times X^{f,f'}c^\dagger_{\mathbf{k},i}c_{\mathbf{k}',i'}, \quad \text{(J13)}$$

where ρ_0 is the density of states (29) of itinerant atoms.

The commutators of the octuple operators $\hat{F}^{\alpha,\alpha',\alpha''}$ are given by eq. (A8), whereas the commutators of the octuple operators $\hat{I}^{\alpha,\alpha',\alpha''}$ are given by eq. (A9). Then eq. (J13) takes the form,

$$\delta H^{(2)}_{\rm o,o} = \frac{1469664\lambda^2_{\rm o}\rho_0}{D_0}\sum_{\alpha}\sum_{f,f'}\sum_{i,i'}\sum_{\mathbf{k},\mathbf{k}'}F^{\alpha}_{f,f'}I^{\alpha}_{i',i}\times \times X^{f,f'}\ c^\dagger_{\mathbf{k}',i'}c_{\mathbf{k},i} - -\frac{306\lambda^2_{\rm o}\rho_0}{5}\sum_{\alpha,\alpha',\alpha''}\sum_{f,f'}\sum_{i,i'}\sum_{\mathbf{k},\mathbf{k}'}\times \times F^{\alpha,\alpha',\alpha''}_{f,f'}I^{\alpha'',\alpha',\alpha}_{i',i}X^{f,f'}\ c^\dagger_{\mathbf{k}',i'}c_{\mathbf{k},i}. \quad \text{(J14)}$$

Appendix K: Derivation of δE, Eq. (34)

The second order correction to the energy is illustrated by the diagrams displayed in Fig. 7. is decomposed into its multiple components as,

$$\delta E = \delta E_{\rm d} + \delta E_{\rm q} + \delta E_{\rm o}. \quad \text{(K1)}$$

Here $\delta E_{\rm d}$, $\delta E_{\rm q}$ and $\delta E_{\rm o}$ are dipole, quadruple and octuple contributions to δE, given explicitly as,

$$\delta E_{\rm d} = -\lambda_{\rm d}^2 \frac{E}{D^2} \sum_{f,f'} X^{f,f'} \sum_{\alpha_1,\alpha_2} \Big(\hat{F}^{\alpha_1}\hat{F}^{\alpha_2}\Big)_{f,f'} \times \times {\rm Tr}\Big(\hat{I}^{\alpha_1}\hat{I}^{\alpha_2}\Big)\ \mathfrak{G}, \tag{K2a}$$

$$\delta E_{\rm q} = -\lambda_{\rm q}^2 \frac{E}{D^2} \sum_{f,f'} X^{f,f'} \times \times \sum_{\alpha_1,\alpha_1'} \sum_{\alpha_2,\alpha_2'} \Big(\hat{F}^{\alpha_1,\alpha_1'}\hat{F}^{\alpha_2,\alpha_2'}\Big)_{f,f'} \times \times {\rm Tr}\Big(\hat{I}^{\alpha_1,\alpha_1'}\hat{I}^{\alpha_2,\alpha_2'}\Big)\ \mathfrak{G}, \tag{K2b}$$

$$\delta E_{\rm o} = -\lambda_{\rm o}^2 \frac{E}{D^2} \sum_{f,f'} X^{f,f'} \sum_{\alpha_1,\alpha_1',\alpha_1''} \sum_{\alpha_2,\alpha_2',\alpha_2''} \times \times \Big(\hat{F}^{\alpha_1,\alpha_1',\alpha_1''}\hat{F}^{\alpha_2,\alpha_2',\alpha_2''}\Big)_{f,f'} \times \times {\rm Tr}\Big(\hat{I}^{\alpha_1,\alpha_1',\alpha_1''}\hat{I}^{\alpha_2,\alpha_2',\alpha_2''}\Big)\ \mathfrak{G}, \tag{K2c}$$

where $\mathfrak{G}$ is given by eq. (37). We consider dipole, quadruple and octuple contributions to δE in turn.

1. Dipole contribution: The trace of the product of two spin matrices is,

$$\sum_{i_1,i_2} I_{i_1,i_2}^{\alpha_1} I_{i_2,i_1}^{\alpha_2} = \frac{1}{3}\ I(I+1)(2I+1)\ \delta^{\alpha_1,\alpha_2}. \tag{K3}$$

Using eq. (K3), we can write

$$\sum_{\alpha}\sum_{f_1} F_{f,f_1}^{\alpha} F_{f_1,f'}^{\alpha} = F(F+1)\ \delta_{f,f'}. \tag{K4}$$

Finally, the dipole contribution to the self energy is,

$$\delta E_{\rm d} = -\frac{2\delta D}{3D}\ E\ \lambda_{\rm d}^2\rho_0^2\ F(F+1)I(I+1)(2I+1).$$

Taking into account that $F=\frac{3}{2}$ and $I=\frac{5}{2}$, we get

$$\delta E_{\rm d} = -\frac{525}{4}\ \frac{\delta D}{D}\ E\ \lambda_{\rm d}^2\rho_0^2. \tag{K5}$$

2. Quadruple contribution: The trace of the product of two quadruple matrices is,

$$\sum_{i_1,i_2} I_{i_1,i_2}^{\alpha_1,\alpha_1'} I_{i_2,i_1}^{\alpha_2,\alpha_2'} = -\frac{112}{3}\Big\{2\ \delta_{\alpha_1,\alpha_1'}\ \delta_{\alpha_2,\alpha_2'} - 3\ \big[\delta_{\alpha_1,\alpha_2}\ \delta_{\alpha_1',\alpha_2'} + \delta_{\alpha_1,\alpha_2'}\ \delta_{\alpha_1',\alpha_2}\big]\Big\}. \tag{K6}$$

Using eq. (K6), we can write

$$\sum_{\alpha_1,\alpha_1'}\sum_{\alpha_2,\alpha_2'} \hat{F}^{\alpha_1,\alpha_1'}\hat{F}^{\alpha_2,\alpha_2'}\ {\rm Tr}\big(\hat{I}^{\alpha_1,\alpha_1'}\hat{I}^{\alpha_2,\alpha_2'}\big) = = 6720\ \hat{1}_4, \tag{K7}$$

where $\hat{1}_4$ is the 4×4 identity matrix.

Finally, quadruple contribution to the self energy is,

$$\delta E_{\rm q} = -13440\ \frac{\delta D}{D}\ E\ \lambda_{\rm q}^2\rho_0^2. \tag{K8}$$

3. Octuple contribution: The trace of the product of two quadruple matrices is,

$$\sum_{\alpha_1,\alpha_1',\alpha_1''}\sum_{\alpha_2,\alpha_2',\alpha_2''} \hat{F}^{\alpha_1,\alpha_1',\alpha_1''}\hat{F}^{\alpha_2,\alpha_2',\alpha_2''} \times \times {\rm Tr}\big(\hat{I}^{\alpha_1,\alpha_1',\alpha_1''}\hat{I}^{\alpha_2,\alpha_2',\alpha_2''}\big) = 1653372\ \hat{1}_4, \tag{K9}$$

where $\hat{1}_4$ is the 4×4 identity matrix.

Finally, octuple contribution to the self energy is,

$$\delta E_{\rm o} = -3306744\ \frac{\delta D}{D}\ E\ \lambda_{\rm q}^2\rho_0^2. \tag{K10}$$

Finally, the second order correction to the energy is,

$$\delta E = -\frac{\delta D}{D}\ E\ \Big\{\frac{525}{4}\ \lambda_{\rm d}^2\rho_0^2 + 13440\ \lambda_{\rm q}^2\rho_0^2 + + 3306744\ \lambda_{\rm o}^2\rho_0^2\Big\}. \tag{K11}$$

Appendix L: Derivation of $\delta H^{(3)}_{\beta,\beta',\beta}$, Eq. (36)

We consider $\delta H^{(3)}_{\beta',\beta,\beta'}$ for $\beta,\beta'={\rm d,q,o}$, in turn.

1. Dipole-dipole contribution: The correction $\delta H^{(3)}_{\rm d,d,d}$ is,

$$\delta H^{(3)}_{\rm d,d,d} = \frac{2\lambda_{\rm d}^3\rho_0^2\delta D}{D} \sum_{\alpha_1,\alpha_2,\alpha_3}\sum_{f,f'} \Big(\hat{F}^{\alpha_1}\hat{F}^{\alpha_2}\hat{F}^{\alpha_3}\Big)_{f,f'} \times \times X^{f,f'} \sum_{i,i'}\sum_{\mathbf{k},\mathbf{k}'} I_{i,i'}^{\alpha_2} c_{\mathbf{k},i}^{\dagger} c_{\mathbf{k}',i'} \times \times {\rm Tr}\Big(\hat{I}^{\alpha_1}\hat{I}^{\alpha_3}\Big). \tag{L1}$$

In order to simplify the expression in the right hand side of eq. (L1), we use the following equalities,

$$\begin{aligned} {\rm Tr}\Big(\hat{I}^{\alpha_1}\hat{I}^{\alpha_3}\Big) &= \frac{1}{3}\ I(I+1)(2I+1) = \\ &= \frac{35}{2}\ \delta_{\alpha_1,\alpha_3}, \end{aligned} \tag{L2}$$

$$\begin{aligned} \sum_{\alpha_1} \hat{F}^{\alpha_1}\hat{F}^{\alpha_2}\hat{F}^{\alpha_1} &= \Big(F(F+1)-1\Big)\ \hat{F}^{\alpha_2} = \\ &= \frac{11}{4}\ \hat{F}^{\alpha_2}. \end{aligned} \tag{L3}$$

Then the dipole-dipole contribution takes the form,

$$\delta H^{(3)}_{\rm d,d,d} = \frac{385}{4}\ \frac{\lambda_{\rm d}^3\rho_0^2\delta D}{D} \sum_{\alpha}\sum_{f,f'}\sum_{i,i'}\sum_{\mathbf{k},\mathbf{k}'} \times \times F_{f,f'}^{\alpha} I_{i,i'}^{\alpha} X^{f,f'}\, c_{\mathbf{k},i}^{\dagger} c_{\mathbf{k}',i'}. \tag{L4}$$

2. **Dipole-quadruple contribution**: The correction $\delta H^{(3)}_{\rm q,d,q}$ is,

$$\delta H^{(3)}_{\rm q,d,q} = \frac{2\lambda_{\rm d}\lambda_{\rm q}^2\rho_0^2\delta D}{D}\sum_{\alpha_1,\alpha_1'}\sum_{\alpha_2}\sum_{\alpha_3,\alpha_3'}\sum_{f,f'}\times \times\Big(\hat{F}^{\alpha_1,\alpha_1'}\hat{F}^{\alpha_2}\hat{F}^{\alpha_3,\alpha_3'}\Big)_{f,f'}\times \times X^{f,f'}\sum_{i,i'}\sum_{\mathbf{k},\mathbf{k}'}I^{\alpha_2}_{i,i'}c^\dagger_{\mathbf{k},i}c_{\mathbf{k}',i'}\times \times{\rm Tr}\Big(\hat{I}^{\alpha_1,\alpha_1'}\hat{I}^{\alpha_3,\alpha_3'}\Big). \quad \text{(L5)}$$

Using eqs. (K6) and (K7), we can write

$$\sum_{\alpha_1,\alpha_1'}\sum_{\alpha_3,\alpha_3'}\hat{F}^{\alpha_1,\alpha_1'}\hat{F}^{\alpha_2}\hat{F}^{\alpha_3,\alpha_3'}\,{\rm Tr}\Big(\hat{I}^{\alpha_1,\alpha_1'}\hat{I}^{\alpha_3,\alpha_3'}\Big) = = 1344\;\hat{F}^{\alpha_2}.$$

Then the dipole-quadruple contribution can be written as,

$$\delta H^{(3)}_{\rm q,d,q} = 2688\;\frac{\lambda_{\rm d}\lambda_{\rm q}^2\rho_0^2\delta D}{D}\sum_{\alpha}\sum_{f,f'}\sum_{i,i'}\sum_{\mathbf{k},\mathbf{k}'}\times \times F^{\alpha}_{f,f'}I^{\alpha}_{i,i'}X^{f,f'}c^\dagger_{\mathbf{k},i}c_{\mathbf{k}',i'}. \quad \text{(L6)}$$

3. **Dipole-octuple contribution**: The correction $\delta H^{(3)}_{\rm o,d,o}$ is,

$$\delta H^{(3)}_{\rm o,d,o} = \frac{2\lambda_{\rm d}\lambda_{\rm o}^2\rho_0^2\delta D}{D}\sum_{\alpha_1,\alpha_1',\alpha_1''}\sum_{\alpha_2}\sum_{\alpha_3,\alpha_3',\alpha_3''}\sum_{f,f'}\times \times\Big(\hat{F}^{\alpha_1,\alpha_1',\alpha_1''}\hat{F}^{\alpha_2}\hat{F}^{\alpha_3,\alpha_3',\alpha_3''}\Big)_{f,f'}\times \times X^{f,f'}\sum_{i,i'}\sum_{\mathbf{k},\mathbf{k}'}I^{\alpha_2}_{i,i'}c^\dagger_{\mathbf{k},i}c_{\mathbf{k}',i'}\times \times{\rm Tr}\Big(\hat{I}^{\alpha_1,\alpha_1',\alpha_1''}\hat{I}^{\alpha_3,\alpha_3',\alpha_3''}\Big). \quad \text{(L7)}$$

Equation (L7) can be simplified by using eq. (K9),

$$\sum_{\alpha_1,\alpha_1',\alpha_1''}\sum_{\alpha_3,\alpha_3',\alpha_3''}\hat{F}^{\alpha_1,\alpha_1',\alpha_1''}\hat{F}^{\alpha_2}\hat{F}^{\alpha_3,\alpha_3',\alpha_3''}\times \times{\rm Tr}\Big(\hat{I}^{\alpha_1,\alpha_1',\alpha_1''}\hat{I}^{\alpha_3,\alpha_3',\alpha_3''}\Big) = = -\frac{4960116}{5}\;\hat{F}^{\alpha_2}.$$

Then the dipole-quadruple contribution can be written as,

$$\delta H^{(3)}_{\rm o,d,o} = -\frac{9920232}{5}\;\frac{\lambda_{\rm d}\lambda_{\rm o}^2\rho_0^2\delta D}{D}\sum_{\alpha}\sum_{f,f'}\sum_{i,i'}\sum_{\mathbf{k},\mathbf{k}'}\times \times F^{\alpha}_{f,f'}I^{\alpha}_{i,i'}X^{f,f'}c^\dagger_{\mathbf{k},i}c_{\mathbf{k}',i'}. \quad \text{(L8)}$$

4. **Quadruple-dipole contribution**: The correction $\delta H^{(3)}_{\rm d,q,d}$ is,

$$\delta H^{(3)}_{\rm d,q,d} = \frac{2\lambda_{\rm q}\lambda_{\rm d}^2\rho_0^2\delta D}{D}\sum_{\alpha_1}\sum_{\alpha_2,\alpha_2'}\sum_{\alpha_3}\sum_{f,f'}\times \times\Big(\hat{F}^{\alpha_1}\hat{F}^{\alpha_2,\alpha_2'}\hat{F}^{\alpha_3}\Big)_{f,f'}\times \times X^{f,f'}\sum_{i,i'}\sum_{\mathbf{k},\mathbf{k}'}I^{\alpha_2,\alpha_2'}_{i,i'}c^\dagger_{\mathbf{k},i}c_{\mathbf{k}',i'}\times \times{\rm Tr}\Big(\hat{I}^{\alpha_1}\hat{I}^{\alpha_3}\Big). \quad \text{(L9)}$$

In order to simplify eq. (L9), we use eq. (K3) and the following equality,

$$\sum_{\alpha}\hat{F}^{\alpha}\hat{F}^{\alpha_2,\alpha_2'}\hat{F}^{\alpha} = \frac{3}{4}\;\hat{F}^{\alpha_2,\alpha_2'}.$$

Then the quadruple-dipole contribution can be written as,

$$\delta H^{(3)}_{\rm d,q,d} = \frac{105}{4}\;\frac{\lambda_{\rm q}\lambda_{\rm d}^2\rho_0^2\delta D}{D}\sum_{\alpha}\sum_{f,f'}\sum_{i,i'}\sum_{\mathbf{k},\mathbf{k}'}\times \times F^{\alpha}_{f,f'}I^{\alpha}_{i,i'}X^{f,f'}c^\dagger_{\mathbf{k},i}c_{\mathbf{k}',i'}. \quad \text{(L10)}$$

5. **Quadruple-quadruple contribution**: The correction $\delta H^{(3)}_{\rm q,q,q}$ is,

$$\delta H^{(3)}_{\rm q,q,q} = \frac{2\lambda_{\rm q}^3\rho_0^2\delta D}{D}\sum_{\alpha_1,\alpha_1'}\sum_{\alpha_2,\alpha_2'}\sum_{\alpha_3,\alpha_3'}\sum_{f,f'}\times \times\Big(\hat{F}^{\alpha_1,\alpha_1'}\hat{F}^{\alpha_2,\alpha_2'}\hat{F}^{\alpha_3,\alpha_3'}\Big)_{f,f'}\times \times X^{f,f'}\sum_{i,i'}\sum_{\mathbf{k},\mathbf{k}'}I^{\alpha_2,\alpha_2'}_{i,i'}c^\dagger_{\mathbf{k},i}c_{\mathbf{k}',i'}\times \times{\rm Tr}\Big(\hat{I}^{\alpha_1,\alpha_1'}\hat{I}^{\alpha_3,\alpha_3'}\Big). \quad \text{(L11)}$$

Using eqs. (K6) and (K7), we can write

$$\sum_{\alpha_1,\alpha_1'}\sum_{\alpha_3,\alpha_3'}\hat{F}^{\alpha_1,\alpha_1'}\hat{F}^{\alpha_2,\alpha_2'}\hat{F}^{\alpha_3,\alpha_3'}{\rm Tr}\Big(\hat{I}^{\alpha_1,\alpha_1'}\hat{I}^{\alpha_3,\alpha_3'}\Big) = = -4032\;\hat{F}^{\alpha_2,\alpha_2'}.$$

Then $\delta H^{(3)}_{\rm q,q,q}$ takes the form,

$$\delta H^{(3)}_{\rm q,q,q} = -8064\;\frac{\lambda_{\rm q}^3\rho_0^2\delta D}{D}\sum_{\alpha,\alpha'}\sum_{f,f'}\sum_{i,i'}\sum_{\mathbf{k},\mathbf{k}'}\times \times F^{\alpha,\alpha'}_{f,f'}I^{\alpha_2,\alpha_2'}_{i,i'}X^{f,f'}c^\dagger_{\mathbf{k},i}c_{\mathbf{k}',i'}. \quad \text{(L12)}$$

6. **Quadruple-octuple contribution**: The correction $\delta H^{(3)}_{\rm o,q,o}$ is,

$$\delta H^{(3)}_{\rm o,q,o} = \frac{2\lambda_{\rm q}\lambda_{\rm o}^2\rho_0^2\delta D}{D}\sum_{\alpha_1,\alpha_1',\alpha_1''}\sum_{\alpha_2,\alpha_2'}\sum_{\alpha_3,\alpha_3',\alpha_3''}\sum_{f,f'}\times \times\Big(\hat{F}^{\alpha_1,\alpha_1',\alpha_1''}\hat{F}^{\alpha_2,\alpha_2'}\hat{F}^{\alpha_3,\alpha_3',\alpha_3''}\Big)_{f,f'}\times \times X^{f,f'}\sum_{i,i'}\sum_{\mathbf{k},\mathbf{k}'}I_{i,i'}^{\alpha_2,\alpha_2'}c^\dagger_{\mathbf{k},i}c_{\mathbf{k}',i'}\times \times{\rm Tr}\Big(\hat{I}^{\alpha_1,\alpha_1',\alpha_1''}\hat{I}^{\alpha_3,\alpha_3',\alpha_3''}\Big). \quad \text{(L13)}$$

In order to simplify eq. (L13), we use the following equality,

$$\sum_{\alpha_1,\alpha_1',\alpha_1''}\sum_{\alpha_3,\alpha_3',\alpha_3''}\hat{F}^{\alpha_1,\alpha_1',\alpha_1''}\hat{F}^{\alpha_2,\alpha_2'}\hat{F}^{\alpha_3,\alpha_3',\alpha_3''}\times \times{\rm Tr}\Big(\hat{I}^{\alpha_1,\alpha_1',\alpha_1''}\hat{I}^{\alpha_3,\alpha_3',\alpha_3''}\Big) = = \frac{1153372}{5}\;\hat{F}^{\alpha_2,\alpha_2'}.$$

Then eq. (L13) takes the form,

$$\delta H^{(3)}_{\rm o,q,o} = \frac{2306744}{5}\;\frac{\lambda_{\rm q}\lambda_{\rm o}^2\rho_0^2\delta D}{D}\sum_{\alpha,\alpha'}\sum_{f,f'}\sum_{i,i'}\sum_{\mathbf{k},\mathbf{k}'}\times \times F^{\alpha,\alpha'}_{f,f'}I^{\alpha,\alpha'}_{i,i'}X^{f,f'}c^\dagger_{\mathbf{k},i}c_{\mathbf{k}',i'}. \quad \text{(L14)}$$

7. **Octuple-dipole contribution**: The correction $\delta H^{(3)}_{\rm d,o,d}$ is,

$$\delta H^{(3)}_{\rm d,o,d} = \frac{2\lambda_{\rm o}\lambda_{\rm d}^2\rho_0^2\delta D}{D}\sum_{\alpha_1}\sum_{\alpha_2,\alpha_2',\alpha_2''}\sum_{\alpha_3}\sum_{f,f'}\times \times\Big(\hat{F}^{\alpha_1}\hat{F}^{\alpha_2,\alpha_2',\alpha_2''}\hat{F}^{\alpha_3}\Big)_{f,f'}\times \times X^{f,f'}\sum_{i,i'}\sum_{\mathbf{k},\mathbf{k}'}I_{i,i'}^{\alpha_2,\alpha_2',\alpha_2''}c^\dagger_{\mathbf{k},i}c_{\mathbf{k}',i'}\times \times{\rm Tr}\Big(\hat{I}^{\alpha_1}\hat{I}^{\alpha_3}\Big). \quad \text{(L15)}$$

In order to simplify eq. (L15), we use the following equality,

$$\sum_{\alpha_1,\alpha_3}\hat{F}^{\alpha_1}\hat{F}^{\alpha_2,\alpha_2',\alpha_2''}\hat{F}^{\alpha_3}\;{\rm Tr}\Big(\hat{I}^{\alpha_1}\hat{I}^{\alpha_3}\Big) = = -\frac{315}{8}\;\hat{F}^{\alpha_2,\alpha_2',\alpha_2''}.$$

Then the octuple-dipole contribution can be written as,

$$\delta H^{(3)}_{\rm d,o,d} = -\frac{315}{4}\;\frac{\lambda_{\rm o}\lambda_{\rm d}^2\rho_0^2\delta D}{D}\sum_{\alpha,\alpha',\alpha''}\sum_{f,f'}\sum_{i,i'}\sum_{\mathbf{k},\mathbf{k}'}\times \times F^{\alpha,\alpha',\alpha''}_{f,f'}I^{\alpha,\alpha',\alpha''}_{i,i'}X^{f,f'}c^\dagger_{\mathbf{k},i}c_{\mathbf{k}',i'}. \quad \text{(L16)}$$

8. **Octuple-quadruple contribution**: The correction $\delta H^{(3)}_{\rm q,o,q}$ is,

$$\delta H^{(3)}_{\rm q,q,q} = \frac{2\lambda_{\rm o}\lambda_{\rm q}^2\rho_0^2\delta D}{D}\sum_{\alpha_1,\alpha_1'}\sum_{\alpha_2,\alpha_2',\alpha_2''}\sum_{\alpha_3,\alpha_3'}\sum_{f,f'}\times \times\Big(\hat{F}^{\alpha_1,\alpha_1'}\hat{F}^{\alpha_2,\alpha_2',\alpha_2''}\hat{F}^{\alpha_3,\alpha_3'}\Big)_{f,f'}\times \times X^{f,f'}\sum_{i,i'}\sum_{\mathbf{k},\mathbf{k}'}I_{i,i'}^{\alpha_2,\alpha_2',\alpha_2''}c^\dagger_{\mathbf{k},i}c_{\mathbf{k}',i'}\times \times{\rm Tr}\Big(\hat{I}^{\alpha_1,\alpha_1'}\hat{I}^{\alpha_3,\alpha_3'}\Big). \quad \text{(L17)}$$

Using eqs. (K6) and (K7), we can write

$$\sum_{\alpha_1,\alpha_1'}\sum_{\alpha_3,\alpha_3'}\hat{F}^{\alpha_1,\alpha_1'}\hat{F}^{\alpha_2,\alpha_2',\alpha_2''}\hat{F}^{\alpha_3,\alpha_3'}{\rm Tr}\Big(\hat{I}^{\alpha_1,\alpha_1'}\hat{I}^{\alpha_3,\alpha_3'}\Big) = = 1344\;\hat{F}^{\alpha_2,\alpha_2',\alpha_2''}.$$

Then $\delta H^{(3)}_{\rm q,o,q}$ takes the form,

$$\delta H^{(3)}_{\rm q,o,q} = 2688\;\frac{\lambda_{\rm o}\lambda_{\rm q}^2\rho_0^2\delta D}{D}\sum_{\alpha,\alpha',\alpha''}\sum_{f,f'}\sum_{i,i'}\sum_{\mathbf{k},\mathbf{k}'}\times \times F^{\alpha,\alpha',\alpha''}_{f,f'}I^{\alpha,\alpha',\alpha''}_{i,i'}X^{f,f'}c^\dagger_{\mathbf{k},i}c_{\mathbf{k}',i'}. \quad \text{(L18)}$$

9. **Octuple-octuple contribution**: The correction $\delta H^{(3)}_{\rm o,o,o}$ is,

$$\delta H^{(3)}_{\rm o,o,o} = \frac{2\lambda_{\rm o}^3\rho_0^2\delta D}{D}\sum_{\alpha_1,\alpha_1',\alpha_1''}\sum_{\alpha_2,\alpha_2',\alpha_2''}\sum_{\alpha_3,\alpha_3',\alpha_3''}\sum_{f,f'}\times \times\Big(\hat{F}^{\alpha_1,\alpha_1',\alpha_1''}\hat{F}^{\alpha_2,\alpha_2',\alpha_2''}\hat{F}^{\alpha_3,\alpha_3',\alpha_3''}\Big)_{f,f'}\times \times X^{f,f'}\sum_{i,i'}\sum_{\mathbf{k},\mathbf{k}'}I_{i,i'}^{\alpha_2,\alpha_2',\alpha_2''}c^\dagger_{\mathbf{k},i}c_{\mathbf{k}',i'}\times \times{\rm Tr}\Big(\hat{I}^{\alpha_1,\alpha_1',\alpha_1''}\hat{I}^{\alpha_3,\alpha_3',\alpha_3''}\Big). \quad \text{(L19)}$$

In order to simplify eq. (L19), we use the following equality,

$$\sum_{\alpha_1,\alpha_1',\alpha_1''}\sum_{\alpha_3,\alpha_3',\alpha_3''}\hat{F}^{\alpha_1,\alpha_1',\alpha_1''}\hat{F}^{\alpha_2,\alpha_2',\alpha_2''}\hat{F}^{\alpha_3,\alpha_3',\alpha_3''}\times \times{\rm Tr}\Big(\hat{I}^{\alpha_1,\alpha_1',\alpha_1''}\hat{I}^{\alpha_3,\alpha_3',\alpha_3''}\Big) = = -\frac{236196}{5}\;\hat{F}^{\alpha_2,\alpha_2',\alpha_2''}.$$

Then eq. (L19) takes the form,

$$\delta H^{(3)}_{\rm o,o,o} = -\frac{472392}{5}\;\frac{\lambda_{\rm o}^3\rho_0^2\delta D}{D}\sum_{\alpha,\alpha',\alpha''}\sum_{f,f'}\sum_{i,i'}\sum_{\mathbf{k},\mathbf{k}'}\times \times F^{\alpha,\alpha',\alpha''}_{f,f'}I^{\alpha,\alpha',\alpha''}_{i,i'}X^{f,f'}c^\dagger_{\mathbf{k},i}c_{\mathbf{k}',i'}. \quad \text{(L20)}$$

Appendices I, J, K, L main points: The second order correction terms are defined in Eqs. (26, 27), while the third ordered correction terms are defined in Eqs. (36). The formidable task of evaluating these terms is carried out in these subsections.

Appendix M: Eigenfunctions and Eigenenergy of the Dipole-Dipole, Quadruple-Quadruple and Octuple-Octuple Interactions

Consider four atoms, such that one atom (an "impurity atom") has spin $F = \frac{3}{2}$ and the three other atoms ("itinerant atoms") have spin $I = \frac{5}{2}$. The interaction between the itinerant atoms and the impurity is dipole-dipole, quadruple-quadruple and octuple-octuple interactions. We derive here eigenfunctions and corresponding eigenenergies of the Hamiltonians of the dipole-dipole, quadruple-quadruple and octuple-octuple interactions, in turn.

1. Eigenfunctions of the Dipole-Dipole Interaction

The Hamiltonian of the dipole-dipole interaction between the atoms is,

$$\mathcal{H}_{\rm d} \;=\; \lambda_{\rm d}\,\Big(\hat{\mathbf{F}}\cdot\hat{\mathbf{S}}\Big), \tag{M1}$$

where $\hat{\mathbf{F}}$ is a vector of the spin-$\frac{3}{2}$ operators, $\hat{\mathbf{S}} = \hat{\mathbf{I}}_1 + \hat{\mathbf{I}}_2 + \hat{\mathbf{I}}_3$, where $\hat{\mathbf{I}}_a$ $(a = 1, 2, 3)$ is a vector of the spin-$\frac{5}{2}$ operators.

Note that $\mathcal{H}_{\rm d}$ can be expressed in terms of the two-atonic spin $\hat{\mathbf{L}}$,

$$\mathcal{H}_{\rm d} \;=\; \frac{\lambda_{\rm d}}{2}\,\Big(\hat{\mathbf{L}}^2 - F(F+1) - S(S+1)\Big), \tag{M2}$$

where

$$\hat{\mathbf{L}} \;=\; \hat{\mathbf{F}} + \hat{\mathbf{S}},$$

Eq. (M2) shows that $\mathcal{H}_{\rm d}$ commutes with $\hat{\mathbf{L}}^2$, $\hat{\mathbf{F}}^2$ and $\hat{\mathbf{F}}^2$. In addition, $\mathcal{H}_{\rm d}$ commutes with $\hat{\mathbf{L}}^z$, but neither with $\hat{\mathbf{F}}^z$ nor $\hat{\mathbf{I}}^z$. The eigenfunctions of $\mathcal{H}_{\rm d}$, $|L, L_z\rangle$, are defined as

$$\begin{aligned}\hat{\mathbf{L}}^2\,\big|L,L_z\big\rangle \;&=\; L(L+1)\,\big|L,L_z\big\rangle,\\ \hat{\mathbf{L}}^z\,\big|L,L_z\big\rangle \;&=\; L_z\,\big|L,L_z\big\rangle,\end{aligned}$$

where $L = 1, 2, 3, 4$.

Corresponding eigenvalues of $\mathcal{H}_{\rm d}$ are,

$$\mathcal{E}_L^{(\rm d)} = \lambda_{\rm d}\,\mathcal{D}_L, \tag{M3}$$

where

$$\mathcal{D}_L = \frac{1}{2}\,\Big(L(L+1) - F(F+1) - S(S+1)\Big). \tag{M4}$$

When $\lambda_{\rm d} > 0$, the lowest energy level has maximal value of S and minimal value of L. For $I = \frac{5}{2}$, this is the level $S = \frac{9}{2}$ and $L = 3$ (see discussions in Sec. IX). Therefore, we conclude that the interaction is antiferromagnetic.

2. Eigenfunctions of the Quadruple-Quadruple Interaction

The Hamiltonian of the quadruple-quadruple interaction between the atoms is,

$$\mathcal{H}_{\rm q} \;=\; \lambda_{\rm q}\,\sum_{\alpha,\alpha'}\hat{F}^{\alpha,\alpha'}\hat{S}^{\alpha,\alpha'}, \tag{M5}$$

where $\hat{F}^{\alpha,\alpha'}$ or $\hat{S}_a^{\alpha,\alpha'}$ is a quadruple operator for the atom with spin-$\frac{3}{2}$ or spin-$\frac{9}{2}$,

$$\begin{aligned}\hat{F}^{\alpha,\alpha'} \;&=\; \hat{F}^{\alpha}\hat{F}^{\alpha'} + \hat{F}^{\alpha'}\hat{F}^{\alpha} - \frac{2}{3}\,F(F+1)\,\delta_{\alpha,\alpha'},\\ \hat{S}^{\alpha,\alpha'} \;&=\; \hat{S}^{\alpha}\hat{S}^{\alpha'} + \hat{S}^{\alpha'}\hat{S}^{\alpha} - \frac{2}{3}\,S(S+1)\,\delta_{\alpha,\alpha'}.\end{aligned}$$

$\mathcal{H}_{\rm q}$ can be expressed in terms of $(\hat{\mathbf{F}}\cdot\hat{\mathbf{S}})$ as,

$$\begin{aligned}\mathcal{H}_{\rm q} \;=\; \lambda_{\rm q}\,\Big\{&4\,\big(\hat{\mathbf{F}}\cdot\hat{\mathbf{S}}\big)^2 + 2\,\big(\hat{\mathbf{F}}\cdot\hat{\mathbf{S}}\big) -\\ &-\frac{4}{3}\,F(F+1)\,S(S+1)\Big\}.\end{aligned}$$

Eigenfunctions of $\mathcal{H}_{\rm q}$ are $|L, L_z\rangle$. Corresponding eigenenergies are,

$$\mathcal{E}_L^{(\rm q)} \;=\; \lambda_{\rm q}\,\mathcal{Q}_L, \tag{M6}$$

where

$$\mathcal{Q}_L = 4\,\mathcal{D}_L^2 + 2\,\mathcal{D}_L - \frac{4}{3}\,F(F+1)\,S(S+1),$$

$\mathcal{D}_L$ is given by eq. (M4).

The spin L takes the values $L = 3, 4, 5, 6$. Corresponding energies are,

$$\begin{aligned}\mathcal{E}_3^{(\rm q)} \;&=\; 132\,\lambda_{\rm q},\\ \mathcal{E}_4^{(\rm q)} \;&=\; -60\,\lambda_{\rm q},\\ \mathcal{E}_5^{(\rm q)} \;&=\; -120\,\lambda_{\rm q},\\ \mathcal{E}_6^{(\rm q)} \;&=\; 72\,\lambda_{\rm q}.\end{aligned} \tag{M7}$$

It is seen that when $\lambda_{\rm q} < 0$, the lowest energy level is the $L = 1$ energy level. For $\lambda_{\rm q} > 0$, the lowest energy level is the $L = 5$ energy level.

3. Eigenfunctions of the Octuple-Octuple Interaction

The Hamiltonian of the octuple-octuple interaction between the impurity and the itinerant atoms is,

$$\mathcal{H}_{\rm o} \;=\; \lambda_{\rm o}\,\sum_{\alpha,\alpha',\alpha''}\hat{F}^{\alpha,\alpha',\alpha''}\hat{S}^{\alpha,\alpha',\alpha''}, \tag{M8}$$

where $\hat{F}^{\alpha,\alpha',\alpha''}$ or $\hat{S}^{\alpha,\alpha',\alpha''}$ is an octuple operator for the atom with spin-$\frac{3}{2}$ or spin-$\frac{9}{2}$, see eq. (5).

Substituting eq. (5) into eq. (M8), we get

$$\mathcal{H}_{\rm o} = \lambda_{\rm o}\Big\{36\,\big(\hat{\mathbf{F}}\cdot\hat{\mathbf{I}}\big)^3+72\,\big(\hat{\mathbf{F}}\cdot\hat{\mathbf{I}}\big)^2+12\,\big(\hat{\mathbf{F}}\cdot\hat{\mathbf{I}}\big)- -\frac{12}{5}\,\big(3F(F+1)-1\big)\big(3S(S+1)-1\big)\big(\hat{\mathbf{F}}\cdot\hat{\mathbf{I}}\big)- -18\,F(F+1)\,S(S+1)\Big\}.$$

The spin L takes the values $L=3,4,5,6$. Corresponding energies are,

$$\begin{aligned}\mathcal{E}^{(\rm o)}_3 &= -\frac{11088}{5}\,\lambda_{\rm o},\\ \mathcal{E}^{(\rm o)}_4 &= \frac{22368}{5}\,\lambda_{\rm o},\\ \mathcal{E}^{(\rm o)}_5 &= -\frac{14787}{5}\,\lambda_{\rm o},\\ \mathcal{E}^{(\rm o)}_6 &= 2997\,\lambda_{\rm o}.\end{aligned}\qquad\text{(M9)}$$

It is seen that when $\lambda_{\rm o}<0$, the lowest energy level is the $L=4$ energy level. When $\lambda_{\rm o}>0$, the lowest energy level is the $L=5$ energy level.

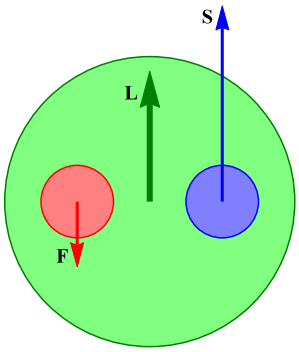


FIG. 12: (color online) Impurity atom with spin F (red disk), itinerant atoms with total spin S (blue disk) creating a cloud screening the spin of the impurity. The "dressed" spin of the impurity is $L=S-F$.

Screening of the impurity spin by a cloud of itinerant atoms is illustrated in Fig. 12. Here the red disk denotes the impurity atom with spin F, the blue disk denotes a cloud of itinerant atoms with the total spin S. The green arrow is a "dressed" spin of the impurity $\mathbf{L}=\mathbf{F}+\mathbf{S}$. When the lowest energy state is $|3,L_z\rangle$ or $|4,L_z\rangle$, the "dressed" spin of the impurity $\mathbf{L}$ is antiparallel to the "bare" spin $\mathbf{F}$ [see inequality (53)], and therefore we deal with over-screened Kondo effect.

Appendix M main points The dipole-dipole, quadruple-quadruple and octopod-octopod Hamiltonians are defined in Eqs. (M1, M5, M8) respectively. Their eigenfunctions and eigenenergies, required for the calculations of the exchange constants, are explicitly elucidated in this Appendix.

Appendix N: ^{3}P$_2$ Yb Atom in Magnetic Field

Consider an ^{3}P$_2$ Yb atom in external magnetic field. The Hamiltonian of the atom is,

$$\mathcal{H}_{\rm at} = \mathcal{H}^{(0)}_{\rm at}+\mathcal{H}_B,\qquad\text{(N1)}$$

where $\mathcal{H}^{(0)}_{\rm at}$ is a Hamiltonian of the isolated ^{173}Yb atom in the ^{3}P$_2$ state and $\mathcal{H}_B$ describes interaction of the atom with the magnetic field,

$$\mathcal{H}^{(0)}_{\rm at} = A_{\rm d}\sum_{\alpha}\hat{I}^{\alpha}\hat{J}^{\alpha}+A_{\rm q}\sum_{\alpha,\alpha'}\hat{I}^{\alpha,\alpha'}\hat{J}^{\alpha,\alpha'},\qquad\text{(N2)}$$

$$\mathcal{H}_B = -g\mu_B B\,\hat{J}^z.\qquad\text{(N3)}$$

Here $\hat{I}^{\alpha}$ and $\hat{I}^{\alpha,\alpha'}$ are spin and quadruple momentum operators for the nucleus, whereas J^{α} and $J^{\alpha,\alpha'}$ are orbital momentum and quadruple momentum operators of the ^{3}P$_2$ electronic configuration. g is the electronic g-factor of the Yb atom in the ^{3}P$_2$ state, see eq. (55).

The constants $A_{\rm d}$ and $A_{\rm q}$ are[31],

$$\frac{A_{\rm d}}{h} = -738\ \text{MHz},\quad \frac{A_{\rm q}}{h} = 1312\ \text{MHz},\qquad\text{(N4)}$$

where h is the Planck constant, or

$$A_{\rm d} = -3.052\ \mu\text{eV},\quad A_{\rm d} = 5.426\ \mu\text{eV}.$$

Taking into account definition (3) for the quadruple momentum operators, we can write the Hamiltonian (N2) in the form,

$$\mathcal{H}^{(0)}_{\rm at} = \big(A_{\rm d}-2\,A_{\rm q}\big)\,\big(\hat{\mathbf{I}}\cdot\hat{\mathbf{J}}\big)+4\,A_{\rm q}\,\big(\hat{\mathbf{I}}\cdot\hat{\mathbf{J}}\big)^2- -\frac{4}{3}\,A_{\rm q}I(I+1)J(J+1).\qquad\text{(N5)}$$

Eq. (N5) shows that eigenfunctions of $\mathcal{H}^{(0)}_{\rm at}$ are also eigenfunctions of the operators $\hat{\mathbf{F}}^2$ and $\hat{F}^z$ [where $\hat{\mathbf{F}}=\hat{\mathbf{I}}+\hat{\mathbf{J}}$ is the operator of the total atomic orbital momentum],

$$\big|F,f\big\rangle = \sum_{i,j}C^{F,f}_{I,i;J,j}\big|I,i;\ J,j\big\rangle,\qquad\text{(N6)}$$

where i, j and f are nuclear, electronic and total atomic magnetic quantum numbers. The wave functions $|I,i;J,j\rangle$ as eigenfunctions of the operators $\hat{I}^z$ and $\hat{J}^z$,

$$\begin{aligned}\hat{I}^z\,\big|I,i;\ J,j\big\rangle &= i\,\big|I,i;\ J,j\big\rangle,\\ \hat{J}^z\,\big|I,i;\ J,j\big\rangle &= j\,\big|I,i;\ J,j\big\rangle.\end{aligned}$$

Corresponding eigenenergies $\mathcal{E}^{(0)}_L$ are

$$\begin{aligned}\mathcal{E}^{(0)}_{\frac{1}{2}} &= -7A_{\rm d}+140A_{\rm q} = 781.0\ \mu\text{eV},\\ \mathcal{E}^{(0)}_{\frac{3}{2}} &= -\frac{11}{2}\,A_{\rm d}+62A_{\rm q} = 353.2\ \mu\text{eV},\\ \mathcal{E}^{(0)}_{\frac{5}{2}} &= -3A_{\rm d}-28A_{\rm q} = -142.8\ \mu\text{eV},\\ \mathcal{E}^{(0)}_{\frac{7}{2}} &= \frac{1}{2}\,A_{\rm d}-70\,A_{\rm q} = -381.3\ \mu\text{eV},\\ \mathcal{E}^{(0)}_{\frac{9}{2}} &= 5\,A_{\rm d}+20\,A_{\rm q} = 93.2\ \mu\text{eV}.\end{aligned}$$

The interaction Hamiltonian $\mathcal{H}_B$, eq. (N3), commutes with the operator $\hat{F}^z$, but nt with $\hat{\mathbf{F}}^2$. Therefore, eigenfunctions of the Hamiltonian $\mathcal{H}_{\rm at}$, eq. (N1), are described by the magnetic quantum numbers f, but not by the total atomic spin F.

In order to find eigenenergies of the Hamiltonian (N1), we find the matric elements of $\mathcal{H}_B$,

$$V^{(f)}_{F,F'} \;=\; \big\langle F,f\big|\mathcal{H}_B\big|F',f\big\rangle = \\ =\; -g\mu_B B\;\mathcal{C}^{(f)}_{F,F'}, \qquad \text{(N7)}$$

where

$$\mathcal{C}^{(f)}_{F,F'} \;=\; \sum_{i,j} j C^{F,f}_{I,i;J,j} C^{F',f}_{I,i;J,j},$$

where $f=-\frac{9}{2},-\frac{7}{2},\ldots,\frac{9}{2}$ and $f\le F,F'\le\frac{9}{2}$. Then the eigenenergies of $\hat{\mathcal{H}}_{\rm at}$ are found from diagonalization of the matrices $\hat{h}^{(f)}$ with matrix elements $h^{(f)}_{F,F'}$ given by,

$$h^{(f)}_{F,F'} \;=\; \mathcal{E}^{(0)}_F\;\delta_{F,F'} + V^{(f)}_{F,F'}. \qquad \text{(N8)}$$

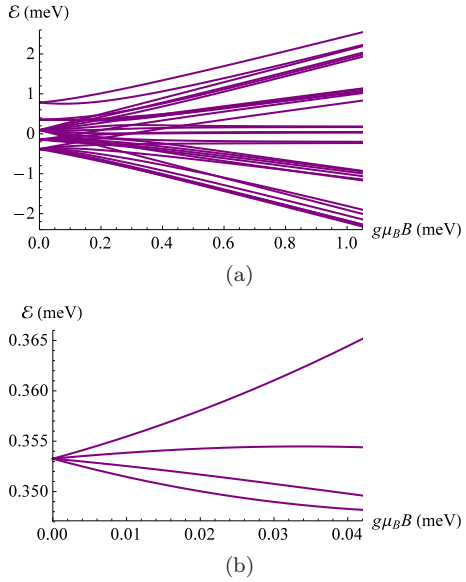


FIG. 13: (color online) Energy spectrum of the ^{173}Yb atom in the ^{3}P$_2$ quantum state [panel (a)]. Zeeman splitting of the $F=\frac{3}{2}$ energy level by a weak magnetic field [panel (b)].

Eigenenergies of the Hamiltonian (N1) as functions of the magnetic field are shown in Fig. 13(a). It is seen that for weak magnetic field [when $g\mu_B B$ is small with respect to the hyperfine splitting], every energy level $\mathcal{E}^{(0)}_F$ splits into $2F+1$ spectral lines with energies $\mathcal{E}_{F,f}$ given by

$$\mathcal{E}_{F,f} \;=\; \mathcal{E}^{(0)}_F - g\mu_B B\;\mathcal{C}^{(f)}_{F,F}. \qquad \text{(N9)}$$

For strong magnetic field [when $g\mu_B B$ is large with respect to the hyperfine splitting], the ^{3}P$_2$ energy level splits into 5 levels with $j_z=0,\pm1,\pm2$, and every level splits into six levels by the hyperfine interaction.

Splitting of the $F=\frac{3}{2}$ energy level (that we are interested in) is,

$$\mathcal{E}_{\frac{3}{2},f} \;=\; \mathcal{E}^{(0)}_F - \frac{13}{30}\;g\mu_B B - f\;g\mu_B B. \qquad \text{(N10)}$$

Energies $\mathcal{E}_{\frac{3}{2},f}$ calculated numerically by diagonalization of the matrices (N8) are shown in Fig. 13(b) as functions of the magnetic field. The energies are almost linear with the magnetic field which agrees with equation (N10).

Appendix O: Averaged Dipole, Quadruple and Octuple Moments

The density matrix of the impurity atom placed in the magnetic field $\mathbf{B}=B\mathbf{e}_z$ is,

$$\hat{\varrho}_{\rm i} \;=\; \frac{1}{Z_{\rm i}}\sum_f e^{\beta g\mu_B B f}\;X^{f,f}, \qquad \text{(O1)}$$

where $\beta=\frac{1}{T}$,

$$Z_{\rm i} \;=\; \sum_f e^{\beta g\mu_B B f}.$$

Expectation value of an operator $\hat{\mathcal{O}}$ acting in the Hilbert state of quantum states of the isolated impurity is,

$$\big\langle\hat{\mathcal{O}}\big\rangle \;=\; \frac{1}{Z_{\rm i}}\sum_f \mathcal{O}_{f,f},$$

where $\mathcal{O}_{f,f}=\langle f|\hat{\mathcal{O}}|f\rangle$.

1. Expectation value of the magnetic dipole momentum operator is,

$$\big\langle\hat{F}^\alpha\big\rangle \;=\; -\mathcal{F}_{\rm d}\;\delta^{\alpha,z}, \qquad \text{(O2)}$$

where

$$\mathcal{F}_{\rm d} \;=\; \frac{1}{2}\;\tanh\left(\frac{g\mu_B B}{2T}\right)+\tanh\left(\frac{g\mu_B B}{T}\right).$$

When $g\mu_B B\ll T$, $\mathcal{F}_d$ can be written in the linear with B approximation as,

$$\mathcal{F}_{\rm d} \;=\; \frac{5}{4}\;\frac{g\mu_B B}{T}+O\!\left(\frac{\mu_B^3 B^3}{T^3}\right).$$

2. Expectation value of the magnetic quadruple momentum operator is,

$$\big\langle\hat{F}^{\alpha,\alpha'}\big\rangle \;=\; -\mathcal{F}_{\rm q}\;\delta^{\alpha,\alpha'}\left\{\delta^{\alpha,x}+\delta^{\alpha,y}-2\delta^{\alpha,z}\right\}, \qquad \text{(O3)}$$

where

$$\mathcal{F}_{\rm q} \;=\; \frac{2\;\sinh^2\left(\frac{g\mu_B B}{2T}\right)}{\cosh\left(\frac{g\mu_B B}{2T}\right)}.$$

When $g\mu_B B \ll T$, $\mathcal{F}_q$ can be expanded with B as,

$$\mathcal{F}_{\rm q} \;=\; \frac{1}{2}\;\frac{\left(g\mu_B B\right)^2}{T^2} + O\!\left(\frac{\mu_B^4 B^4}{T^4}\right).$$

3. Expectation value of the magnetic octuple momentum operator is,

$$\left\langle \hat{F}^{\alpha,\alpha',\alpha''}\right\rangle \;=\; \mathcal{F}_{\rm o}\,\Big\{\delta^{\alpha,\alpha'}\delta^{\alpha'',z} + \delta^{\alpha,\alpha''}\delta^{\alpha',z} + \\ +\;\delta^{\alpha',\alpha''}\delta^{\alpha,z} - 5\;\delta^{\alpha,z}\delta^{\alpha',z}\delta^{\alpha'',z}\Big\}, \quad \text{(O4)}$$

where

$$\mathcal{F}_{\rm o} \;=\; \frac{36}{5}\;\frac{2\;\sinh^4\left(\frac{g\mu_B B}{2T}\right)}{\sinh\left(\frac{2g\mu_B B}{2T}\right)}.$$

When $g\mu_B B \ll T$, $\mathcal{F}_o$ can be expanded with B as,

$$\mathcal{F}_{\rm o} \;=\; \frac{9}{40}\;\frac{\left(g\mu_B B\right)^3}{T^3} + O\!\left(\frac{\mu_B^5 B^5}{T^4}\right).$$

4. Expectation value of $F^{\alpha_1}F^{\alpha_2}$ is,

$$\frac{1}{2}\left\langle \hat{F}^{\alpha_1}\hat{F}^{\alpha_2} + \hat{F}^{\alpha_2}\hat{F}^{\alpha_1}\right\rangle = \left(\frac{5}{4} + \mathcal{F}^{\alpha_1}_{\rm d,d}\right)\,\delta^{\alpha_1,\alpha_2}, \quad \text{(O5)}$$

where

$$\mathcal{F}^{\alpha}_{\rm d,d} \;=\; \left(3\;\delta^{\alpha,z} - 1\right)\;\frac{2\;\sinh^2\left(\frac{g\mu_B B}{2T}\right)}{\cosh\left(\frac{g\mu_B B}{2T}\right)}.$$

When $g\mu_B B \ll T$, $\mathcal{F}_{d,d}$ can be expanded with B as,

$$\mathcal{F}^{\alpha}_{\rm d,d} \;=\; \left(3\;\delta^{\alpha,z} - 1\right)\;\frac{1}{2}\;\frac{\left(g\mu_B B\right)^2}{T^2} + O\!\left(\frac{\mu_B^4 B^4}{T^4}\right).$$

5. Expectation value of $F^{\alpha_1}F^{\alpha_2,\alpha_2'}$ is,

$$\frac{1}{2}\left\langle \hat{F}^{\alpha_1}\hat{F}^{\alpha_2,\alpha_2'} + \hat{F}^{\alpha_2,\alpha_2'}\hat{F}^{\alpha_1}\right\rangle = \\ = \Big(\delta^{\alpha_1,\alpha_2}\delta^{\alpha_2',z} + \delta^{\alpha_1,\alpha_2'}\delta^{\alpha_2,z} - \\ -\,2\;\delta^{\alpha_1,z}\delta^{\alpha_2,z}\delta^{\alpha_2',z}\Big)\;\mathcal{F}^{(1)}_{\rm d,q} + \\ +\,\delta^{\alpha_2,\alpha_2'}\left(\delta^{\alpha_1,z} - 2\;\delta^{\alpha_1,z}\delta^{\alpha_2,z}\right)\mathcal{F}^{(2)}_{\rm d,q}, \quad \text{(O6)}$$

where

$$\mathcal{F}^{(1)}_{\rm d,q} \;=\; -\frac{3}{2}\;\tanh\left(\frac{g\mu_B B}{T}\right), \\ \mathcal{F}^{(2)}_{\rm d,q} \;=\; \tanh\left(\frac{g\mu_B B}{2T}\right) - \frac{1}{2}\;\tanh\left(\frac{g\mu_B B}{T}\right).$$

When $g\mu_B B \ll T$, $\mathcal{F}^{(1,2)}_{d,q}$ can be expanded with B as,

$$\mathcal{F}^{(1)}_{\rm d,q} \;=\; -\frac{3}{2}\;\frac{g\mu_B B}{T} + O\!\left(\frac{\mu_B^3 B^3}{T^3}\right), \\ \mathcal{F}^{(2)}_{\rm d,q} \;=\; \frac{g\mu_B B}{T} + O\!\left(\frac{\mu_B^3 B^3}{T^3}\right).$$

6. Expectation value of $F^{\alpha_1}F^{\alpha_2,\alpha_2',\alpha_2''}$ is,

$$\frac{1}{2}\left\langle \hat{F}^{\alpha_1}\hat{F}^{\alpha_2,\alpha_2',\alpha_2''} + \hat{F}^{\alpha_2,\alpha_2',\alpha_2''}\hat{F}^{\alpha_1}\right\rangle = \\ = \mathcal{A}^{\alpha_1;\alpha_2,\alpha_2',\alpha_2''}\mathcal{F}_{\rm d,o}, \quad \text{(O7)}$$

where $\mathcal{A}^{\alpha_1;\alpha_2,\alpha_2',\alpha_2''}$ is symmetric with $\alpha_2,\alpha_2',\alpha_2''$ tensor which does not depend on temperature or magnetic field,

$$\mathcal{F}_{\rm d,o} \;=\; \frac{2\;\sinh^2\left(\frac{g\mu_B B}{2T}\right)}{\cosh\left(\frac{g\mu_B B}{2T}\right)}.$$

When $g\mu_B B \ll T$, $\mathcal{F}_{d,o}$ can be expanded with B as,

$$\mathcal{F}_{\rm d,o} \;=\; \frac{1}{2}\;\frac{\left(g\mu_B B\right)^2}{T^2} + O\!\left(\frac{\mu_B^4 B^4}{T^4}\right).$$

Appendices N and O main points: Although we do not subject our system to an external magnetic field (since it is detrimental for the Kondo effect) we find it useful to employ our detailed analysis of Yb atoms and inspect their properties under an application of a weak magnetic field. In particular, the multiple analysis worked out in this paper helps us to elucidate the pattern of the dependence of energy levels on the magnetic field, both for the ground-state $^1S_0$ and the excited state $^3P_2$. This is shown in Figs. 13(a), and 13(b).

[1] J.Kondo, Progr. Theor. Phys. **32**, 37 (1964).
[2] P. Coleman, Physics World **12**, 29 (1995).
[3] P. W. Anderson, Physics World **12**, 37 (1995).
[4] A. C. Hewson, The Kondo Problem to Heavy Fermions (Cambridge University Press, Cambridge, 1993).
[5] V. T. Rajan, Phys. Rev. Lett. **51**, 308 (1983).
[6] P. Schlottmann, Zeitschrift für Physik B: Condensed Matter **51**, 223 (1983).
[7] Andrés Jerez, Natan Andrei, and Gergely Zaránd, Phys. Rev. B **58**, 3814 (1998).
[8] P. Noziéres and A. Blandin, J. Phys. (Paris) **41**, 193 (1980).
[9] Y. Oreg and D. Goldhaber-Gordon, Phys. Rev. Lett. **90**, 136602 (2003).
[10] A. M. Sengupta and Y. B. Kim, Phys. Rev. B **54**, 14918 (1996).
[11] C. Silber, S. Gunther, C. Marzok, B. Deh, P. W. Courteille, and C. Zimmermann, Phys. Rev. Lett. 95, 170408 (2005).
[12] T. Onimaru, K. Izawa, K. T. Matsumoto, T. Yoshida, Y. Machida, T. Ikeura, K. Wakiya, K. Umeo, S. Kittaka, K. Araki, T. Sakakibara, T. Takabatake, Phys. Rev. B **94**,

075134 (2016); arXiv:1606.09571.
[13] I. Kuzmenko, T. Kuzmenko, Y. Avishai and K. A. Kikoin, Phys. Rev. B **91**, 165131 (2015); arXiv:1402.0187.
[14] Olivier Parcollet, Antoine Georges, Gabriel Kotliar, and Anirvan Sengupta, Phys. Rev. B **58**, 3794 (1998); arXiv:cond-mat/9711192.
[15] T.Fukuhara, Y.Takasu, M.Kumakura, Y.Takahashi, Phys. Rev. Lett. **98**, 030401 (2007).
[16] Ren Zhang, Yanting Cheng, Hui Zhai, Peng Zhang, Phys. Rev. Lett. **115**, 135301 (2015); arXiv:1504.02864.
[17] Ren Zhang, Deping Zhang, Yanting Cheng, Wei Chen, Peng Zhang, Hui Zhai, Phys. Rev. A **93**, 043601 (2016); arXiv:1509.01350.
[18] G. Pagano, M. Mancini, G. Cappellini, L. Livi, C. Sias, J. Catani, M. Inguscio, and L. Fallani, Phys. Rev. Lett. 115, 265301 (2015).
[19] G. Pagano, M. Mancini, G. Cappellini, P. Lombardi, F. Schäfer, H. Hu, X.-J. Liu, J. Catani, C. Sias, M. Inguscio, et al., Nature Physics **10**, 198 (2014).
[20] Giacomo Cappellini, Marco Mancini, Guido Pagano, Pietro Lombardi, Lorenzo Livi, Mario Siciliani de Cumis, Pablo Cancio, Marco Pizzocaro, Davide Calonico, Filippo Levi, Carlo Sias, Jacopo Catani, Massimo Inguscio, Leonardo Fallani, Phys. Rev. Lett. **113**, 120402 (2014).
[21] F. Scazza, C. Hofrichter, M. Höfer, P. C. De Groot, I. Bloch, and S. Folling, Nature Physics **10**, 779 (2014).
[22] T. D. Ladd, F. Jelezko, R. Laflamme, Y. Nakamura, C. Monroe, and J. L. O'Brien, Nature **464**, 45 (2010).
[23] A. J. Daley, Quantum Information Processing **10**, 865 (2011).
[24] X. Zhang, M. Bishof, S. L. Bromley, C. V. Kraus, M. S. Safronova, P. Zoller, A. M. Rey, and J. Ye, Science **345**, 1467 (2014).
[25] B. Song, C. He, S. Zhang, E. Hajiyev, W. Huang, X.-J. Liu, and G.-B. Jo, arXiv:1608.00478.
[26] S. Kolkowitz, S. L. Bromley, T. Bothwell, M. L. Wall, G. E. Marti, A. P. Koller, X. Zhang, A. M. Rey, and J. Ye, arXiv:1608.03854.
[27] L. F. Livi, G. Cappellini, M. Diem, L. Franchi, C. Clivati, M. Frittelli, F. Levi, D. Calonico, J. Catani, M. Inguscio, L. Fallani, arXiv:1609.04800.
[28] Igor Kuzmenko, Tetyana Kuzmenko, Yshai Avishai, Gyu-Boong Jo, Phys. Rev. B **93**, 115143 (2016); arXiv:1512.00978.
[29] A. Yamaguchi, S. Uetake, S. Kato, H. Ito, and Y. Takahashi, New Journal of Physics **12**, 103001 (2010).
[30] A. Khramov, A. Hansen,W. Dowd, R. J. Roy, C. Makrides, A. Petrov, S. Kotochigova, and S. Gupta, Physical Rev. Lett. **112**, 033201 (2014).
[31] S.G. Porsev, Yu.G. Rakhlina, M.G. Kozlov, J. Phys. B **32**, 1113-20 (1999); arXiv:physics/9810011.
[32] Masses, nuclear spins, and magnetic moments: I. Mills, T. Cvitas, K. Homann, N. Kallay, and K. Kuchitsu, in Quantities, Units and Symbols in Physical Chemistry, Blackwell Scientic Publications, Oxford, UK, 1988.
[33] S.G. Porsev, M.S. Safronova, A. Derevianko, Charles W. Clark, Phys. Rev. A **89**, 012711 (2014); arXiv:1307.2656 .
[34] W. F. Meggers and J. L. Tech, J. Res. Natl. Bur. Stand. (U.S.) **83**, 13 (1978).
[35] T. Andersen, "Atomic negative ions: Structure, dynamics and collisions". Physics Reports **394**, 157 (2004).
[36] G. F. Gribakin and V. V. Flambaum, Phys. Rev. A **48**, 546 (1993).
[37] Masaaki Kitagawa, Katsunari Enomoto, Kentaro Kasa, Yoshiro Takahashi, Roman Ciuryło, Pascal Naidon, and Paul S. Julienne, Phys. Rev. A **77**, 012719 (2008); arXiv:0708.0752.
[38] Shinya Kato, Seiji Sugawa, Kosuke Shibata, Ryuta Yamamoto, and Yoshiro Takahashi, Phys. Rev. Lett. 110, 173201 (2013); arXiv:1210.2483.
[39] L. D. Landau and E. M. Lifshitz, Quantum Mechanics, A Course of Theoretical Physics Vol. 3 (Pergamon, New York, 1965).
[40] Sanner, Christian and Su, Edward J and Keshet, Aviv and Huang, Wujie and Gillen, Jonathon and Gommers, Ralf and Ketterle, Wolfgang, Physical Review Letters 106 010402 (2011)
[41] Navon, Nir and Piatecki, Swann and Günter, Kenneth and Rem, Benno and Nguyen, Trong Canh and Chevy, Frédéric and Krauth, Werner and Salomon, Christophe, Physical Review Letters 107 135301 (2011)
[42] Nascimbène, S and Navon, N and Jiang, K J and Chevy, F. and SALOMON, C, Nature 463, 1057 (2010)
[43] Hofrichter, Christian and Riegger, Luis and Scazza, Francesco and Höfer, Moritz and Fernandes, Diogo Rio and Bloch, Immanuel and Fölling, Simon, Physical Review X, 6, 021030 (2016)